# DECIPHERING THE FUNCTION OF G PROTEIN-COUPLED RECEPTOR 30

## DISSERTATION

zur Erlangung des akademischen Grades

**doctor rerum naturalium**

**(Dr. rer. nat.)**

im Fach Biologie

eingereicht an der

Mathematisch-Naturwissenschaftlichen Fakultät I

der Humboldt Universität zu Berlin

von

Jörg Isensee

geboren am 13.11.1975 in Hannover, Deutschland

Präsident der Humboldt-Universität zu Berlin
Prof. Dr. Dr. h.c. Christoph Markschies

Dekan der Mathematisch-Naturwissenschaftlichen Fakultät I
Prof. Dr. Lutz-Helmut Schön

Gutachter/innen:

1. Prof. Dr. rer. nat. Klaus Peter Hofmann
2. Prof. Dr. rer. nat. Patricia Ruiz Noppinger
3. Prof. Dr. rer. nat. Werner Kloas

Tag der mündlichen Prüfung: 01.07.2009

**Für Sabina und Alma**

# ZUSAMMENFASSUNG

Der G Protein-gekoppelte Rezeptor 30 (GPR30) wurde vornehmlich im Kontext von schnellen Östrogeneffekten auf zelluläre Signaltransduktionskaskaden untersucht und stellt möglicherweise einen neuen Östrogenrezeptor dar. Die physiologische Funktion von GPR30 *in vivo* konnte jedoch bisher nicht ermittelt werden.

Daher wurde in dieser Arbeit ein Gpr30-defizientes Mausmodell charakterisiert, bei dem ein Teil der kodierenden Sequenz durch einen LacZ-Reporter ersetzt wurde (Gpr30-lacZ). Die Integration des Konstruktes in den Gpr30-Locus wurde mittels *Southern blotting* und *Real-time PCR* verifiziert. Gpr30-positive Zelltypen wurden durch Kolokalisation von LacZ mit zelltyp-spezifischen Markerproteinen identifiziert. Weitere Versuche dienten der Aufklärung des Phänotyps von Gpr30-lacZ Mäusen. Zur Identifizierung von Proteinen des GPR30-Signalkomplexes wurden *Yeast-Two-Hybrid* Analysen mit der N- bzw. C-terminalen Domäne des Rezeptors durchgeführt.

Die wesentlichen LacZ-positiven Zellpopulationen waren (i) Endothelzellen in kleinen arteriellen Gefäßen, (ii) glatte Muskelzellen, Perizyten und neuronale Subpopulationen im Gehirn, (iii) Hauptzellen in der Magenschleimhaut, (iv) Zellpopulationen in der Adenohypophyse und dem Hypophysenzwischenlappen sowie (vi) chromaffine Zellen im Nebennierenmark. Während der Phenotypisierung des Mausmodells wurde eine Reduktion der CD62L+ T-Zellen von ca. 50% im peripheren Blut festgestellt. Mittels Y*east Two-Hybrid* Analyse wurden *Pals1-associated tight junction protein* (PATJ) und *FUN14 domain-containing 2* (FUNDC2) als mögliche Interaktionspartner identifiziert.

Zusammenfassend wurde in dieser Arbeit eine zelluläre Basis für die Funktion von Gpr30 *in vivo* ermittelt. Der Phänotyp in Gpr30-lacZ Mäusen ist wahrscheinlich durch eine verringerte Produktion von naiven T-Zellen im Thymus bedingt. PATJ bindet die C-terminalen Aminosäuren von GPR30 mit einer PDZ-Domäne und könnte ein Gerüstprotein des GPR30-Signalkomplexes darstellen.

Schlagwörter: *G protein-gekoppelter Rezeptor 30, GPR30, LacZ Reporter Maus, PATJ, FUNDC2*

## ABSTRACT

The orphan G protein coupled receptor 30 (GPR30) was predominantly analyzed in the context of membrane-initiated estrogen signaling suggesting that GPR30 represents a novel estrogen receptor. However, the physiological function of GPR30 *in vivo* remained unknown.

To unravel the physiological role of murine Gpr30 *in vivo*, a Gpr30-deficient mouse model was analyzed that harbors a LacZ reporter (Gpr30-lacZ) within the Gpr30 locus. The targeting of Gpr30 was verified by Southern blotting and real-time PCR. Gpr30-expressing cell types were identified by colocalization of LacZ along with cell type-specific markers. Further experiments aimed to decipher the phenotype of Gpr30-lacZ mice. To gain information about the signaling complex of human GPR30, yeast two-hybrid screenings were performed with the N- and C-terminal domains as bait.

The main LacZ-positive cell populations were (i) endothelial cells in small arterial vessels of various tissues, (ii) smooth muscle cells, pericytes, and neuronal subpopulations in the brain, (iii) gastric chief cells in the stomach, (iv) cells in the intermediate and anterior pituitary, and (v) chromaffin cells in the adrenal glands. Extensive phenotype screening at the German Mouse Clinic revealed reduced numbers of T cells in the peripheral blood of Gpr30-lacZ mice. Especially the proportion of CD62L+ cells was decreased by approx. 50%. Yeast two-hybrid screening led to the identification of Pals1-associated tight junction protein (PATJ) and FUN14 domain-containing 2 (FUNDC2).

In conclusion, this study provides a cellular basis for the function of Gpr30 *in vivo*. Since CD62L+ cells represent the naive T cell compartment, the phenotype of Gpr30-lacZ mice suggests an impaired production of T cells in the thymus. PATJ likely binds the C-terminus of GPR30 with one of its PDZ domains and may represent a scaffolding protein of the GPR30 signaling complex.

Keywords: *G protein coupled receptor 30, GPR30, LacZ reporter mouse, PATJ, FUNDC2*

# TABLE OF CONTENTS

# ABBREVIATIONS

| | |
|---|---|
| 7TMR | Seven transmembrane receptor |
| Akt | Protein kinases B |
| α-SMC | α-Smooth muscle cell actin |
| ATP | Adenosine-5'-triphosphate |
| cDNA | Complementary DNA |
| CFP | Cyan fluorescent protein |
| CoIP | Co-immunoprecipitation |
| DMEM | Dulbecco's modified Eagle medium |
| DMSO | Dimethyl sulfoxide |
| DNA | Deoxyribonucleic acid |
| E2 | 17β-estradiol |
| EDTA | Ethylendiaminotetraacetic acid |
| EGFR | Epidermal growth factor receptor |
| ER | Estrogen receptor |
| ERK | Extracellular signal-regulated kinases |
| FBS | Fetal bovine serum |
| FLAG-tag | FLAG octapeptide (DYKDDDDK) |
| FUNDC2 | FUN14 domain-containing 2 |
| GFAP | Glial fibrillary acidic protein |
| GFP | Green fluorescent protein |
| GPCR | G protein-coupled receptor |
| GPR30 | Human G protein-coupled receptor 30 |
| Gpr30 | Murine G protein-coupled receptor 30 |
| GRK | G protein-coupled receptor kinase |
| GTP | Guanosine-5'-triphosphate |
| HA | Hemagglutinin epitope |
| His-tag | Polyhistidine-tag |
| IP3 | Inositol triphosphate |
| IRES | Internal ribosomal entry site |
| LacZ | β-galactosidase |
| mRNA | Messenger RNA |
| Myc-tag | Myc decapeptide (EQKLISEEDL) |
| neoR | Neomycin-resistance |
| NO | Nitric oxide |
| PATJ | Pals1-associated tight junction protein |
| ORF | Open reading frame |
| NP-40 | Nonidet P-40 |
| OD | Optical density |
| PEG | Polyethylene glycol |
| PAGE | Polyacrylamide gel electrophoresis |
| SHBG | Sex hormone binding globulin |
| PBS | Phosphate buffered saline |
| PCR | Polymerase chain reaction |
| SV40 pA | SV40 polyadenylation site |
| PDZ domain | Post-synaptic density 95, Discs Large, Zona Occludens 1 domain |
| PECAM-1 | Platelet/endothelial cell adhesion molecule 1 |
| PGK | Phosphoglycerate kinase promoter |
| PI3K | Phosphatidylinositol 3-kinase |
| PIP2 | Phosphatidylinositol 4,5-bisphosphate |
| PLCβ | Phospholipase C-β |
| PMSF | Phenylmethylsulfonylfluoride |
| SDS | Sodium dodecylsulphate |
| TE | Tris-EDTA solution |
| Tris | Tris(hydroxymethyl)-aminomethane hydrochloride |
| X-gal | 5-chlor-4-brom-3-indolyl-β-galactoside |
| YFP | Yellow fluorescent protein |

# 1 INTRODUCTION

The superfamily of G protein-coupled receptors (GPCRs) is one of the largest protein families encoded in mammalian genomes. In humans more than 800 members are known, of which ≈400 are likely olfactory receptors involved in the perception of odors by specific neurons in the olfactory bulb (Fredriksson *et al.* 2003). Of the remaining 376 GPCRs, 139 are still classified as orphan receptors with unknown ligands according to the IUPHAR database (The International Union of Basic and Clinical Pharmacology, http://www.iuphar-db.org). The already identified ligands of GPCRs represent an extremely heterogeneous set of molecules including ions, biogenic amines, nucleotides, amino acid metabolites such as dopamine and norepinephrine, peptides, proteins, large glycoprotein hormones, bioactive lipids, odorants, tastants and even photons are detected by GPCRs.

Members of the GPCR family are among the most pursued targets for the development of therapeutic drugs. Approximately 30% of the clinically marketed drugs target GPCR function, representing approximately 9% of global pharmaceutical sales with several GPCR ligands belonging to the top-100-selling pharmaceutical products worldwide (Drews 2000; Brink *et al.* 2004). These available drugs target only a small number of GPCRs, which implicates that there is still an enormous potential for drug discovery within the field (Fredriksson *et al.* 2003).

The first main requirement for a protein to be classified as a GPCR are seven hydrophobic stretches of about 25 to 35 consecutive amino acids, which are believed to represent seven α-helices that span the plasma membrane in an counter-clockwise manner. The second requirement is the ability of the GPCR to assemble a signaling unit (e.g. interaction with a G protein) enabling the activation of multiple signaling pathways within the cell. However, interaction with a specific G protein has not been demonstrated for most GPCRs (Fredriksson *et al.* 2003). Therefore the more concise term seven transmembrane receptor (7TMR) will be preferentially used as a synonym for GPCR in the following text. Since the three-dimensional structure of 7TMRs is far greater conserved than the primary sequence, classification systems have been developed that integrate sequence data as well structural motifs and functional properties (Davies *et al.* 2008). The standard classification is implemented in the GPCRDB database (http://www.gpcr.org/7tm/) (Horn *et al.* 2003), which divides 7TMRs of all species into six classes (Class A: Rhodopsin-like, Class B: Secretin-like; Class C:

Metabotropic glutamate receptors; Class D: Pheromone receptors; Class E: cAMP receptors; Class F: Frizzled/smoothened family). The six classes are further divided into sub-families and sub-sub-families based on the function and ligand. Classes A, B, C and F are found in mammalians, whereas over 75% of all human non-olfactory 7TMRs belong to class A (http://www.iuphar-db.org).

The deorphanization and functional analysis of novel 7TMRs represents a wide field of current research. This work is dedicated to the functional analysis of the orphan 7TMR GPR30 (formerly known as CMKRL2, LyGPR, CEPR, GPCR-Br, or FEG-1) which belongs to the class A (Rhodopsin like) receptors, sub-family peptide receptors, sub-sub family chemokine receptor-like 2 which contains only GPR30 orthologs of different species.

## 1.1 Signaling Complexes of seven transmembrane receptors

7TMRs are nowadays recognized as elements of large signaling units composed of multiple proteins that interact with each other in a complex fashion. These units are sometimes referred to as receptosomes and are believed to be organized by scaffolding proteins. Many of the known scaffolding proteins contain multiple PDZ (Post-synaptic density 95, Discs Large, Zona Occludens 1) domains. PDZ domains generally, but not always, interact with the extreme C-terminal tail of a 7TMR (Bockaert *et al.* 2004).

Signaling occurs primarily through heterotrimeric G proteins consisting of an α-, β-, and γ-subunit, whereas the β- and γ-subunit are tightly associated. Although several isoforms of each subunit exist (20 α, 6 β, and 12 γ proteins are known), four main classes of G proteins can be distinguished based on the functional properties of the α-subunit designated as $G_s$, $G_i$, $G_q$, and $G_{12/13}$ (Hamm 1998).

G proteins are inactive in the heterotrimeric state when GDP is bound to the α subunit. Ligand-binding changes the conformation of the intracellular domain of the GPCR resulting in receptor-mediated guanine nucleotide exchange of GDP with GTP, dissociation of the $G_\alpha$-GTP and $G_{\beta\gamma}$ subunit, and subsequent activation of downstream effectors. Different $G_\alpha$ isoforms activate different effector proteins. $G_{\alpha s}$ stimulates the production of cAMP from ATP by direct interaction with the membrane-associated enzyme adenylate cyclase. Cyclic AMP activates protein kinase A (PKA) resulting in the phosphorylation of multiple downstream targets. In contrast, $G_{\alpha i}$ inhibit the production of cAMP. $G_{\alpha q}$ activates the membrane-bound enzyme phospholipase C-β (PLCβ), which cleaves phosphatidylinositol 4,5-bisphosphate ($PIP_2$) into inositol triphosphate

($IP_3$) and diacylglycerol (DAG). $IP_3$ then activates its receptors within the smooth endoplasmic reticulum leading to the opening of calcium channels followed by the release of calcium ions into the cytosol. $G_{\alpha 12/13}$ is involved in Rho family GTPase signaling. The $G_{\beta\gamma}$ subunit itself has also active functions, e.g. the transactivation of the epidermal growth factor receptor (EGFR). Some receptors are coupled primarily to one G protein subtype, whereas others bind members of several G protein subtypes. Therefore, GPCR signaling may act specifically on one downstream effector or result in the activation of multiple effectors (Premont and Gainetdinov 2007).

However, 7TMRs are now recognized to interact not only with G proteins but also with several accessory proteins. These proteins have important functions such as targeting to specific cellular compartments, assembling into large functional complexes (receptosomes), trafficking to and from the plasma membrane, and the fine-tuning of signaling properties (Bockaert *et al.* 2004). 7TMRs desensitize upon prolonged exposure to high concentrations of agonist and resensitize when not exposed to agonist for some time. The most important pathway that mediates sensitization involves G protein-coupled receptor kinases (GRKs) and arrestins. Activated 7TMRs are recognized by GRKs and rapidly phosphorylated on specific serine and threonine residues located within the intracellular loops and the C-terminal tail (Moore *et al.* 2007; Premont and Gainetdinov 2007). Seven GRKs (GRK1-7) have been identified in humans so far (Premont and Gainetdinov 2007). Due to tissue-specific expression of some isoforms, most 7TMRs in the body are potentially regulated by GRKs 2, 3, 5, or 6 (Premont and Gainetdinov 2007). The analysis of mouse models deficient for GRKs revealed that some 7TMRs are regulated by one particular GRK, whereas others are regulated by several GRK subtypes in a tissue-specific manner (Premont and Gainetdinov 2007).

Phosphorylated 7TMRs are able to recruit the protein β-arrestin, which prevents the receptor from activating additional G proteins. Moreover, β-arrestins act as adapters for the AP2 complex that directs activated receptors to clathrin-coated pits to facilitate their internalization (Goodman *et al.* 1996; Laporte *et al.* 2002). Recent findings indicate that β-arrestins are also involved in the activation of signaling cascades independent of G protein signaling by serving as multiprotein scaffolds for a number of signaling molecules such as extracellular signal-regulated kinases (ERKs), c-Jun N-terminal kinases (JNKs), p38 MAP kinases, protein kinase B (Akt), phosphatidylinositol 3-kinase (PI3K), and the small GTPase RhoA (DeWire *et al.* 2007). Four arrestin isoforms (arrestin 1-4) have been identified in the human genome. Two of these isoforms show

cell type-restricted expression indicating that most 7TMRs bind either arrestin 2 (β-arrestin 1) or arrestin 4 (β-arrestin 2) (Premont and Gainetdinov 2007). Knockout mice of either β-arrestin 1 or 2 are viable (Conner *et al.* 1997; Bohn *et al.* 1999), whereas the double-knockout phenotype is embryonic lethal (Kohout *et al.* 2001) implying that β-arrestin isoforms are able to substitute each other to some degree (DeWire *et al.* 2007).

Further enhancing the complexity of 7TMR signaling, several of them have been found to form homo- or heterodimers, a concept which may imply important functions of real orphan 7TMRs as modulators of other ligand-binding receptors (Luttrell 2006).

## 1.2 The G protein-coupled Receptor 30

Human GPR30 was initially cloned in 1996-97 by five different research groups from several sources. The cloning was performed either with degenerated polymerase chain reaction (PCR) primers to amplify the transmembrane domains of novel 7TMRs from cDNA of Burkitt's lymphoblasts (Owman *et al.* 1996), B cells (Kvingedal and Smeland 1997), shear-stressed human umbilical vein endothelial cells (Takada *et al.* 1997), and human genomic DNA (Feng and Gregor 1997) or by differential cDNA library screening between MCF-7 and MDA-MB-231 breast cancer cell lines (Carmeci *et al.* 1997).

The genomic context as well as the gene structure of GPR30 is well conserved in different species (Fig. 1A,B). The GPR30 gene is localized on human chromosome 7p22.3 or on mouse homolog 5G1. Upstream of GPR30 resides another 7TMR designated as GPR146 suggesting a gene duplication event. However, a similar function of both proteins is unlikely, since they share only ≈20% sequence identity. Three alternative splicing variants of 2-3 exons with different 5' untranslated regions (5'-UTR) encoding the same GPR30 protein are known in humans (Fig. 1B). In the mouse, a single Gpr30 transcript that contains three exons was found so far.

The GPR30 protein consists of about 375 amino acids and is encoded in an intronless open reading frame (ORF) in all species. The protein is highly conserved in mammalians with 87% sequence identity between human and mouse (Fig. 1C), whereas most amino acid exchanges are within the N-terminal domain. Especially the transmembrane domains, the third intracellular domain (IC3), and the C-terminal domain are highly conserved in mammalian species. The N- and C-terminal domains of GPR30 are rather short compared to most 7TMRs.

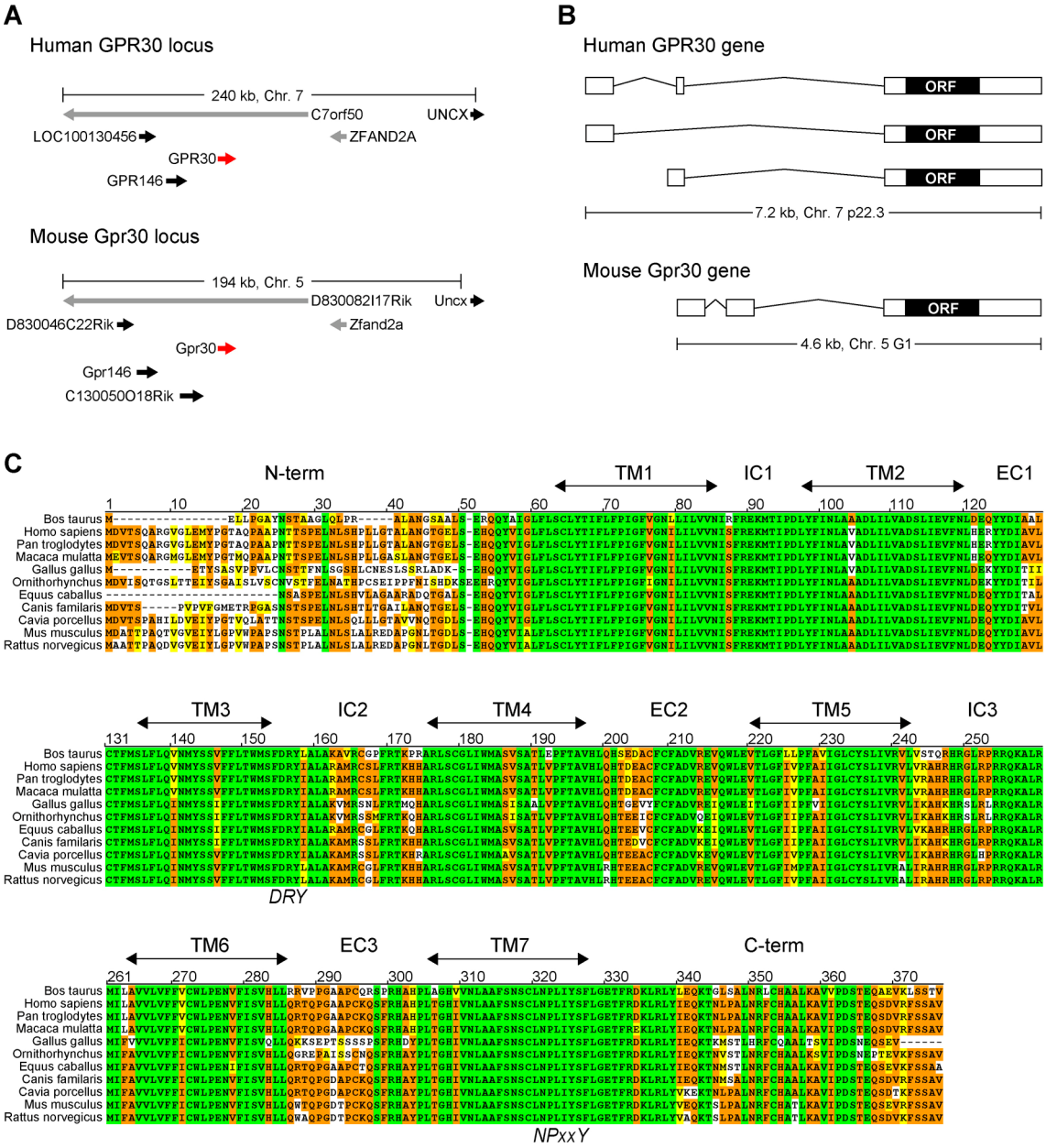


**Fig. 1:** (A) Genomic locus of the human and mouse GPR30 gene (red arrows). Genes on the same strand are shown in black; genes on the complementary strand are depicted in grey. (B) Exon/Intron structure of the human and mouse GPR30 gene. White squares indicate exons. The open reading frame (ORF) encoding the protein is shown in black. Three spicing variants of 2-3 exons are known in humans. The mouse Gpr30 gene encodes a single transcript that contains three exons. (C) Sequence alignment of GPR30 orthologs from several mammalian species, the chicken (*Gallus gallus*), and the platypus (*Ornithorhynchus anatinus*). The GPR30 protein contains seven transmembrane domains (TM1-7), three intracellular- (IC1-3) or extracellular loops (EC1-3) as well as an N- and C-terminal domain. Especially the transmembrane domains, the third intracellular loop (IC3), and the C-terminal domain are highly conserved in mammalian species.

The closest relatives of GPR30 in the human genome (≈30-35% sequence identity) are the interleukin 8 receptor alpha (IL8RA, CXCR1) on chromosome 2q35 and the angiotensin II receptor, type 1 (AGTR1) on chromosome 3q21 (Owman *et al.* 1996; Feng and Gregor 1997). However, GPR30 could not be included in any of the five main families

identified in a phylogenetic analyses of all human 7TMRs outlining its unique structure (Fredriksson *et al.* 2003). GPR30 contains the DRY motif located at the boundary between transmembrane domain (TM) III and intracellular loop (IC) 2 of class A GPCRs. This highly conserved stretch plays a pivotal role in regulating the GPCR conformational states and mutations within the motif often results in constitutive activation of the GPCR (Rovati *et al.* 2007). Moreover, the conserved NPxxY motif located at the end of TM7 of GPR30 was shown to mediate the association of 7TMRs with the ADP-ribosylation factor ARF1, which may couple these receptors to phospholipases (Robertson *et al.* 2003; Johnson *et al.* 2006). Concerning the association of GPR30 with G proteins, coupling to $G_s$ and $G_q$ has been suggested (Filardo *et al.* 2002; Revankar *et al.* 2005), which may indicate cell type-specific differences (for further details see 1.3.1). If GPR30 activity is regulated by the GRK-arrestin pathway has not been investigated so far, but recent bioinformatic tools to identify potential phosphorylation sites (Xue *et al.* 2008) predict one GRK2 site ($S_{367}$), two GRK3 sites ($T_{170}$, $S_{373}$), and two GRK5 sites ($T_{343}$, $S_{367}$, $S_{373}$) within the GPR30 sequence.

## 1.3 Molecular Pathways of Estrogen Signaling

Estrogens including 17β-estradiol (E2) are a group of steroid hormones which have been implicated in the regulation of a variety of physiological processes such as reproduction, mammary gland development, bone turnover, cardiovascular function, spermatogenesis, and neuroprotection (Simpson *et al.* 2005). Estrogens are the primary sex steroid hormones in females and are predominantly synthesized by developing follicles in the ovaries, corpus luteum, placenta, and breast, but males produce small amounts of estrogen within the testis as well. Moreover, estrogens are produced locally within some somatic tissues such as the liver and adrenal glands. The biosynthesis starts from cholesterol and involves the conversion of testosterone to E2 or androstenedione to estrone by the enzyme aromatase. Sex steroid hormones are transported in complex with the sex hormone binding globulin (SHBG) within the circulation. Concerning the uptake of steroid hormones by target cells expressing intracellular receptors, SHBG was believed to keep sex steroids inactive and to control the amount of free hormones that enter cells by passive diffusion. However, it is now well documented that pathways for the cellular uptake of steroid-SHBG complexes exist (Hammes *et al.* 2005). The active uptake of sex steroids involves the interaction of SHBG and its steroid hormone cargo with megalin, a member of the low-density lipoprotein receptor-related protein family,

in clathrin coated pits at the plasma membrane (Adams 2005). The steroid-SHBG-megalin complex is then internalized in endocytic vesicles followed by the release of the hormone from its binding globulin (Hammes *et al.* 2005).

Estrogens classically regulate gene expression via nuclear estrogen receptors ERα and ERβ (ERs) acting primarily as ligand-activated transcription factors (McKenna and O'Malley 2002). ERα was characterized in 1973 based on its specific binding activity in rat uterus extracts (Jensen and DeSombre 1973; Greene *et al.* 1986), whereas the related ERβ was cloned later in 1996 from a rat prostate cDNA library (Kuiper *et al.* 1996). Both receptors are highly homologous in their DNA- and ligand-binding domains, but lack relative homology in their transcriptional activation domains (Kuiper *et al.* 1997). Since tissue distribution, expression levels, and phenotypes of knockout models differ between the two receptors, functional differences are apparently present (Kuiper *et al.* 1997; Antal *et al.* 2008). Subsequent to hormone binding, conformational changes induce chaperone dissociation and dimerization of ERs followed by binding to specific estrogen responsive elements (EREs) located in the promoters of target genes and the recruitment of coactivators and/or corepressors (Klein-Hitpass *et al.* 1986; McKenna and O'Malley 2002). Moreover, ERs regulate transcription by tethering to other transcription factor complexes that contact DNA at alternative response elements, a mode of action commonly referred to as transcriptional cross-talk (Gottlicher *et al.* 1998). These rather slow genomic effects are sensitive towards inhibitors of transcription and translation and have been extensively investigated.

In contrast to the direct effects of estrogens on transcription, estrogens also induce rapid nongenomic effects on different components of signal transduction pathways. E2 was found to induce the release of second messengers such as calcium, cAMP, cGMP, and NO as well as to activate several protein kinases (e.g. ERKs, PI3K, Akt) in various cell types (Losel *et al.* 2003; Edwards 2005; Hammes and Levin 2007). Nongenomic effects of estrogens take place within seconds or minutes at the plasma membrane and are insensitive towards inhibition of transcription and translation. Since membrane-initiated estrogen signaling resembles the action of 7TMRs, the identification of a 7TMR that binds and signals upon estrogen stimulation has been awaited. In this context, multiple reports suggested that GPR30 might be a G protein-coupled estrogen receptor.

### 1.3.1 Membrane-initiated Estrogen Signaling mediated by GPR30

Initially, Filardo and colleagues observed that the estrogen-induced phosphorylation of ERK requires the expression of GPR30 in the breast cancer cell line SKBR3 lacking classical ERs (Filardo *et al.* 2000). Transient expression of GPR30 in MDA-MB-231 breast cancer cells (ERα-negative, ERβ-positive) resulted in the conversion to an estrogen-responsive phenotype. Consistent with acting through a GPCR, E2-induced phosphorylation of ERK involved the transactivation of the epidermal growth factor receptor (EGFR). EGFR transactivation is a common mechanism of G protein signaling (Prenzel *et al.* 1999) and occurs through the activation of $G_{\beta\gamma}$ and the subsequent liberation of heparin-bound EGF (HB-EGF) from the cell surface by matrix metalloproteinases (MMPs). EGFR transactivation and downstream signaling to ERK is a well known nongenomic effect of estrogen which is essential for uterine epithelial cell proliferation as well as ductal elongation and endbud growth in the mammary gland (Mukku and Stancel 1985; Nelson *et al.* 1991; Ankrapp *et al.* 1998). Interestingly, the selective ER modulator tamoxifen and the ER antagonist ICI182780 (ICI) acted as agonists on the EGFR transactivation. In subsequent studies, Filardo *et al.* showed that ERK activity was rapidly restored to basal levels through PKA-dependent inhibition of Raf-1 activity (Filardo *et al.* 2002). Since this mechanism involves the stimulation of adenylate cyclase and subsequent cAMP production, coupling of GPR30 to $G_{\alpha s}$ was assumed. Moreover, transcriptional up-regulation of the proto-oncogene c-fos was shown to occur through the activation of ERK by GPR30 in SKBR3 breast cancer cells (ERα- and ERβ-negative, GPR30-positive) by estrogen and phytoestrogens (Maggiolini *et al.* 2004). The c-fos response was repressed in SKBR3 cells transfected with an antisense oligonucleotide against GPR30 and reconstituted in GPR30-deficient MDA-MB 231 and BT-20 breast cancer cells transiently transfected with GPR30.

In the following, two different groups claimed in 2005 that GPR30 directly binds E2 and mediates rapid nongenomic signaling (Revankar *et al.* 2005; Thomas *et al.* 2005). Thomas *et al.* described the specific binding of heavy hydrogen labeled E2 ($[^3H]$E2) to membranes of SKBR3 cells and to GPR30-transfected human embryonic kidney (HEK) cells with a dissociation constant ($K_i$) of approximately 3 nM (Thomas *et al.* 2005). The binding sites were absent in untransfected HEK293 or SKBR3 cells with siRNA-mediated knockdown of GPR30. The authors suggest that the binding was specific, since progesterone, testosterone, and cortisol were unable to compete with $[^3H]$E2. In a second study, Revankar *et al.* used fluorescently labeled E2 (E2-Alexa) to directly

visualize the cellular and subcellular binding properties of GPR30 (Revankar *et al.* 2005). Binding of E2-Alexa was proportional to the GFP signal in GPR30-GFP transfected COS7 cells supporting the hypothesis that expression of GPR30 generates estrogen-binding sites. Competition binding of E2-Alexa with unlabeled E2 revealed a $K_i$ of ≈6 nM. In contrast to most 7TMRs expressed at the plasma membrane, GPR30 expression was observed mainly in the endoplasmic reticulum, with weaker staining also present in the Golgi apparatus and nuclear membrane. To compare the signaling capabilities of ERα and GPR30, Revankar *et al.* evaluated the accumulation of phosphatidylinositol (3,4,5)-trisphosphate (PIP3) using a fluorescent protein-tagged plekstrin homology domain from Akt (PH-FP) in transfected COS7 cells. When cells expressing PH-FP were stimulated with EGF to activate the EGFR at the cell surface, PH-FP accumulated at the plasma membrane. Upon E2 stimulation, cells expressing either ERα-GFP or GPR30-GFP accumulated the PH-FP reporter in the nucleus, which was prevented by the PI3K inhibitor LY294002. The authors state that this novel finding may be explained by the intracellular localization of ERα-GFP in the nucleus or GPR30-GFP in the endoplasmic reticulum, respectively. In line with previous data (Filardo *et al.* 2000), stimulation with the partial ER antagonist 4-hydroxytamoxifen activated PI3K only in GPR30-transfected cells. Moreover, the EGFR inhibitor AG1478 blocked PI3K activation only in GPR30- and not ERα-transfected cells. In addition to PI3K activation, Revankar *et al.* showed that E2 stimulation induced an increase in intracellular calcium levels in COS7 cells transfected with either ERα or GPR30. The GPR30-mediated calcium increase was blocked by the EGFR inhibitor AG1478 and was partly sensitive towards pertussis toxin, but not by the phospholipase C inhibitor U73122. In contrast, the ERα-mediated calcium release was not sensitive to the EGFR inhibitor AG1478 and blocked by U73122 and pertussis toxin. These results demonstrate that E2-induced PI3K activation and calcium release occurred through different pathways, depending on the receptor being utilized (Prossnitz *et al.* 2008).

However, the number of reports that question the function of GPR30 as a transmembrane estrogen receptor is growing (Pedram *et al.* 2006; Otto *et al.* 2008b). Pedram *et al.* found that E2 failed to bind to Gpr30-expressing endothelial cells from ERα/ERβ double knockout mice and did not activate cAMP, ERK, or PI3K (Pedram *et al.* 2006). In contrast to Filardo *et al.*, the production of cAMP or ERK activation could not be demonstrated in SKBR3 cells (GPR30-positive, ER-negative) and nongenomic E2 responses were blocked by ICI in MCF-7 cells (ER-positive, GPR30-positive).

In a recent publication, saturable and specific binding of radioactive E2 was observed only to ERα, but not to GPR30 (Otto *et al.* 2008b). E2 stimulation of GPR30-expressing cells had no impact on intracellular cAMP levels or calcium release (Otto *et al.* 2008b). Whereas radioactive E2 is cell membrane-permeable, the use of Alexa-labeled E2 required the permeabilization of cells with saponin, which might have impact on GPR30 or other unknown proteins that start to bind the E2-Alexa conjugate under these conditions (Otto *et al.* 2008b). Of note, saturable and specific binding of E2-Alexa to GPR30 has never been analyzed (Otto *et al.* 2008b). Therefore, definitive proof awaits binding studies with purified, detergent-solubilized receptor; a challenging task that has been accomplished only for few GPCRs (Prossnitz *et al.* 2008).

Concerning the E2-induced signaling of GPR30, several issues need to be considered in detail. For instance, long-lasting calcium currents were described after E2 stimulation of COS-7 cells transiently transfected with GPR30 (Revankar *et al.* 2005); a finding typical for agents which severely disturb the integrity of cellular membranes (Otto *et al.* 2008b). Unfortunately, the type and final concentration of vehicle applied in the experiments of Revankar *et al.* remained unclear. In the same line of evidence, appropriate vehicle controls were missing in other studies reporting ERK phosphorylation in response to E2-stimulation (Filardo *et al.* 2000; Filardo *et al.* 2002; Maggiolini *et al.* 2004; Vivacqua *et al.* 2006). Instead, untreated cells were often used as controls and exceedingly high concentrations of E2 up to 1 μM were applied (maximal free E2 plasma levels are 2 nM in cycling women and 0.1 nM in rodents), leading to the analysis of effects that are most likely not receptor-mediated (Otto *et al.* 2008b).

In conclusion, the question if GPR30 represents a novel estrogen receptor remains controversial implicating that GPR30 may still be an orphan receptor. However, despite the lack of convincing experimental evidence, GPR30 was already renamed in most databases to G protein coupled estrogen receptor (GPER) in 2007.

### 1.3.2 Membrane-initiated Estrogen Signaling mediated by ERα and ERβ

On the other hand, substantial evidence was provided that a small fraction of endogenous cellular ERα is targeted to the plasma membrane by a palmitoylation site within the E domain, which facilitates association with caveolin-1 and subsequent membrane localization within caveolae rafts (Razandi *et al.* 2002; Razandi *et al.* 2003a; Pedram *et al.* 2006; Pedram *et al.* 2007). Membrane-bound ERα variants are believed to physically interact with G proteins implicating that classical ERs act similar to GPCRs (Razandi *et*

*al.* 1999; Wyckoff *et al.* 2001; Kumar *et al.* 2007). In transfected Chinese hamster ovary cells, membrane-associated ERα or ERβ co-precipitate with and activate $G_{\alpha s}$ and $G_{\alpha q}$ leading to the generation of cAMP and $IP_3$ (Razandi *et al.* 1999). Moreover, it has been shown in endothelial cells that endogenous membrane-bound ERα associates with the p85α regulatory subunit of PI3K and $G_{\alpha i}$ leading to the activation of endothelial nitric-oxide synthase (eNOS) after E2 stimulation (Simoncini *et al.* 2000; Wyckoff *et al.* 2001). Since ERα and eNOS are organized in a functional signaling module within caveolae of endothelial cells (Chambliss *et al.* 2000), E2 induces the rapid release of nitric oxide (NO) and thereby contributes to cardiovascular protection. NO, synthesized by eNOS, plays multiple roles in the cardiovascular system including the regulation of vascular tone, leukocyte adhesion to the endothelium, inhibition of platelet aggregation, and vascular smooth muscle cell proliferation (Mendelsohn and Karas 2005). In contrast to findings reported in the previous section, Razandi *et al.* found that the transactivation of the EGFR required the expression of classical ERs in breast cancer and endothelial cells (Razandi *et al.* 2003b). Using pull-down experiments with purified recombinant proteins, Kumar *et al.* recently demonstrated that ERα binds directly to $G_{\alpha i}$ and $G_{\beta\gamma}$ via amino acids 251–260 and 271–595 of ERα, respectively (Kumar *et al.* 2007). Of note, E2 caused the release of both $G_{\alpha i}$ and $G_{\beta\gamma}$ without stimulating GTP binding to $G_{\alpha i}$ suggesting that the mechanism of E2-induced activation of G proteins by ERα is independent of guanine nucleotide exchange and therefore differs significantly from GPCR-induced signaling.

In conclusion, there are still controversies in the field concerning the physiological relevance of nongenomic signaling *in vivo* and whether or not these effects are exclusively mediated by classical ERs or if novel receptors such as GPR30 are involved as well (Warner and Gustafsson 2006).

## 1.4 Potential Physiological Functions of GPR30 *in vivo*

Several studies investigated the expression of GPR30 by real-time PCR (Martensson *et al.* 2008), RNase protection assays (Otto *et al.* 2008a), Northern (Owman *et al.* 1996; Carmeci *et al.* 1997; Feng and Gregor 1997), or western blotting (Pedram *et al.* 2006; Wang *et al.* 2007) in various tissues of rodent and human origin. The findings indicate that GPR30 is expressed at low levels in multiple tissues. However, the findings are partially inconsistent and the applied methods do not provide information about the relevant cell types. Therefore, several tissues have been investigated in more detailed

studies with immunohistochemistry as well as *in situ* hybridization (Sakamoto *et al.* 2007; Matsuda *et al.* 2008). Nevertheless, the major drawback of these studies is the lack of critical experiments clearly confirming the specificity of used antibodies and probes. So far no study reported the absence of a signal obtained by immunohistochemistry or western blotting in a Gpr30-deficient mouse model (Martensson *et al.* 2008; Otto *et al.* 2008a; Wang *et al.* 2008a).

Since GPR30 mRNA and protein expression was found to be regulated by gonadotrophic hormones in granulosa and theca cells of hamster ovaries, a possible role of GPR30 for the reproductive system was suggested (Wang *et al.* 2007; Prossnitz *et al.* 2008). Moreover, GPR30 expression was found in primordial follicles of the hamster ovary (Wang *et al.* 2008b). GPR30 mRNA and protein levels decreased from the 13th day of gestation (E13) through the second day of postnatal (P2) life, followed by steady increases from P3 through P6. Exposure to GPR30 small interfering RNA *in vitro* significantly reduced GPR30 mRNA and protein levels in cultured hamster ovaries, attenuated E2-BSA-FITC binding to cultured P6 ovarian cells, and markedly suppressed estrogen-stimulated primordial follicle formation (Wang *et al.* 2008b). Supporting a potential function of GPR30 in the hypothalamic-pituitary-gonadal axis, GPR30 expression colocalized with oxytocin-positive neurons in the rat hypothalamus (Brailoiu *et al.* 2007; Sakamoto *et al.* 2007). Oxytocin is involved in the regulation of reproductive functions and its release is influenced by ovarian steroids (Russell and Leng 1998). However, the GPR30-selective agonist G1 (Bologa *et al.* 2006; Revankar *et al.* 2007) did not stimulate estrogenic effects in the uterus or mammary gland of mice (Otto *et al.* 2008b). Gpr30-deficient mouse models are fertile and exhibit normal reproductive organs as well as reproductive functions (Otto *et al.* 2008a).

Wang *et al.* implicated the function of Gpr30 with estrogen-induced thymic atrophy (Wang *et al.* 2008a), which normally occurs during pregnancy or prolonged estrogen treatment. Thymic atrophy triggered by estrogens might contribute to sexual dimorphism in the immune response, susceptibility to autoimmune disease, and maternal tolerance towards the fetus during pregnancy (Aluvihare *et al.* 2004). Studies with ERα- and ERβ-deficient mice showed that ERα is at least partially responsible for the reduction in thymus size, whereas ERβ is not relevant (Staples *et al.* 1999; Erlandsson *et al.* 2001; Wang *et al.* 2008a). The authors of the study therefore suggested that another receptor may contribute to estrogen-induced thymic atrophy and analyzed Gpr30- as well as ERα-, and ERβ-deficient mice in a side by side comparison. Thymo-

cytes are T cell precursors ultimately derived from bone marrow haematopoietic progenitors cells which develop in the thymus and are classified into a number of distinct maturational stages based on the expression of cell surface markers such as CD4 and CD8 (Petrie *et al.* 1990). The earliest thymocyte stage is the double negative stage (DN, CD4- CD8-) which can be divided into four substages (DN1-4). The next major stage is the double positive stage (DP, CD4+ CD8+). The final stage in maturation is the single positive stage of mature T cells (SP, positive for either CD4 or CD8). CD4 is expressed on T helper cells, regulatory T cells, monocytes, macrophages, and dendritic cells and functions as a co-receptor that assists the T cell receptor (TCR) to interact with class II MHC molecules on the surface of antigen presenting cells. In contrast, CD8 is predominantly expressed on cytotoxic T cells and serves as a co-receptor for the TCR to recognize class I MHC molecules. The maturation of T cells involves several steps of selection to ensure specificity against foreign pathogens and tolerance towards self antigens. The first step (β selection) eliminates thymocytes of the DN3 stage with defective TCRs. Then DP cells are selected which are able to bind MHC molecules during positive selection. Finally, apoptosis becomes induced while negative selection in DP or SP cells with high affinity for self antigens. The findings of Wang *et al.* suggest that ERα exclusively mediates an early developmental blockage of DN thymocytes after E2 treatment, whereas Gpr30 was indispensable for thymocyte apoptosis that preferentially occurs in TCR β-chain$^{-/low}$ DP thymocytes (Wang *et al.* 2008a).

A recent study of Martensson *et al.* reported that female Gpr30-deficient mice had hyperglycemia and impaired glucose tolerance, reduced body growth, increased blood pressure, and reduced serum insulin-like growth factor-I levels (Martensson *et al.* 2008). These metabolic consequences of Gpr30-deficiency were associated with decreased serum insulin levels in ovariectomized females *in vivo*. In addition, Gpr30-deficiency abolished the E2-stimulated increase in insulin release after glucose stimulation from isolated pancreatic islets of both sexes *in vitro*. The results presented by Martensson *et al.* are consistent with earlier observations showing that E2 acts directly on β-cells to trigger insulin release (Nadal *et al.* 1998; Ropero *et al.* 1999). The fact that this E2 response was found to be membrane-dependent and insensitive to the selective estrogen receptor modulator tamoxifen and the ER antagonist ICI 182,780 (Nadal *et al.* 1998; Ropero *et al.* 1999), suggests that membrane receptors are involved.

## 1.5 Research Aims and Objectives

The first major aim of this thesis was to understand the function of Gpr30 *in vivo* in the mouse as a model system. Therefore, a mutant mouse model was analyzed that harbors a LacZ reporter (Gpr30-lacZ) in the Gpr30 locus leading to a partial deletion of the Gpr30 coding sequence. Initial objectives concerning the molecular characterization of Gpr30-lacZ mice were (i) the establishment of genotyping procedure, (ii) the verification of the successful targeting of Gpr30 by Southern blotting, (iii) the backcrossing to the two mouse strains C57BL/6J an 129OlaHsd, and (iv) the quantification of the wildtype and the targeted transcript by real time PCR in various tissues to exclude that the integration of the reporter cassette changes the endogenous Gpr30 promoter activity. Objectives concerning the cell type-specific expression of Gpr30 were (i) the analysis of the tissue distribution of the LacZ reporter using X-gal assays, (ii) the colocalization of LacZ-positive cells along with cell type-specific markers, and (iii) the detection of the endogenous Gpr30 protein by immunohistochemistry. To establish the detection of the Gpr30 protein, antibodies directed against several domains of Gpr30 were tested on transfected cells and sections of homozygous Gpr30-lacZ mice and wildtype controls. Further studies addressed the function of Gpr30 *in vivo* by analyzing the phenotype of Gpr30-lacZ mice potentially caused by Gpr30-deficiency. The objectives were (i) to perform a general necropsy and histopathological examination of sectioned tissues, (ii) to send Gpr30-lacZ mice to the German Mouse Clinic for a comprehensive primary phenotype screen, and (iii) to design and conduct reasonable animal experiments based on the identification of Gpr30-positive cell types and results from the primary screen.

The second major aim of this thesis was to identify proteins that interact with human GPR30 to provide insight into the signaling complex and potential functions of the receptor at the molecular level. The objectives to achieve this aim were (i) to perform a yeast two-hybrid screening with the N- and C-terminal domains of GPR30, (ii) to verify the identified interactions in mammalian cells by an independent approach, e.g. co-immunoprecipitation in transiently transfected cells and cells endogenously expressing both interacting proteins, and (iii) to colocalize GPR30 and the interacting protein(s) by immunocytochemistry.

# 2 MATERIALS AND METHODS

Standard protocols for various techniques in molecular biology were mainly performed according to *Molecular Cloning* (3rd edition, Sambrook & Russel, Cold Spring Harbor Laboratory Press, 2001).

## 2.1 Cloning

Overview tables of all constructs and primers were placed in section 2.8.2 and 2.8.3. Detailed cloning strategies for constructs generated within the scope of this thesis can be found in section 2.1.9 - 2.2.1. Vector cards, complete sequences of all constructs, and sequencing results are provided within the electronic supplement.

### 2.1.1 Bacterial *E. coli* strains

Electrocompetent DH5α (Invitrogen) were used for the propagation of standard vectors and routine subcloning. Chemically competent KC8 (Clontech) were used to amplify prey plasmids based on pACT2 from yeast 2-hybrid screening. The auxotrophic leuB, trpC, and hisB mutations of KC8 can be complemented by transformation with plasmids bearing the wild-type allele of the analogous gene from yeast (LEU2, TRP1, and HIS3). Chemically competent DB3.1 (Invitrogen) or One Shot ccdB Survival Phage-Resistant cells (Invitrogen) were used for maintenance and propagation of Gateway vectors containing the ccdB gene. The strains contain a gyrase mutation (*gyr*A462) that renders them resistant to otherwise lethal CcdB effects. Bacteria were propagated in standard LB medium (QBIOgene) or LB agar (MP Biomedicals) at 37°C unless noted.

### 2.1.2 Polymerase Chain Reaction (PCR)

PCR reactions for cloning approaches were performed with Pfx50 DNA polymerase (Invitrogen), since this enzyme possesses proofreading exonuclease activity. If 3'-A overhangs were necessary (e.g for TOPO cloning) Platinum Taq DNA polymerase (Invitrogen) was used. Analytical PCR reactions were conducted with standard Taq DNA Polymerase (Eppendorf). Standard reactions were performed after an initial denaturation (95°C, 5 min) for 20-35 cycles of denaturation (95°C, 30 sec), annealing (55-65°C, 30 sec), and extension (72 °C, 30-120 sec) followed by a final extension step (72 °C, 5 min).

### 2.1.3 Agarose Gel Electrophoresis

DNA molecules were separated by gel electrophoresis in gels containing 1-3% agarose. Standard electrophoresis grade agarose (Invitrogen) was used for analytical gels. If gel extraction of the DNA fragment was required for cloning purposes, gels were prepared with SeaKem GTC agarose (Cambrex). The electrophoresis was performed in a custom system (Bächler Feintech) at 50 V for 20-40 min. The buffer system was TBE (45 mM Tris-borate, 1 mM EDTA, pH 8.3) in case of analytical gels and TAE (40 mM Tris-acetate, 1 mM EDTA, pH 8.0) for cloning approaches. Ethidium bromide (50 µg/l) was included in the buffer and gel to visualize DNA bands by UV light (Syngene).

### 2.1.4 Plasmid Isolation

For small scale plasmid isolations (max 10 µg), 5 ml LB medium including antibiotics was inoculated with one colony and cultured overnight at 37 °C while shaking (225 rpm). Cells grown in 2 ml overnight culture were pelleted and plasmids were isolated using the QIAprep Spin Miniprep Kit (QIAGEN) according to the manufacturer's protocol and eluted in 30 µl $H_2O$. If larger amounts (max 500 µg) of plasmid DNA were desired, 100-200 µl of the overnight cultures were used to inoculate 50 ml LB medium. On the next day, plasmids were isolated with the QIAGEN Plasmid Maxi Kit (QIAGEN) according to the instruction manual.

### 2.1.5 PCR Purification and Gelextraction

PCR products were purified by QIAquick PCR Purification Kit (QIAGEN) and eluted in 30 µl $dH_2O$. Restricted DNA fragments were separated from linearized vectors by gel electrophoresis, cut from the gel, extracted using the QIAquick Gel Extraction Kit (QIAGEN), and eluted in 30 µl $dH_2O$. PCR products containing attB-sites for Gateway cloning were generally purified by PEG purification. For PEG purification, 150 µl TE buffer (pH 8.0) was added to a 50 µl PCR reaction. Then 100 µl of 30% PEG containing 30 mM $MgCl_2$ was added, vortexed, and centrifuged immediately at 10,000 x g for 15 min at room temperature. The pellet was dissolved in 30-50 µl TE buffer (pH 8.0).

### 2.1.6 Ligation

DNA inserts and linearized vectors were ligated by T4 DNA ligase (Invitrogen) according to the manufacturer's protocol. Ligations were incubated overnight at 16 °C and diluted 5-fold in TE buffer (10 mM Tris, 1 mM EDTA, pH 7.5) before transformation.

### 2.1.7 Transformation of Electro- and Chemically Competent Bacteria

Electrocompetent DH5α cells (40 µl) were thawed on ice and mixed with 1 µl plasmid DNA (50 pg) or diluted ligation reaction (1-10 ng). The reaction was transferred into a pre-chilled 0.1 cm electroporation cuvette (Bio Rad) and pulsed in an electroporator (Bio Rad). The cells were resuspended in 1 ml SOC medium, incubated at 37 °C for 1 h while shaking, and plated onto selection agar plates. For transformation of chemically competent cells, 50 µl cell suspension was mixed with 1 µl plasmid DNA (50 pg) or diluted ligation reaction (1-10 ng). The reaction was chilled on ice for 30 min, heat-shocked for 45 sec at 42 °C in a water bath, and placed on ice for additional 2 min. Subsequently, 0.9 ml SOC medium was added. Cells were regenerated at 37 °C for 1 h while shaking and plated onto selection agar plates.

### 2.1.8 Gateway Cloning

The construction strategy of several constructs was based on Gateway cloning technology, which utilizes the site-specific recombination properties of the bacteriophage lambda (Snyder *et al.* 1989) and provides a rapid and efficient way to move the gene of interest into multiple vector systems. Gateway cloning technology constitutes two essential recombinant reactions (i.e. BP and LR reaction) that are directed with so-called att-sites. BP reactions were performed with attB-site containing PCR products (or attB-site containing Gateway expression vectors) and the attP-site containing donor vector pDONR221 (Invitrogen) to generate "entry" clones designated as pENTR221 constructs. BP reactions were performed in 10 µl scale including 6 µl TE buffer (10 mM Tris, 1 mM EDTA, pH 8.0), 1 µl attB PCR product (50-100 ng, 50 fmol), 1 µl donor vector (150 ng, 50 fmol), and 2 µl BP Clonase™ II enzyme mix (Invitrogen) for 1-5 h at room temperature. Reactions were stopped by adding 1 µl proteinase K solution and incubation at 37 °C for 10 min. During the reaction the attB site of the PCR product recombines with the attP-sites of the vector replacing an insert containing a ccdB gene and a chloramphenicol resistance marker. To select for positive clones, 1 µl of the BP reaction was transformed in 40 µl electro-competent DH5α cells, which are ccdB sensitive, and plated on LB agar plates (50 µg/ml kanamycin). Plasmids of positive clones were isolated and controlled by BsrG1 (Bsp1407I, Fermentas) digestion. Through LR recombination reactions, target sequences were transferred from the entry clone containing attL-sites into destination vectors (pDEST) containing attR-sites to generate mammalian expression clones (pEXP) containing attB-sites. The destination

vectors included N- or C-terminal sequences encoding various tags leading to the expression of fusion protein in mammalian cells. Several vectors (i.e. pDEST474, pDEST475, pDEST515, pDEST701) were a gift from Dominic Esposito (NCI-Frederick Vector Engineering Group, USA); others were from Invitrogen (i.e. pDEST26) or constructed according to section 2.1.9. LR reactions were performed using LR Clonase™ II enzyme mix (Invitrogen) in 10 µl total volume with 50-150 ng (50 fmol) entry vector and 150 ng (50 fmol) destination vector for 1-5 h at room temperature. Reactions were stopped by adding 1 µl proteinase K solution and incubation at 37 °C for 10 min. LR reactions (1 µl) were transformed into 40 µl of electro-competent DH5α cells; positive clones were selected on LB agar plates containing 100 µg/ml ampicillin. Plasmids were isolated from resistant colonies, controlled by BsrG1 digestion, and sequenced.

### 2.1.9 Construction of Gateway Compatible Vectors

Gateway compatible vectors based on pcDNA3 containing N- or C-terminal CFP tags (i.e. pcDNA3-NCFP, pcDNA3-CFP) (Schaefer *et al.* 2001) as well as vectors containing N- or C-terminal YFP tags (i.e. pcDNA3-NYFP, pcDNA3-YFP) (Voigt *et al.* 2005) were kindly provided by Prof. Dr. Michael Schaefer (Department of Molecular Pharmacology and Cell Biology, Charite – Universitätsmedizin, Berlin). These vectors were converted into Gateway destination vectors by subcloning Gateway cassettes containing attR recombination sites flanking a *ccd*B gene and a chloramphenicol-resistance gene into the multiple cloning sites of FRET vectors using the Gateway vector conversion system (Invitrogen). To convert pcDNA3-NCFP and pcDNA3-NYFP into destination vectors (i.e. pcDNA3NCFP-DEST, pcDNA3NYFP-DEST), they were cut using EcoRV, dephosphorylated with calf intestinal alkaline phosphatase (Invitrogen), and blunt-end ligated with the RfC.1 cassette using T4 DNA ligase (Invitrogen) according the instruction manual. The ligation reactions were diluted 5-fold in TE buffer (10 mM Tris, 1 mM EDTA, pH 8.0) and transformed into chemically competent One shot ccdB Survival™ Phage-Resistant cells. For the construction of destination vectors containing C-terminal tags (i.e. pcDNA3CFP-DEST, pcDNA3YFP-DEST) the same strategy was applied except that the cassette RfB was subcloned to account for the reading frame. Transformed bacteria were plated onto selection agar plates containing 30 µg/ml chloramphenicol. The integration of the cassette was controlled by BsrGI digestion, the correct orientation was determined by sequencing using the CMV forward primer (P1).

### 2.1.10 GPR30 Constructs

Two OmicsLink™ clones encoding GPR30 with C-terminal His-tag (EX-M0792-M01) or GFP-tag (EX-M0792-M03) were obtained from the German Resource Center for Genome Research (RZPD). The constructs are based on the vectors pReceiver-M01 or pReceiver-M02, respectively. Sequencing of the constructs revealed a frame shift mutation in the His-tagged clone and several point mutations in the GFP-tagged one. However, no mutations were found in the sequences encoding the N- or C-terminal domain in EX-M0792-M03. Therefore, the clone was used to construct bait vectors for yeast 2-hybrid screening (see 2.2.1). Furthermore, a construct encoding GPR30 tagged with EGFP based on pcDNA3 (i.e. pcDNA3-GPR30-EGFP) was kindly provided by Prof. Eric Prosnitz (University of New Mexico, Albuquerque, USA).

The pcDNA3-GPR30-EGFP construct was used as a template to amplify GPR30 by PCR and to subclone the product into pcDNA3.1(+) for native expression without tag. The forward primer P13 included a HindIII site and the reverse primer P14 included a NotI site, respectively. In addition, the reverse primer had a two bps mismatch to introduce a stop codon. The PCR was performed using Pfx50 DNA polymerase (55 °C annealing temperature, see 2.1.2). The 1185 bps product was purified (QIAquick PCR Purification), cut using HindIII and NotI according to the instruction manual, again cleaned by gel extraction, and finally ligated with linearized pcDNA3(+) using T4 DNA ligase at 16 °C overnight. Electrocompetent DH5α were transformed with the ligation reaction and plated onto selection agar plates containing 100 µg/ml ampicillin. Plasmids were isolated from positive clones and controlled by restriction endonuclease digestion and sequencing.

To shuttle GPR30 into Gateway compatible FRET vectors with C-terminal tags, the entry clone pENTR221-GPR30-C was generated by recombining an attB PCR product (1187 bps) with pDONR221 in a BP reaction. The PCR reaction (Pfx50 DNA polymerase, 55 °C annealing temperature, see 2.1.2) was performed using primers P279 and P280 and pcDNA3-GPR30-EGFP as template. The GPR30 insert was shuttled by LR recombinations into destination vectors pcDNA3CFP-DEST and pcDNA3YFP-DEST to create the expression constructs pcDNA3CFP-EXP-GPR30 and pcDNA3YFP-EXP-GPR30. All constructs have been controlled by BsrGI digestion and partial sequencing using the CMV forward primer (P1).

### 2.1.11 FUNDC2 Constructs

The Gateway expression clone pdEYFPEXP-FUNDC2 was obtained from the German Resource Center for Genome Research (RZPD, IOH40818-pdEYFP-C1amp). The construct generates a fusion protein of FUNDC2 N-terminally tagged with EYFP if transfected in mammalian cells. This construct was used to generate an entry clone for N-terminal fusions by performing a BP reaction with pDONR221. Prior to the BP reaction, pdEYFPEXP-FUNDC2 was linearized by HindIII restriction endonuclease digestion. The digestion was performed in a 25 µl scale containing 4 µg plasmid DNA and 40 units HindIII (New England Biolabs) for 1 h at 37 °C according to the manufacturer's instructions. The linearized vector was gel purified and eluted in 25 µl $dH_2O$. The BP reaction was performed according to section 2.1.8 and transformed into electrocompetent DH5α as well as in chemically competent DB3.1 cells (1 µl per transformation). Plating of transformed DH5α cells on selection agar plates containing kanamycin (50 µg/ml) enabled the selection of entry clones pENTR221-FUNDC2-N; plating of transformed DB3.1 on selection agar plates containing chloramphenicol (30 µg/ml) enabled the selection of clones containing the Gateway destination vector pdEYFP-C1amp (referred to as pdEYFP-DEST in the following). Both constructs were controlled by BsrGI digestion and pENTR221-FUNDC2-N has been sequenced using M13 forward (P2) and reverse primers (P3).

The entry clone pENTR221-FUNDC2-N was then used in LR reactions to shuttle FUNDC2 into destination vectors pDEST26, pDEST475, pDEST515, pDEST701, pcDNA3NCFP, and pcDNA3NYFP. The LR reactions were performed according to section 2.1.8, transformed into electrocompetent DH5α and plated onto selection agar plates (100 µg/ml ampicillin). The resulting expression clones generate N-terminal fusion proteins of FUNDC2 tagged with His (pEXP26-FUNDC2), Myc (pEXP475-FUNDC2), HA (pEXP515-FUNDC2), Flag (pEXP701-FUNDC2), CFP (pcDNA3CFP-EXP-FUNDC2), or YFP (pcDNA3YFP-EXP-FUNDC2). All constructs have been controlled by BsrGI digestion and partial sequencing using primer P1.

To tag FUNDC2 at the C-terminus, the entry clone pENTR221-FUNDC2-C was generated by a BP recombination of an attB-site containing PCR product and the donor vector pDONR221 (Invitrogen). The PCR was performed using primer P300 and P301 (Pfx50 DNA polymerase, 55 °C annealing temperature, see 2.1.2). The product was purified (PEG purification, see 2.1.5) and controlled by gel electrophoresis.

The FUNDC2 sequence was finally shuttled by LR recombinations into destination vectors pDEST474, pcDNA3CFP-DEST, and pcDNA3YFP-DEST.

## 2.2 Yeast Two-Hybrid Screening

To identify proteins interacting with GPR30, the N- and C-terminal domains were subcloned into the EcoRI/BamHI site of the bait vector pBTM116. The vector has a polylinker downstream of a LexA coding sequence driven by an ADH1 promoter (Bartel and Fields 1995). Thus, activation of the promoter in yeast leads to the expression of a LexA protein fused N-terminally to the subcloned fragment. LexA consists of a C-terminal dimerization domain and an N-terminal DNA binding domain that specifically recognizes palindromic sequences containing the CTGTNNNN consensus half-site. In addition, the vector carries the TRP1 gene that encodes an enzyme essential for tryptophan biosynthesis and enables yeast auxotrophs to grow in the absence of tryptophan.

A human heart cDNA library (Clontech #638815) subcloned in the XhoI restriction site of the pACT2 prey vector was co-transformed to screen for interacting proteins. The vector has a polylinker downstream of the GAL4 activation domain (amino acids 768–881) fused to an HA epitope tag. The prey vector generates a fusion protein of the GAL4 activation domain, an HA epitope tag, and a protein encoded by a library cDNA cloned into the polylinker in the correct orientation and reading frame. The vector also contains the LEU2 gene that allows yeast auxotrophs to grow in the absence of leucine.

Interaction of bait and prey proteins leads to the formation of an active transcription factor that induces the expression of the two reporter genes HIS3 and lacZ in LV40 yeasts. Both reporter genes are driven by minimal GAL1 promoters fused to multimerized LexA binding sites. Therefore, yeast expressing LexA activators can be detected as histidine prototrophs or by β-galactosidase activity.

Bait plasmids and library were sequentially introduced into the host *S. cerevisiae* L40 yeast strain to improve the efficiency of transformation. Yeasts were initially transformed with the bait plasmid in a small-scale procedure (see 2.2.3), and then library screens (see 2.2.4) were performed using a large-scale transformation procedure (Fields and Song 1989). Reagents and methods for yeast two-hybrid analyses were mainly adapted from the Yeast Protocols Handbook (PT3024-1, Clontech).

### 2.2.1 Construction of Yeast Two-Hybrid Bait Vectors

To generate a yeast bait encoding the N-terminal domain (pBTM116-Nterm) a sequence encoding amino acids 1-54 of the human GPR30 (MDVTSQARGVGLE-MYPGTAQPAAPNTTSPELNLSHPLLGTALANGTGELSEHQQ) was amplified by PCR (Eppendorf; 25 Cycles; 55 °C, 187 bps) using the OmicsLink™ clone EX-M0792-M03 (RZPD) as template. The forward primer P109 included an EcoRI site; the reverse primer P110 was flanked by BamHI. The PCR product was purified (PCR Purification Kit, QIAGEN) and controlled by gel electrophoresis. The PCR product as well as the empty pBTM116 vector (Bartel and Fields 1995) were digested using EcoRI/BamHI restriction enzymes, purified, ligated, and transformed into electrocompetent DH5α cells. Plasmids were isolated and sequenced using the sequencing primer P4 and P5. To construct a yeast bait encoding the C-terminal domain (i.e. pBTM116-Cterm) the sequence encoding amino acids 330-375 (TFRDKLRLYIEQKTNLPALNRFCHAAL-KAVIPDSTEQSDVRFSSAV) was amplified from pcDNA3-GPR30-GFP (PCR product 187 bps) and subcloned downstream of the LexA into the polylinker of pBTM116 using the same strategy described before. The forward primer P111 included an EcoRI site; the reverse primer P112 was flanked by BamHI, respectively.

### 2.2.2 Library Amplification

The human heart cDNA library (Clontech #638815) was amplified to gain enough plasmids for large-scale yeast transformations. According to the manufacturer the library contains $3.6x10^6$ independent clones with a size of 0.6-3 kb. To guarantee the complete amplification of the whole library, approximately twice as much transformed clones as the estimated number of individual clones in the library were plated. Electro-competent DH5α (40 µl) were transformed with 1 µg library DNA. A dilution series ($10^{-2}$-$10^{-6}$) was plated to estimate the library titer (number of colony forming units per ml of bacterial suspension). The whole remaining transformation reaction was spread onto 40 large plates (15 cm diameter) and incubated at 37 °C overnight. On the next day the number of colony forming units per ml was calculated. All colonies were scraped of the plates and resuspended in 2.5 l LB medium including ampicillin (50µg/ml). The cell suspension was incubated with shaking for 2 h at 37 °C, bacteria were pelleted, and large-scale plasmid isolation was performed (QIAGEN Maxiprep Kit).

### 2.2.3 Small-Scale Transformation

To prepare competent yeast for a small scale transformation, a single yeast colony (max 2 weeks old) was inoculated in 20 ml YPDA medium (20.0 g/l Difco Peptone; 10.0 g/l Yeast Extract; 20 g/l glucose; 15 ml/l 0.2% adenine hemisulfate stock; 50 mg/l ampicillin; 50 mg/l tetracycline) at 30 °C overnight. On the next day, 10 ml of the overnight culture was transferred to 150 ml YPDA medium ($OD_{600}$ = 0.2-0.3) and cultured until $OD_{600}$ = 0.5-0.6 (3-6 h). Cells were pelleted, washed once with sterile $H_20$ and resuspended in 1.5 ml of sterile TE/LiAc (100 mM LiAc, 10 mM Tris-HCL, 1 mM EDTA, pH 8.0) and stored on ice. 50 µl competent yeast cells were mixed with 0.5 µg plasmid DNA, 50 µg denatured YEASTMAKER carrier DNA (Clontech), and 300 µl PEG/TE/LiAc (40% polyethylene glycol, 100 mM LiAc, 10 mM Tris-HCL, 1 mM EDTA, pH 8.0) and incubated at 30 °C for 30 min while shaking. Heat-shock transformation was performed at 42 °C for 15 min after adding 35 µl DMSO and chilled on ice. Cells were pelleted, resuspended in 100 µl $H_20$, and spread onto selection agar plates (6.7 g/l Yeast Nitrogen Base; 100 ml/l 10X amino acids (1200 mg/l L-adenine hemisulfate, 200 mg/l L-arginine HCL, 200 mg/l L-histidine HCL monohydrate, 300 mg/l L-isoleucine, 1000 mg/l L-leucine, 300 mg/l L-lysine HCL, 200 mg/l L-methionine, 500 mg/l L-phenylalanine, 2000 mg/l L-threonine, 200 mg/l L-tryptophane, 300 mg/l L-tyrosine, 200 mg/l uracil, 1500 mg/l L-valine); 20 g/l glucose; 50 mg/l ampicillin; 50 mg/l tetracycline; 20-100 ml 1M aminotriazole stock (THULL only), 20 g/l agar). Colonies appeared after 2-3 days culture at 30 °C.

### 2.2.4 Library Screening

For the library screening, 20 ml selection medium without tryptophan (-T medium, see 2.2.3) was inoculated with one single colony of the bait transformants and cultured at 30 °C overnight. The culture was then transferred to 200 ml -T medium and grown at 30 °C overnight to obtain a saturated cell suspension ($OD_{600}$ > 1). Approximately 50 ml of this culture was added to 800 ml YPD medium ($OD_{600}$ = 0.15-0.2) and grown until OD = 0.5 (3-6 h). The cells were used to prepare 20 ml of competent yeast cells as described above. Competent cells were split in two Erlenmeyer flasks (one for the library screen, the other for the autoactivator screen) and incubated at room temperature for 10 min. 250 µg library DNA (library screen) or empty pACTII vector (autoactivator screen), 5 mg denatured carrier DNA, and 70 ml PEG/TE/LiAc was added to competent yeast and incubated at 30 °C for 30 min with shaking (100 rpm). The heat-shock trans-

formation was performed after adding 8.8 ml DMSO at 42 °C for 15 min in a water bath (swirl occasionally). Co-transformed yeast cells were pelleted and resuspended in 1 liter YPD and incubated at 30 °C for 1 h. Cells were pelleted, resuspended in selection medium lacking tryptophan and leucine and further incubated at 30 °C for 8 h. Finally, cells were resuspended in 10 ml water and 200 µl of a dilution series was plated onto 50 selection agar plates without tryptophan, leucine and histidine in the presence of 80 mM 3-aminotriazole (-THULL medium, see 2.2.3) and incubated at 30 °C. Double transformants that express interacting proteins rendered colonies within 8-10 days, which were re-plated onto fresh selection agar plates for further analysis. Positive colonies were resuspended in YPD medium with 25% glycerol and stored at -70 °C.

### 2.2.5 Verification of the Interactions in Yeast

Interaction between bait and preys was confirmed by re-transfection of bait and prey plasmids back into yeast and LacZ activity filter assays. For LacZ activity filter assays, colonies from selection plates (without tryptophan and leucine) were replica-transferred onto a Whatman Nr.1 filter. The replica filter was submerged in liquid nitrogen to permeabilize cells, and then allowed to thaw. The filter was placed (colonies facing up) onto another filter presoaked in Z buffer/X-gal solution (60 mM $Na_2HPO_4$, 40 mM $NaH_2PO_4$, 10 mM KCl, 1 mM $MgSO_4$, pH 7.0, 0.27% β-mercaptoethanol and 0.334 g/l X-gal) and incubated at 30 °C. Colonies expressing β-galactosidase appeared blue within 1-12 h. For yeast re-transformation, library plasmids encoding interacting proteins were isolated from individual positive colonies. To remove the bait plasmid from double transformed yeast, colonies were inoculated in 3 ml medium lacking leucine and cultured at 30 °C for 1 day. Growth in the absence of tryptophan selection allows survival of yeast segregants without bait plasmid, which is randomly lost. The cells were pelleted, lysed in 200 µl of lysis buffer (2% Triton X-100, 1% SDS, 100 mM NaCl, 1 mM EDTA, 10 mM Tris, pH 8.0), and disrupted in the presence of 200 µl phenol/chloroform/isoamyl alcohol (25:24:1) and 0.3 g of acid-washed glass beads by vortexing for 2 min. The suspension was clarified by centrifugation and plasmids were recovered from the supernatant by standard ethanol precipitation. The DNA pellet was resuspended in 20 µl $H_2O$. The library plasmids were amplified in KC8 cells, which are leucine auxotroph due to a leuB mutation. Chemically competent KC8 (100 µl) were heat-shock transformed using 10 µl prey plasmid and spread onto M9 minimal medium agar plates (200 ml/l 5X M9 salts (43.0 g/l $Na_2HPO_4$ dihydrate, 15.0 g/l $KH_2PO_4$, 2.5 g/l

NaCl, 5.0 g/l $NH_4Cl$), 100 ml/l 10X amino acids without leucine (–L, see 2.2.3); 20 g/l glucose; 50 mg/l ampicillin; 50 mg/l kanamycin; 1 mM thiamine; 2 mM $MgSO_4$; 100 µM $CaCl_2$). Transformed clones can be selected by complementation with the yeast LEU2 gene from the pACT2 library plasmid. Bait and prey plasmids were re-transformed into yeast according to the small-scale transformation protocol described previously (see 2.2.3). True positive interacting clones grew again on selective agar plates without tryptophan, leucine and histidine and were positive in LacZ activity filter assays. Verified prey plasmids were sequenced using primers P31 and P32.

## 2.3 Mammalian Cell Culture and Immunocytochemistry

### 2.3.1 Cell Lines

Cell lines HeLa, T47D, and SKBR3 were cultured in Dulbecco's Modified Eagle Medium (DMEM) containing 10% FBS including antibiotics (penicillin/streptomycin, Biochrom) in a humidified incubator with 5% $CO_2$ at 37 °C.

### 2.3.2 Transfections

Mammalian cell lines were either transfected with FuGENE 6 reagent (Roche Applied Science) or Polyethylenimin (PEI, 50% solution in $H_2O$, Sigma-Aldrich Cat# 18,197-8). For transfection with FuGENE 6 reagent, the cells were seeded 24 h prior transfection at a density of 10,000-20,000 cells/$cm^2$. For transfections in 10 cm plates (55 $cm^2$ surface area, 10 ml medium), 18 µl Fugene 6 reagent was diluted in 582 µl serum free medium (OptiMEM, Gibco) and incubated 5 min at room temperature. Then 6 µg plasmid DNA (≈1 µg/µl) was added, vortexed for a second, and incubated for at least 15 min at room temperature. Finally the transfection complex was added to the cell culture vessel in a drop wise manner while swirling. In case of chamber slides (0.69 $cm^2$, 400 µl medium), 0.6 µl Fugene 6 reagent was diluted in 10 µl serum free medium and 0.1 µg DNA was added. The expression of transfected constructs was assayed 24-48 h later. Since large quantities of transfected cells were need for co-immunoprecipitations, PEI transfections were performed in 15 cm plates. About $7x10^6$ were seeded per 15 cm plate and grown over night. Before starting the transfection, the standard medium was replaced with 20 ml DMEM containing 2% FBS. Then 1235 µl serum-free OptiMEM were mixed with 65 µl PEI (1mg/ml, pH 7.0) and 26 µg DNA (DNA conc. of 0.5-2 µg/µl) and incubated for 10 min at room temperature. The transfection mixture was added in a drop wise manner while swirling. The expression of transfected constructs was assayed 24 h later.

### 2.3.3 Immunocytochemistry

The cells were cultured and transfected in chamber slides (BD Biosciences) or 24 well plates and fixed with 4% paraformaldyde in PBS (Riedel-de Haen) for 10 min at room temperature. The fixed cells were rinsed twice for 2 min in washing buffer (PBS, 0.05% Tween 20, pH 7.2) and incubated in serum blocking (2% serum, 1% BSA, 0.1% fish skin gelatin, 0.1% Triton X-100, 0.05% Tween 20) for 30 min at room temperature or overnight at 4 °C. The used serum was derived from the same species as the secondary antibody (normally goat). The fixed cells were incubated with the primary antibody diluted in PBS with 1% BSA (100 µl per chamber) for 1 hour at room temperature or overnight at 4 °C. The cells were rinsed several times in washing buffer and then incubated with the secondary antibody (Alexa Fluor 568- or Alexa Fluor 488 conjugated, Molecular Probes) diluted 1:500 in PBS for 30 min at room temperature. Cell nuclei were counterstained with DAPI (0.2 ng/µl). Slides were coversliped with aqueous Antifade fluorescent mounting medium (Vector Labs) or Flouromount-G (Southern Biotech) and sealed with nail polish.

## 2.4 Western Blotting and Co-immunoprecipitation

Information regarding the used antibodies is provided in the materials section 2.8.1.

### 2.4.1 Standard SDS-PAGE Protocol

For SDS-PAGE, the samples were mixed with 4x SDS loading buffer (300 mM Tris pH 6.8, 12% SDS, 0.6% bromphenol blue, 60% glycerol, 12% fresh β-mercaptoethanol), denatured by cooking or at 37 °C for 20 min (GPR30 only), loaded onto a polyacrylamide gel composed of a 4% stacking gel and a 10-15% separating gel, and separated by gel electrophoresis (BioRad) in Laemmli buffer (25 mM Tris, 192 mM glycine, 0.1% SDS, pH 8.3) at 90 V until the sample focussed in the stacking gel and then at 120 V until the dye runs off the gel. The separated proteins were transferred onto a PVDF membrane (Hybond-P, Amersham) using a semi dry blotter (Bio Rad). PVDF membranes were equilibrated in methanol for 30 sec. The gel, the PVDF membrane, and extra thick Whatmann 3MM papers were pre-soaked in Towbin buffer (25 mM Tris, 192 mM glycine, 200 ml/l methanol) for 20 min prior to use. The transfer was conducted with 100 mA per gel for 1 h at room temperature. The membrane was blocked in TBST (125 mM Tris-HCl, 625 mM NaCl, 0.05% Tween 20, pH 8.0) containing 5% low fat milk powder for 1h and incubated with the primary antibody dissolved

in blocking buffer for 1 h at room temperature or at 4 °C over night while shaking. The membrane was washed 6x in TBST for 5 min and incubated with the secondary antibody diluted in TBST (sheep anti-mouse peroxidase conjugated, Amersham, 1:7500; goat anti rabbit peroxidase conjugated, Calbiochem, 1:7500) for 1 h at room temperature. The immune complexes were detected with an ECL detection system according to the manufacturer's protocol (Amersham).

### 2.4.2 Western Blotting to Detect GPR30 in HeLa Cell Lysates

Total cell lysates were prepared from cells grown in 10 cm plates. Cells were lysed 48 h after transfection in 450 µl lysis buffer (100 mM Tris-HCl pH 8.0, 2% SDS, 3.2 M Urea) supplemented with 64 mM DTT, 0.5 mM phenylmethylsulphonyl fluoride, and 1X complete protease inhibitor mixture (Roche). After 5 min incubation on ice, cells lysates were sonicated for 20 sec (4x for 5 sec) on ice and mixed with 4x SDS loading buffer. Finally, the cell lysates were denatured at 37 °C for 20 min and separated by SDS-PAGE in a 10% polyacrylamid gel (see 2.4.1). The blocked membrane was incubated with the rabbit anti-GPR30 3$^{rd}$ extracellular domain antibody diluted 1:500 at 4 °C overnight.

### 2.4.3 Western Blotting to Detect Mouse Gpr30 in Tissue Lysates

Three different approaches were tested to detect murine Gpr30 by western blotting. Initially, a modified protocol already established to detect human GPR30 in transfected HeLa cells was used (see 2.4.2). Briefly, hippocampus and stomach tissue of wildtype as well as Gpr30-lacZ mice was homogenized in liquid nitrogen. Pulverized tissue (50 mg) was placed in an a cooled dounce homogenizer (Wheaton, 7 ml, tight grinder) and 1 ml ice cold lysis buffer (100 mM Tris-HCl pH 8.0, 2% SDS, 3.2 M Urea, 64 mM DTT, 0.5 mM phenylmethylsulphonyl fluoride, 1X complete protease inhibitor mixture (Roche)) was added. The lysate was grinded 15x to disrupt the cells and processed as described previously (see 2.4.1) using primary antibodies directed against the 3$^{rd}$ extracellular domain (1:500) and C-terminal antiserum (1:1000) of human GPR30.

In a second trial, brain vessel were carefully removed from the brain surface of wildtype and Gpr30-lacZ mice (n=3) and stored in ice cold PBS. The vessels were collected by centrifugation, frozen in liquid nitrogen, and transferred into the dounce homogenizer. The tissue was disrupted by grinding in 1 ml lysis buffer (15 mM Tris-HCl pH 7.5, 8.7% glycerol, 1% SDS, 8 M urea, 0.0004% bromphenol blue, 143 mM β-mercapto-

ethanol) and analyzed by SDS-PAGE (see 2.4.1) with antibodies directed against the 3rd extracellular and C-terminal domain of human GPR30.

In a final third trial, a commercial kit specifically designed for the extraction of membrane proteins was used (ProteoExtract Transmembrane Protein Extraction Kit, Calbiochem). Pulverized tissue of the hippocampus and stomach (50 mg) was placed in an a cooled dounce homogenizer (Wheaton, 7 ml, tight grinder) and disrupted in 1 ml extraction buffer 1 including 10 µl proteinase inhibitor mix with 15 strokes. The extraction was performed according to the manufacturer's instructions with Extraction buffer 2B. The lysate was analyzed by SDS-PAGE with antibodies against the 1st extracellular (1:500), 3rd extracellular (1:500), and C-terminal domain (1:1000) of GPR30.

### 2.4.4 Co-immunoprecipitation of GPR30 and FUNDC2

The day before transfection, 2.5 x $10^6$ HEK293 cells were seeded per 10 cm dish. The cells were transfected with HA-GPR30 (pTL1-HA2/GPR30), Myc-FUNDC2 (pEXP701-FUNDC2), GFP, or mock vector (empty pcDNA3.1+) using the PEI transfection procedure with 10 µg plasmid DNA in total (see 2.3.2). To harvest the cells 48 h after transfection, the cells were washed twice with PBS and scraped off the dish with a cell scraper (Nalge Nunc International) in 5 ml PBS on ice. The cells were collected in 15 ml Falcon tubes by centrifugation (500 g for 5 min) and stored at -80°C. The cells were lysed in 500 µl RIPA buffer (50 mM Tris pH 7.5, 150 mM NaCl, 1% NP-40, 0.1% SDS, 1 mM EDTA, 1 mM EGTA) freshly supplemented with 0.5% sodium deoxycholate and 1x protease inhibitors (β-glycerophosphate, aprotinine, leupetine, NaF, Pefabloc). The tube was rotated for 1 h at 4 °C and then centrifuged at 8000g for 10 min. The supernatant was transferred into a new tube; 40 µl aliquots were stored for total lysate (input) western blots. The remaining 440 µl supernatant was incubated with 2 µg of primary antibody (mouse monoclonal anti-Myc, Santa Cruz) for 4 h at 4 °C on a roller shaker, centrifuged at 16000 g for 10 min, and transferred into a new tube. In parallel, 50 µl protein G-sepharose bead slurry was prepared by mixing 25 µl protein G-sepharose beads (GE Healthcare, solution in 20% ethanol) wit 25 µl lysis buffer. The beads were washed with lysis buffer (3x 1 ml lysis buffer, 1000 rpm for 1 min), added to the lysate, and incubated at 4 °C over night. Subsequently, the beads were washed with lysis buffer (3x 1 ml, 1000 rpm for 1 min), resuspended in 40 µl 4x SDS loading buffer, and denatured at 37 °C for 10 min. Finally, the beads were removed and the supernatant was analyzed by SDS-PAGE (see 2.4.1).

### 2.4.5 Co-immunoprecipitation of YFP-FUNDC2 and Myc-FUNDC2

About $7x10^6$ HeLa cells were seeded in 15 cm cell culture dishes and grown over night. The cells were transfected with YFP-FUNDC2 (pdEYFP-EXP-FUNDC2), Myc-FUNDC2 (pEXP701-FUNDC2) or both constructs using the PEI transfection procedure (see 2.3.2). Prior to lysis, the cells were washed twice with PBS and scraped off the dish with a cell scraper (Nalge Nunc International) in 5 ml PBS on ice. The cells were collected in 15 ml Falcon tubes by centrifugation at 500 g for 5 min, resuspended in 1 ml lysis buffer (50 mM Tris, 100 mM NaCl, 5 mM $MgCl_2$, 0.1% NP-40, 1X complete protease inhibitor mixture (Roche Applied Science), pH 7.5) and lysed by passing the cell suspension through a 27 gouge syringe (7x) followed by a 30 gouge syringe (7x). Subsequently the lysates were cleared by centrifugation (2 x 16.000 g for 10 min). The supernatant was incubated with 3 µg primary antibody (mouse monoclonal anti-GFP (Roche Applied Science) or rabbit polyclonal anti-Myc (Sigma)) for 3 h at 4 °C on a roller shaker, centrifuged at 16000 g for 10 min and transferred into a new tube. In parallel, 100 µl protein G-sepharose bead slurry was prepared by mixing 50 µl protein G-sepharose beads (GE Healthcare, solution in 20% ethanol) wit 50 µl lysis buffer. The beads were washed with lysis buffer (5x 1 ml lysis buffer, 1000 rpm for 1 min), added to the lysate, and incubated at 4 °C over night. Subsequently, the beads were washed with lysis buffer (3x, 1000 rpm for 1 min) and resuspended in 30 µl 4x SDS loading buffer. The samples were boiled for 5 min, the beads were removed by centrifugation (1000 g, 1 min), and the supernatant was analyzed by SDS-PAGE (see 2.4.1).

## 2.5 Histology

Information concerning the used antibodies is provided in the materials section 2.8.1.

### 2.5.1 Frozen Sections

Tissues were fixed in fixative (PBS pH 7.4, 2 mM $MgCl_2$, 2% paraformaldehyde,) on ice for 1-4 hours (depending on tissue and size) and rinsed several hours in PBS including 2 mM $Mg^{2+}$. Tissues were then submerged in 30% sucrose in PBS including 2 mM $Mg^{2+}$ at 4 °C overnight. On the next day tissues were embedded in cryomolds in Tissue Tek OCT compound (Sakura), snap frozen on dry ice, and stored at -80ºC. Frozen blocks were cut in 5-25 µm thick sections (CM 1900, Leica) and mounted on slides (Menzel), dried at room temperature for 30 min, and stored in airtight containers at -80ºC. The slides were warmed up to room temperature in closed containers.

### 2.5.2 Paraffin Sections

Tissues were submerged in fixative (PBS; 4% paraformaldehyde) at 4 °C overnight and subsequently washed in PBS for 12 h at 4 °C. Fixed tissues were dehydrated and paraffinized in an embedding machine (Thermo). The embedding program included 70% ethanol for 1h, 80% ethanol for 1h, 96% ethanol for 1h, 100% ethanol for two changes (1h each), xylene for 1h, and paraffin wax for two changes (1 h each). The tissues were embedded into paraffin blocks and cut with a microtome (Microm) in 5-10 µm thick sections, mounted onto slides, dried for 30 min and incubated at 63 °C for 1h.

### 2.5.3 Fixation and Pretreatment

The frozen sections were fixed with pre-cooled (-20 °C) acetone, ethanol, methanol, or ice cold 2% PFA for 10 min. In case of acetone, ethanol, or methanol fixation, the sections were subsequently air dried for 30 min at room temperature.

Paraffin sections were deparaffinized for 3 min each in xylene (3 changes), 100% ethanol, 95% ethanol, 80% ethanol, 70% ethanol, and water. For epitope retrieval either the citrate buffer or proteinase K pretreatment was used. To apply the citrate buffer method, slides were placed in citrate buffer (10 mM sodium citrate, 0.05% Tween 20, pH 6.0) and boiled for 20 min in a microwave, cooled down to room temperature for 20 min, rinsed in $dH_2O$, and stored in PBS. Proteinase K pretreatment (20 µg/ml proteinase K, 10 mM Tris, 1 mM EDTA, pH 8.0) was applied for 10 min at 37 °C.

### 2.5.4 Immunoflourescence Method

The slides were rinsed in washing buffer (PBS, 0.05% Tween 20, pH 7.2) and blocked with serum blocking (2% serum, 1% BSA, 0.1% fish skin gelatin, 0.1% Triton X-100, 0.05% Tween 20) for 30 min at room temperature. The used serum was derived from the same species as the secondary antibody (normally goat). Then the sections were covered with the primary antibody diluted in PBS including 1% BSA for 1 hour at room temperature or overnight at 4 °C and rinsed 3x for 2 min in washing buffer. The sections were then incubated with fluorescently labeled secondary antibodies (Alexa Fluor 568- or Alexa Fluor 488-conjugated, Molecular Probes) diluted 1:500 in PBS for 30 minutes at room temperature and rinsed 3x for 2 min in washing buffer. DAPI (0.2 ng/µl) was included to counterstain nuclei. Slides were coversliped with aqueous Anti-fade Fluorescent Mounting Medium (Vector Labs) or Flouromount-G (Southern Biotech) and sealed with nail polish.

### 2.5.5 Immunoenzyme (HRP) Method

The slides were rinsed in washing buffer (PBS, 0.05% Tween 20, pH 7.2) and blocked with serum blocking (2% serum, 1% BSA, 0.1% fish skin gelatin, 0.1% Triton X-100, 0.05% Tween 20) including 10% avidin blocking solution (0.001% avidin, Vector) for 30 min at room temperature or overnight at 4 °C. The used serum was derived from the same species as the secondary antibody (normally goat). Endogenous peroxidase activity was blocked by incubation in 3% $H_2O_2$ in PBS (paraffin sections) or 0.3% $H_2O_2$ in methanol (frozen sections). Then the sections were covered with the primary antibody diluted in PBS including 1% BSA and 10% biotin blocking solution (0.001% biotin, Vector) for 1 hour at room temperature or overnight at 4 °C and rinsed 3x for 2 min in washing buffer. The sections were then incubated with a biotinylated secondary antibody (1:500, Vector) diluted in PBS for 30 minutes at room temperature and rinsed 3x for 2 min in washing buffer. The biotinylated secondary antibody was detected with a complex of streptavidin conjugated to horseradish peroxidase (Strept ABComplex/HRP, Dako) for 30 min at room temperature. To visualize conjugated horseradish peroxidase, the sections were covered with AEC solution (Dako) or Vector-SG substrate (Vector) and counterstained in Mayers haematoxylin (Sigma) or Nuclear Fast Red (Vector). Finally, sections were cover-slipped in aqueous mounting medium (Glycergel, Dako) in case of AEC substrate or Permount (Fisher Scientific) for Vector-SG substrate and Nuclear Fast Red counterstaining.

### 2.5.6 LacZ Reporter Assay

Whole mount staining was performed after short fixation (PBS, 2-4% paraformaldehyde, 2 mM $MgCl_2$) for 1 h on ice. Tissues were rinsed in PBS including 2 mM $MgCl_2$ for 1 h at 4 °C and directly transferred into X-gal reaction buffer (PBS including 1 mg/ml 5-Brom-4-chlor-3-indoxyl-β-D-galactopyranosid (X-gal), 10 mM potassium ferrocyanide, 10 mM potassium ferricyanide, 2 mM $MgCl_2$, 0.02% Nonidet P-40 substitute, 0.01% sodium deoxycholate) for 1-24 hours at 37 °C. Frozen sections were produced according to section 2.5.1. For LacZ assays, frozen sections were postfixed (PBS, 2% paraformaldehyde, 2 mM $MgCl_2$) for 10 minutes at 4 °C, rinsed in PBS including 2 mM $MgCl_2$ for 20 min at room temperature, and transferred into X-gal reaction buffer for 1-5 h. In case of subsequent antibody staining, the slides were processed according to section 2.5.4. Otherwise they were rinsed again, counterstained

with Nuclear Fast Red (Sigma), dehydrated quickly (70%, 80%, 95%, 100% for 10 sec each) and cover-slipped in Permount mounting medium (Fisher Scientific).

### 2.5.7 Fluorescent Nissl Staining

For fluorescent Nissl staining following the LacZ assay, the sections were placed in PBS (pH 7.2) for 30 min, permeabilized in PBS including 0.1% Triton X-100 for 10 min (without serum blocking), and washed twice for 5 min each in PBS. The green fluorescent Nissl staining (Molecular Probes) was thawed and diluted 1:100 in PBS. The sections were covered with the staining solution for 20 min, washed twice for 5 min in PBS, counterstained with DAPI (0.2 ng/µl), and finally cover-slipped with Anti-fade Fluorescent Mounting Medium (Vector Labs).

## 2.6 Real-time PCR

### 2.6.1 Total RNA isolation

Mouse tissues were withdrawn immediately after scarification and washed in ice-cold Hank's balanced salt solution, flash-frozen in liquid nitrogen, pulverized, and stored at -80 °C. Total RNA of individual tissues was isolated in parallel from wild-type, heterozygote, and homozygote Gpr30-lacZ mice using RNeasy Kit (QIAGEN), RNeasy Fibrous Tissue Kit (QIAGEN), RNeasy Lipid Tissue Kit (QIAGEN), or Trizol (Invitrogen) according to the manufacturer's protocol. Standard RNA isolation from cell lines was performed using NucleoSpin RNA II Kit (Macherey-Nagel). The concentration and integrity of total RNA was measured using a 2100 Bioanalyzer (Agilent Technologies).

### 2.6.2 cDNA-Synthesis

Approximately 500 ng total RNA was reverse transcribed using Multi-Scribe reverse transcriptase (Applied Biosystems) with random hexamers in 20 µl reactions; ribonuclease inhibitor (0.5 U/µl) was included. Reactions were carried out for 10 min at room temperature and 2 h at 37 °C. Finally, cDNAs were diluted to 1 ng/µl and stored at -20 °C.

### 2.6.3 Real-time PCR Quantification

Real-time PCR (qRT-PCR) reactions were performed in triplicate using SYBR-Green I master mix (Applied Biosystems) and 10 ng cDNA as template in 25 µl reactions. No template and no reverse transcriptase controls were included and products were

analysed by gel electrophoresis and inspection of dissociation curves. PCR efficiency was determined for single reactions using DART-PCR Version 1.0 (Peirson *et al.* 2003), and mean PCR efficiency of gene-specific reactions was used for data analysis. Normalisation and error propagation were calculated as described at the geNORM website (Vandesompele *et al.* 2002). The relative quantity of a specific transcript was calculated as Q=E^(Min(mean Ct of all samples)-Ct), whereas E represents the mean PCR efficiency and Ct the threshold cycles. Three different housekeeping genes (Mouse: Hprt1, Gapdh, Rpl13A; Human: HPRT1, GAPDH, 18S RNA) were assayed, and a normalisation factor was calculated from the geometric mean of their expression levels. Normalised expression levels of target genes were calculated by dividing the corresponding relative quantity by the normalisation factor. Statistical significance was assessed using a two-tailed t test assuming unequal variance of the biological replicates. Gene-specific primers were designed using the Primer 3 software (Rozen and Skaletsky 2000); sequences are provided in section 2.8.3.

## 2.7 Gpr30-lacZ Mice

Gpr30-lacZ mice were obtained from Deltagen (USA). The company generated Gpr30-lacZ mice by homologous recombination targeting exon 3 that encodes the ORF of Gpr30 (Fig. 2). Embryonic stem cells derived from the 129Sv strain were transfected with the linearized targeting construct. G418-resistant clones were analyzed by Southern blotting using a probe that hybridized outside of the 5' homology arm of the targeting vector and long range PCR. Positive ES cell clones were injected in C57BL/6 blastocysts and implanted in CD-1 pseudo pregnant recipients to generate chimeric mice. Male chimeras were mated to C57BL/6 females; agouti offspring (F1 generation) that result from the outcross of the 129 sperm and the C57BL/6 ova were genotyped and send to the customer. We backcrossed heterozygous offspring to the C57BL/6J and 129OlaHsd parental strains for six generations and verified the integration of the targeting construct in more detail by southern blotting (see 2.7.2). C57BL/6J and 129/OlaHsd mice were obtained from Harlan-Winkelmann. Mice were maintained under standardized SPF conditions and 12-h-light/12-h-dark cycle with access to food and water *ad libitum*. Animal housing, care and applications of experimental procedures complied with the Guide for the Care and Use of Laboratory Animals of the Government of Berlin, Germany, and are in accordance to the recommendations of the

Society for Laboratory Animal Science (GV-SOLAS) and the Federation of European Laboratory Animal Science Associations (FELASA).

### 2.7.1 Genotyping of Gpr30-lacZ Mice

Tail tips were digested in 100 µl tail lysis buffer (300 mM sodium acetate; 5 mM EDTA; 1% Triton X-100; 10.0 mM Tris-Cl, pH 8.3, 750 µg/ml proteinase K) overnight at 55 °C. The tail DNA was heated to 95 °C for 5 min and diluted 1:10 in 10 mM Tris (pH 8.3). For each tail sample two PCR reactions were performed; one multiplex reaction plus the targeted (F1 generation) or endogenous (F2 generation) allele alone. The endogenous allele was amplified using primers P172 and P173 (433 bp product); the targeted allele was amplified using primers P172 and P174 (618 bp product). For the multiplex primer stock 5 µl P173, 5 µl P174, 10 µl P172, and 180 µl $dH_2O$ were combined. The PCR reaction (1.5 mM $Mg^{2+}$, 200 µM dNTPs, 200 nM primer, 0.05 U Taq, Eppendorf) was performed using 2 µl diluted tail DNA as template. The PCR conditions were 94 °C for 3 min; 94 °C for 10 sec, 60 °C for 30 sec, 68 °C for 60 sec (30 cycles); with a final extension for 7 min at 68 °C. PCR products were separated on a 1.4% agarose gel at 120 V.

### 2.7.2 Southern Blotting

High molecular weight genomic DNA was isolated from liver and spleen using a phenol-based protocol according to Sambrook & Russel (2001). Briefly, about 100 mg of powdered tissue was suspended in 800 µl lyses buffer (10 mM Tris-Cl, 100 mM EDTA, 0.5% SDS, pH 8.0) in a 2.0 ml tube. RNA was digested by adding 1 µl RNase A (30 mg/ml, Sigma) for 1 h at 37 °C. The sample was gently mixed with 10 µl proteinase K (10 mg/ml) and incubated at 50 °C overnight. After adding an equal amount of buffered phenol (Roth), the solution was mixed slowly for 10 min. The emulsion was separated by centrifugation at 5000 g for 15 min at room temperature. The viscous aqueous phase was carefully transferred into a new 2 ml tube using a truncated tip and the extraction was repeated once again. Finally 0.2 volumes of 10 M ammonium acetate and 2 volumes of ethanol were added. The precipitate was collected, washed twice with 70% ethanol, and stored in an open tube at room temperature until the ethanol was evaporated. Finally the DNA was dissolved in 200-500 µl 10 mM Tris at 4 °C for 12 hrs. The obtained high molecular weight DNA was diluted 1:10 in TE and vigorously vortexed before quantification with a Nanodrop at 260 nm.

DIG-labeled probes were constructed that hybridize outside of and adjacent to the 5' and 3' construct arms as well as in the targeting vector (internal probe). The sequences were amplified from genomic DNA by PCR employing primers P302+P303 for the 5' probe, P304+P305 for the 3' probe, and P306+P307 for the internal probe. The probe sequences were subcloned in pCR2.1-TOPO by direct TOPO-cloning. For DIG-labeling the PCR DIG Probe Synthesis Kit (Roche Applied Science) was used with purified plasmid DNA as template. Control reactions without DIG-dUTP were included to control the labeling efficiency by agarose gel electrophoresis.

About 10 µg genomic DNA was digested with 100 Units of the restriction endonucleases EcoRI (NEB), BamHI (NEB), or Hind III (NEB) in a total reaction volume of 50 µl at 37 °C overnight. Digested DNA samples (5 µg) were separated by gel electrophoresis in large gels (0.8% agarose in TBE buffer) at 30 V overnight. As a molecular weight marker, 5 µl of a DIG-labelled DNA marker (Roche Applied Science) were loaded. The gel was briefly stained in 0.3 µg/ml ethidium bromide and examined under UV light. To denaturate the DNA, the gel was submerged in 250 mM HCl for 10 min at room temperature with gentle shaking and placed twice in denaturation solution (0.5 M NaOH, 1.5 M NaCl) for 15 min. Following a quick rinse in double distilled water, the gel was submerged twice in neutralization solution (0.5 M Tris-HCl, pH 7.5; 1.5 M NaCl) for 15 minutes and equilibrated in 20X SSC (3 M NaCl, 300 mM sodium citrate, pH 7.0) for at least 10 min.

The DNA was transferred overnight onto a positively charged nylon membrane (Roche Applied Science) using a downward capillary transfer procedure. On the next day, the damp membrane was placed on Whatman 3MM paper that has been soaked in 2X SSC and exposed to UV light in a transilluminator (Stratagene). The blot was rinsed briefly in double distilled water, air dried and stored at 4 °C.

For hybridization the blots were placed in roller bottles containing 10 ml prewarmed DIG Easy Hyb buffer (Roche Applied Science) and incubated for at least 30 minutes at 46.5 °C in a hybridization oven (Binder). To prepare the hybridization solution, 10 µl of DIG-labeled PCR product was diluted 1:5 in $dH_2O$, denatured at 95 °C for 5 min, chilled on ice, and added to 5 ml prewarmed DIG Easy Hyb buffer (Roche Applied Science). The prehybridization solution was replaced by the hybridization solution and blots were incubated at 46.5 °C overnight. On the next day they were washed twice for 5 min in low stringency buffer (2X SSC, 0.1% SDS) at room temperature in a plastic

tray, transferred into high stringency buffer (0.5X SSC, 0.1% SDS) prewarmed to 68 °C, and incubated twice for 15 min at 68 °C with gentle shaking.

To visualize probe-target hybrids by chemiluminescence, the blots were washed twice for 2 min at room temperature in washing buffer (0.1 M Maleic acid, 0.15 M NaCl, 0.3% (v/v) Tween 20, pH 7.5), transferred into blocking solution (10X blocking solution (Roche Applied Science) diluted 1:10 in maleic acid buffer) for 30 min, and incubated with antibody solution (Anti-Digoxigenin-AP (75 mU/ml), 1:10000 in blocking solution) for 30 min while shaking. After washing twice for 15 min with washing buffer, the blots were equilibrated in detection buffer (0.1 M Tris-HCl, 0.1 M NaCl, pH 9.5) and placed on acetate sheets, covered with 1 ml diluted CSPD, sealed, and incubated for 10 min at 37 °C to enhance the luminescence reaction. Finally X-ray films were exposed to the sealed blots for 30-60 min.

## 2.8 Materials

### 2.8.1 Antibodies

**Tab. 1:** Primary and secondary antibodies.

| Antibody | Company | Cat# | Dilution |
|---|---|---|---|
| **Primary antibodies** | | | |
| rabbit polyclonal anti-GPR30 N-terminal domain | Acris | SP4209P | 1:500 |
| rabbit polyclonal anti-GPR30 1st extracellular domain | MBL | LS-AA1184 | 1:500 |
| rabbit polyclonal anti-GPR30 3rd extracellular domain | MBL | LS-A4271 | 1:500 |
| rabbit polyclonal anti-GPR30 C-terminal domain antiserum | kindly provided by Eric Prossnitz | | 1:1000 |
| rabbit polyclonal anti-glial fibrillary acidic protein (GFAP) | Abcam | Ab48050 | 1:1000 |
| rat monoclonal (MEC 7.46) anti-PECAM-1 (CD31) | GeneTex | GTX27388 | 1:250 |
| mouse monoclonal anti-α-SMC actin conjugated with Cy3 | Sigma | C6198 | 1:500 |
| mouse monoclonal anti-FUNDC2 (clone 2G12) | Abnova | H0065991-M05 | 1:500 |
| mouse monoclonal anti-GFP | Roche Applied Science | 11814460001 | 1:750 |
| rabbit polyclonal anti-Myc | Sigma | C3956 | 1:2000 |
| mouse monoclonal anti-Myc, clone 9E10 | Santa Cruz | sc-40 | 1:1000 |
| mouse monoclonal anti-HA, clone F-7 | Santa Cruz | sc-7392 | 1:1000 |
| mouse monoclonal anti-HA, clone 16B12 | Covance | MMS-101R | 1:1000 |
| **Secondary antibodies for immunofluorescence** | | | |
| Alexa Fluor 488 goat anti-rabbit IgG (H+L) | Molecular Probes | A-11008 | 1:500 |
| Alexa Fluor 568 goat anti-rabbit IgG (H+L) | Molecular Probes | A-11011 | 1:500 |
| Alexa Fluor 488 goat anti-mouse IgG (H+L) | Molecular Probes | A-11001 | 1:500 |
| Alexa Fluor 568 goat anti-mouse IgG (H+L) | Molecular Probes | A-11004 | 1:500 |
| **Secondary antibodies for western blotting** | | | |
| sheep anti-mouse peroxidase conjugated | Amersham | NXA931 | 1:7500 |
| goat anti-rabbit peroxidase conjugated | Calbiochem | DC03L | 1:7500 |

### 2.8.2 Vectors and Constructs

The generation of GPR30 and FUNDC2 constructs is described in section 2.1.10 and 2.1.11, respectively.

**Tab. 2:** Vectors and Constructs

| No. | Construct | Marker | Description |
|---|---|---|---|
| **Empty vectors** | | | |
| 16 | pBTM116 | $A^R$, TRP1 | Y2H bait vector |
| 15 | pACT2 | $A^R$, LEU2 | Y2H prey vector |
| 17 | pcDNA3.1+ | $A^R$, $N^R$ | Empty vector (Invitrogen) |
| 1 | pcDNA3CFP* | $A^R$, $N^R$ | FRET vector for C-term CFP tag |
| 2 | pcDNA3NCFP* | $A^R$, $N^R$ | FRET vector for N-term CFP tag |
| 3 | pcDNA3YFP* | $A^R$, $N^R$ | FRET vector for C-term YFP tag |
| 4 | pcDNA3NYFP* | $A^R$, $N^R$ | FRET vector for N-term YFP tag |
| 22 | pDONR221 | $K^R$, $C^R$, ccdB | Gateway attP donor vector (Invitrogen) |
| 23 | pDEST26 | $A^R$, $N^R$, $C^R$, ccdB | Gateway attR destination vector, N-term His-tag |
| 24 | pDEST474** | $A^R$, $N^R$, $C^R$, ccdB | Gateway attR destination vector, C-term Myc-tag* |
| 25 | pDEST475** | $A^R$, $N^R$, $C^R$, ccdB | Gateway attR destination vector, N-term HA-tag* |
| 26 | pDEST515** | $A^R$, $N^R$, $C^R$, ccdB | Gateway attR destination vector, N-term Flag-tag* |
| 27 | pDEST701** | $A^R$, $N^R$, $C^R$, ccdB | Gateway attR destination vector, N-term Myc-tag* |
| 31 | pdEYFP-DEST | $A^R$, $C^R$, ccdB | Gateway attR destination vector, N-term EYFP-tag |
| 51 | pcDNA3CFP-DEST | $A^R$, $N^R$, $C^R$, ccdB | Gateway attR destination vector, C-terminal YFP tag |
| 52 | pcDNA3YFP-DEST | $A^R$, $N^R$, $C^R$, ccdB | Gateway attR destination vector, C-terminal CFP tag |
| **GPR30 constructs** | | | |
| 13 | pcDNA3-GPR30-EGFP*** | $A^R$, $N^R$ | Expression of GPR30 with C-term EGFP tag** |
| 55 | pBTM116-GPR30Nterm | $A^R$, TRP1 | Yeast two-hybrid bait, encodes the N-terminus of GPR30 |
| 57 | pBTM116-GPR30Cterm | $A^R$, TRP1 | Yeast two-hybrid bait, encodes the C-terminus of GPR30 |
| 18 | pcDNA3.1+/GPR30 | $A^R$, $N^R$ | Expression of full-length GPR30 |
| 19 | pcDNA3.1+/GPR30Δ1-104 | $A^R$, $N^R$ | Expression of N-term truncated GPR30 |
| 32 | pENTR221-GPR30-C | $K^R$ | Entry vector for GPR30 constructs with C-terminal tags |
| 45 | pTL1-HA2/GPR30 | $A^R$ | Expression of GPR30 with N-term HA-tag |
| 59 | pCR2.1-TOPO-3prime | $K^R$ | Southern probe for Gpr30-lacZ mice, 3' |
| 60 | pCR2.1-TOPO-5prime | $K^R$ | Southern probe for Gpr30-lacZ mice, 5' |
| 61 | pCR2.1-TOPO-Internal | $K^R$ | Southern probe for Gpr30-lacZ mice, Internal |
| **FUNDC2 constructs** | | | |
| 33 | pENTR221-FUNDC2-N | $K^R$ | Entry vector for FUNDC2 constructs with N-terminal tags |
| 70 | pENTR221-FUNDC2-C | $K^R$ | Entry vector for FUNDC2 constructs with C-terminal tags |
| 20 | pdEYFPEXP-FUNDC2 | $A^R$ | Gateway attB vector, FUNDC2 with N-term EYFP-tag |
| 21 | pEXP26-FUNDC2 | $A^R$, $N^R$ | Gateway attB vector, FUNDC2 with N-term His-tag |
| 28 | pEXP475-FUNDC2 | $A^R$, $N^R$ | Gateway attB vector, FUNDC2 with N-term HA-tag |
| 29 | pEXP515-FUNDC2 | $A^R$, $N^R$ | Gateway attB vector, FUNDC2 with N-term FLAG-tag |
| 30 | pEXP701-FUNDC2 | $A^R$, $N^R$ | Gateway attB vector, FUNDC2 with N-term Myc-tag |
| 64 | pEXP474-FUNDC2 | $A^R$ | Gateway attB vector, FUNDC2 with C-term Myc-tag |

* provided by Prof. Michael Schaefer, Charité Universitätsmedizin, Berlin, Germany
** provided by Dominic Esposito, NCI-Frederick Vector Engineering Group, USA
*** provided by Eric Prossnitz, University of New Mexico, Albuquerque, USA
Abbreviations: $A^R$, ampicillin resistance; $C^R$, chloramphenicol resistence; $K^R$, kanamycin resistence; $N^R$, neomycin resistance; LEU2, LEU2 gene enabling yeast auxotrophs to grow in the absence of leucine; TRP1, TRP1 gene enabling yeast auxotrophs to grow in the absence of tryptophan; ccdB, lethal ccdB gene

### 2.8.3 Primer

All primers were obtained from MWG Biotech in a 0.01 µmol scale (HPSF purification) and resuspended in $H_2O$ to 100 pmol/µl (100 mM) stock concentration. Equal amounts of forward and reverse primer were combined and diluted to 5 µM each with $dH_2O$.

**Tab. 3:** Primer sequences.

| No. | Sequence (5' → 3') | Comment |
|---|---|---|
| P1 | GTCATAGCTGTTTCCTG | For. sequencing of Gateway destination vectors |
| P287 | ACCACTTTGTACAAGAAAGCTGGG | Rev. sequencing of Gateway destination vectors |
| P2 | GTAAAACGACGGCCAG | M13 forward sequencing primer |
| P3 | CGCAAATGGGCGGTAGGCGTG | M13 reverse sequencing primer |
| P4 | GTTGGGGTTATTCGCAAC | Forward sequencing primer pBTM116 |
| P5 | CATAAGAAATTCGCCCGG | Reverse sequencing primer pBTM116 |
| P31 | AATACCACTACAATGGATGAT | Forward sequencing primer pACT2 |
| P32 | GTGAACTTGCGGGGTT | Reverse sequencing primer pACT2 |
| P79 | GACAGCCACTCTGGAGGAGA | qRT-PCR, mouse Rpl13A |
| P80 | TCTGCCTGTTTCCGTAACCT | qRT-PCR, mouse Rpl13A |
| P69 | CGACCACTTTGTCAAGCTCA | qRT-PCR, human GAPD |
| P70 | TTACTCCTTGGAGGCCATGT | qRT-PCR, human GAPD |
| P71 | TGTTCCTACCCCCAATGTGT | qRT-PCR, mouse Gapdh |
| P72 | CCTGCTTCACCACCTTCTTG | qRT-PCR, mouse Gapdh |
| P73 | TTGTTGTAGGATATGCCCTTGA | qRT-PCR, human HPRT1 |
| P74 | GGCTTTGTATTTTGCTTTTCCA | qRT-PCR, human HPRT1 |
| P75 | TGTTGTTGGATATGCCCTTG | qRT-PCR, mouse Hprt |
| P76 | TTGCGCTCATCTTAGGCTTT | qRT-PCR, mouse Hprt |
| P81 | CCGCAGCTAGGAATAATGGAATA | qRT-PCR, human 18S |
| P82 | TCTAGCGGCGCAATACGAAT | qRT-PCR, human 18S |
| P109 | GATGACGAATTCATGGATGTGACTTCCCAAGCCCG | Y2H bait vector pBTM116-Nterm, EcoRI site |
| P110 | GAGGAGGATCCGACTGCTGGTGCTCCGAGAGCT | Y2H bait vector pBTM116-Nterm, BamHI site |
| P111 | GATGACGAATTCACCTTCAGGGACAAGCTGAGGC | Y2H bait vector pBTM116-Cterm, EcoRI site |
| P112 | GATGAGGATCCGCTACACGGCACTGCTGAACC | Y2H bait vector pBTM116-Cterm, BamHI site |
| P172 | ACCTGTCGAAGCTCATCCAGGTGAG | Genotyping of GPR30KO mice |
| P173 | GGTGGAGATCTACCTAGGTCCCGTG | Genotyping of GPR30KO mice |
| P174 | GGGGATCGATCCGTCCTGTAAGTCT | Genotyping of GPR30KO mice |
| P213 | CCCAAGCTTGCCACCATGGATGTGACTTCC | Construction of pcDNA3(+)-GPR30, HindIII site |
| P214 | TAGTTTAGCGGCCGCACGTTAGCACCTGCATTACCT-ACACGGCACTGCTG | Construction of pcDNA3(+)-GPR30, NotI site |
| P279 | GGGGACAAGTTTGTACAAAAAAGCAGGCTACCATGG-ATGTGACTTCCCAA | Construction of pENTR221-GPR30-C, attB1-site |
| P280 | GGGGACCACTTTGTACAAGAAAGCTGGGTCCACGG-CACTGCTGAACCTCA | Construction of pENTR221-GPR30-C, attB2-site |
| P298 | AGCTGTAGGAGGTGGATTCTTTC | qRT-PCR, mouse Fundc2 |
| P299 | TTGACCTCAGTTGGTATTTGCTT | qRT-PCR, mouse Fundc2 |
| P300 | GGGGACAAGTTTGTACAAAAAAGCAGGCTTCGAAGG AGATAGAACCATGGAAACATCTGCCCCACGTGCCGG | Construction of pENTR221-FUNDC2-C, attB1-site |
| P301 | GGGGACCACTTTGTACAAGAAAGCTGGGTCGGATG-CCATGCCAAGCAG | Construction of pENTR221-FUNDC2-C, attB2-site |
| P302 | CCCGAATTCGTGCCATCTCAGGTAGGAGC | Forward primer for Southern probe (5') |
| P303 | CCCGAATTCCCAGAGCTGAGGTGCTTTCC | Reverse primer for Southern probe (5') |
| P304 | CCCGAATTCTTCTGCGTACTCTCCTATGTACC | Forward primer for Southern probe (3') |
| P305 | CCCGAATTCGCTCTGCCAAGTCCACTAAACC | Reverse primer for Southern probe (3') |
| P306 | CCCGAATTCCACGTCTCTTTCCAACAGCTGC | Forward primer for Southern probe (Internal) |
| P307 | CCCGAATTCAGTAGTCGCATCCATGGCTTCC | Reverse primer for Southern probe (Internal) |

# 3 RESULTS

## 3.1 Molecular Characterization of GPR30-lacZ Mice

To investigate the expression and function of Gpr30 *in vivo*, a mutant mouse model was analyzed that harbors a LacZ reporter (Gpr30-lacZ) in the Gpr30 locus leading to a partial deletion of the Gpr30 coding sequence. The targeting of Gpr30 and the blastocyst injection was performed by Deltagen Inc. (San Mateo, USA). The mice were generated by homologous recombination in embryonic stem (ES) cells derived from the 129/OlaHsd strain targeting exon 3 that encodes the open reading frame (ORF) of Gpr30 (Fig. 2A). The inserted cassette contains a splice acceptor, an internal ribosomal entry site (IRES), a β-galactosidase gene (lacZ), a SV40 polyadenylation site (SV40 pA), and a neomycin-resistance gene (neoR) driven by a phosphoglycerate kinase promoter (PGK). The insertion replaced 349 bps of the ORF encoding amino acids 20-136 of Gpr30 accounting for the first two transmembrane domains as well as the first intra- and extracellular loop (Fig. 2B). Two heterozygous breeding couples of Gpr30-lacZ mice were obtained and subsequently backcrossed to C57BL/6J as well as 129/OlaHsd females for six generations.

Since the integration of the targeting cassette into the mouse genome has not been analyzed sufficiently by Deltagen, the integration was verified in more detail by Southern blotting using probes that hybridize outside of and adjacent to the 5' and 3' construct arms as well as in the cassette (internal probe) (Fig. 2A). Southern blotting (see 2.7.2) was performed with genomic DNA isolated from livers of wildtype, heterozygous as well as homozygous Gpr30-lacZ mice (Fig. 2C). The 5'-external probe detected a 10.5 kb EcoRI-fragments from the wildtype allele and smaller 8.8 kb EcoRI-fragments from the targeted allele which confirms the integration of the 5' construct arm (Fig. 2C, left). The integration of the 3' construct arm was verified with a 3'-external probe detecting fragments of 6.1 kb or 6.8 kb from the wildtype allele as well as 6.8 kb and 10.7 kb for the targeted allele after BamHI- or HindIII-digestion (Fig. 2C, right). The internal probe located within the 5' construct arm detected 6.1 kb or 6.9 kb fragments from the wildtype allele as well as 2.0 kb or 2.5 kb fragments from the targeted allele, respectively, showing the single integration of the construct into the mouse genome (Fig. 2C, middle). Since the detected fragments had always the expected size, the successful homologous recombination event was clearly confirmed.

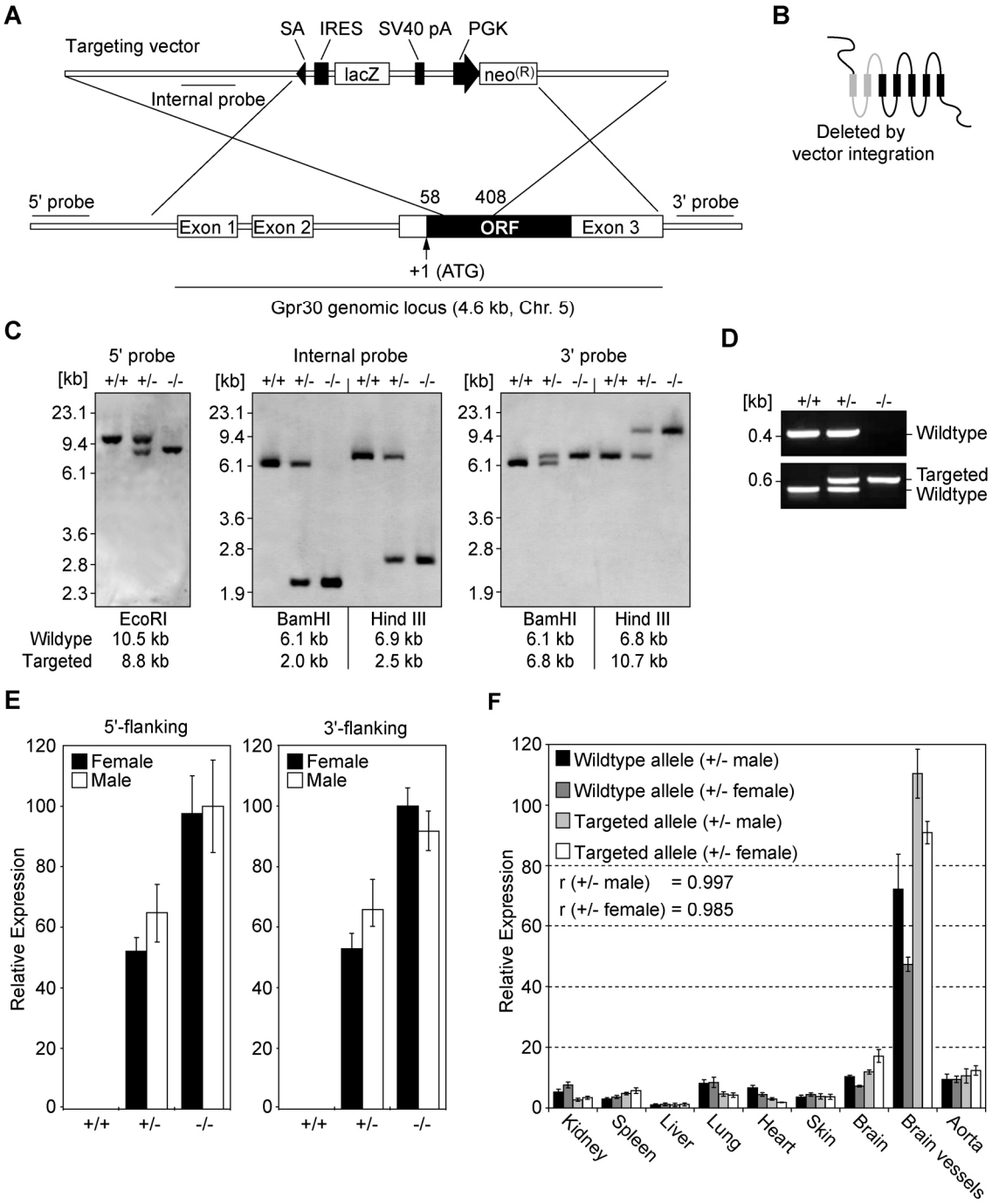


**Fig. 2:** Gene targeting strategy and molecular characteristics of Gpr30-lacZ mice. (A) Exon 3 encoding Gpr30 was disrupted by insertion of a cassette containing a splice acceptor (SA), an internal ribosomal entry site (IRES), a LacZ reporter (lacZ), a SV40 polyadenylation site, and a neomycin-resistance (neoR) driven by a PGK promoter. (B) The insertion deleted 349 bps of the ORF encoding the first two transmembrane domains and the first intra- and extracellular loop. (C) Genomic liver DNA was analyzed by Southern blotting with probes that hybridize outside of and adjacent to the 5' and 3' construct arms as well as in the targeting vector (internal probe). The detected fragments had the expected size verifying the targeting of Gpr30. (D) Genotyping of Gpr30-lacZ mice showing that the wildtype PCR product (433 bps) was absent in Gpr30-lacZ mice, whereas the targeted allele (618 bps) was amplified exclusively in Gpr30-lacZ mice. (E) Real-time PCR quantification of sequences flanking the cassette using brain cDNA. The cassette is spliced to the 5'-region of exon 3 in the mutated transcript. In addition, a fusion transcript of the neoR gene and the remaining 3'-region of exon 3 was detected in Gpr30-lacZ mice. (F) Quantification of the wildtype and targeted allele in various tissues of one male and one female heterozygous Gpr30-lacZ mouse by real-time PCR. The expression of wildtype and targeted allele correlated significantly (Pearson correlation coefficient r > 0.98).

For genotyping, tail cuts of the offspring were collected at an age of 4 weeks, digested, and analyzed by PCR (see 2.7.1). For genotyping reactions, forward primers located upstream (wildtype allele) or in the cassette (targeted allele) were combined with a gene-specific primer binding downstream of the integration site. The wildtype fragment (433 bps) was absent in homozygous Gpr30-lacZ mice, whereas a larger fragment indicating the targeted allele (618 bps) was specifically amplified in the Gpr30-lacZ mice (Fig. 2D).

Real-time PCR quantification of sequences flanking the cassette in brain cDNA samples verified the fusion of the lacZ transcript to the 5'-part of exon 3 (Fig. 2E). In addition, a fusion transcript of the neoR gene and the remaining 3'-region of exon 3 was detected in the Gpr30 mutant mice (Fig. 2E). The expression of this transcript starts at the PGK promoter and leads to overexpression of a truncated Gpr30 transcript in Gpr30-lacZ mice as determined by real-time PCR. However, the expression of a truncated protein is impossible due to stop codons in all three reading frames terminating the neomycin resistance and due to a nonsense reading frame of the remaining transcript.

To assure that the integration of the reporter cassette in the Gpr30 locus did not affect the endogenous promoter activity, the expression of the wildtype and targeted allele was quantified in various tissues of one male and one female heterozygous Gpr30 mutant mouse by real-time PCR (Fig. 2F). The results revealed that the expression of the wild-type and the targeted allele correlated significantly (Pearson correlation coefficient $r > 0.98$) in both animals. Highest expression was detected in isolated brain vessels that have been removed from the brain surface; lowest expression was detected in liver. Of note, the amount of Gpr30 transcript was much lower in the aorta compared to brain vessels.

## 3.2 Tissue Distribution of LacZ Expression

The finding that the expression of the LacZ reporter and the wildtype Gpr30 correlated at transcript level indicated that the expression of the lacZ reporter reflects the endogenous Gpr30 expression. Therefore, Gpr30-positive cells were localized in tissues by X-gal staining and immunohistochemistry with a LacZ-specific antibody. Initially, whole tissue specimens were assayed for LacZ activity by whole mount X-gal staining (see 2.5.6). Subsequently, LacZ-positive cells were colocalized with cell type-specific markers in frozen sections. For all staining procedures, eight weeks old male and female heterozygote mice were used. To ensure specific staining, wildtype littermates were

always stained in parallel as negative controls. Since the employed LacZ reporter included a nuclear localization signal, predominant nuclear staining was expected in case of specific signals. A summary of the LacZ expression data in diverse tissues from Gpr30-lacZ mice is shown in an overview table (Tab. 4).

**Tab. 4:** Summary of LacZ expression in Gpr30-lacZ mice.

| Tissue / Organ | LacZ Expression |
|---|---|
| Brain | Smooth muscle cells and pericytes of all blood vessels, neuronal subpopulations in the lateral part of the cerebral cortex and in the polymorph layer of the dentate gyrus |
| Skeletal muscle | Few small arteries and arterioles |
| Heart | Few small arteries and arterioles |
| Skin | No LacZ expression |
| Peritoneum | All arteries and arterioles |
| Aorta | Small vessels of the *Vasa vasorum* |
| Esophagus | Few small arteries and arterioles of the surrounding muscle layer |
| Stomach | Strong expression in the gastric fundus, probably chief cells |
| Pancreas | LacZ expression is detectable in blood vessels. Isolated islets have not been investigated in detail |
| Gallbladder | No LacZ expression |
| Liver | No LacZ expression |
| Kidney | Endothelial cells in arcuate and interlobular arteries as well as afferent arterioles. Scattered LacZ expression in papilla and medulla. |
| Urinary Bladder | Blood vessels |
| Trachea | No LacZ expression |
| Larynx | No LacZ expression |
| Lung | LacZ expression is detectable in few distinct cells. |
| Thyroid Gland | LacZ expression is detectable in blood vessels |
| Pituitary Gland | Intermediate and anterior lobe |
| Adrenal Glands | Medulla |
| Salivary Glands | No LacZ expression |
| Testis | Few small arteries and arterioles |
| Seminal Vesicles | Few small arteries and arterioles |
| Coagulating Gland | Few small arteries and arterioles |
| Vagina/Cervix | Few small arteries and arterioles |
| Ovary | No LacZ expression |
| Mammary gland | Few small arteries and arterioles |
| Eyes | No LacZ expression |
| Thymus | No LacZ expression |
| Spleen | No LacZ expression |
| Lymph nodes | No LacZ expression |
| Bone marrow | No LacZ expression |

Consistent with the real-time PCR data, multiple LacZ-positive cells were found in surface vessels of the brain (Fig. 3). Of note, arterial vessels such as the middle cerebral artery (MCA, black arrow in Fig. 3D) and its rostral and caudal branches were found to contain more LacZ-positive cells compared to venous vessels (e.g. the caudal rhinal vein, white arrow in Fig. 3D). The vessel-associated LacZ-positive cells were ubiquitously present and appeared to be attached either outside of or inserted into the basal lamina of brain vessels (Fig. 4A-C). LacZ-positive cells colocalized with α-smooth muscle cell (SMC) actin and not with the endothelial cell marker platelet/endothelial cell adhesion molecule 1 (PECAM-1, CD31) clearly indicating that LacZ-positive cells were smooth muscle cells and pericytes in the brain (Fig. 4E-I).

Further analysis revealed prominent expression of LacZ in the vessel system of the peritoneum, which is a serous membrane that forms the lining of the abdominal cavity and covers most of the intra-abdominal organs (Fig. 5A). Moreover, LacZ-positive cells were present in small arterial blood vessels of various tissues including the fat depots, skeletal muscle, and heart (Fig. 5B-D). However, the expression of the reporter appeared to be restricted to cells of special vascular beds. For instance larger vessels such as the thoracic and abdominal aorta (Fig. 5G) and its adjacent branching vessels like the carotid, intercostal, renal, and superior mesenteric arteries were negative for LacZ-positive cells. In contrast, small arterioles in the outer layer of the aorta (Fig. 5E) as well as the final branches of the mesenteric arteries that supply the digestive organs and surrounding fat depots (Fig. 5F) contained large numbers of LacZ-positive cells. Consistent with the real-time PCR data, LacZ expression was absent in the liver (Fig. 5H).

However, the vessel-associated LacZ-positive cells in other tissues than the brain may represent an endothelial subpopulation. For instance in the kidney, LacZ-positive cells were specifically located in smaller arteries (i.e. arcuate and interlobular arteries) and in afferent arterioles supplying the glomeruli (Fig. 6A-D). In contrast to cells detected in the brain, LacZ-positive cells in the kidney were clearly located at the luminal site of the vessel. Furthermore, the elongated nuclei of these cells were in direction of the blood flow, which is known to be characteristic for endothelial cells. They colocalized with PECAM-1, but not with α-SMC actin (Fig. 6E-I).

Further analyses revealed that LacZ-positive vessel-associated cells were present in multiple organs, but restricted to only a few and small arteries/arterioles in most tissues.

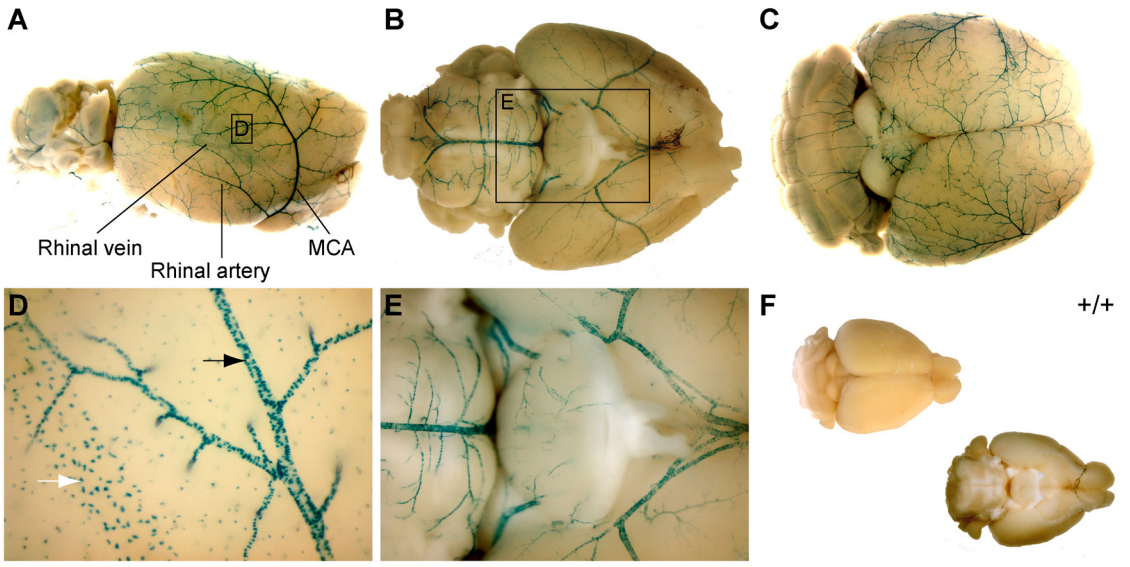


**Fig. 3:** Lateral (A), ventral (B), and dorsal aspect (C) of the brain after whole mount X-gal staining showing vessel-associated expression of the LacZ reporter in heterozygous Gpr30-lacZ mice. The magnification of the lateral aspect in (D) shows an arterial (back arrow) and a venous vessel (white arrow). Of note, arterial vessels contained more LacZ-positive cells than venous vessels. The magnification of the ventral aspect shows the Circle of Willis (E). The staining was absent in wildtype control brains (F). MCA, middle cerebral artery.

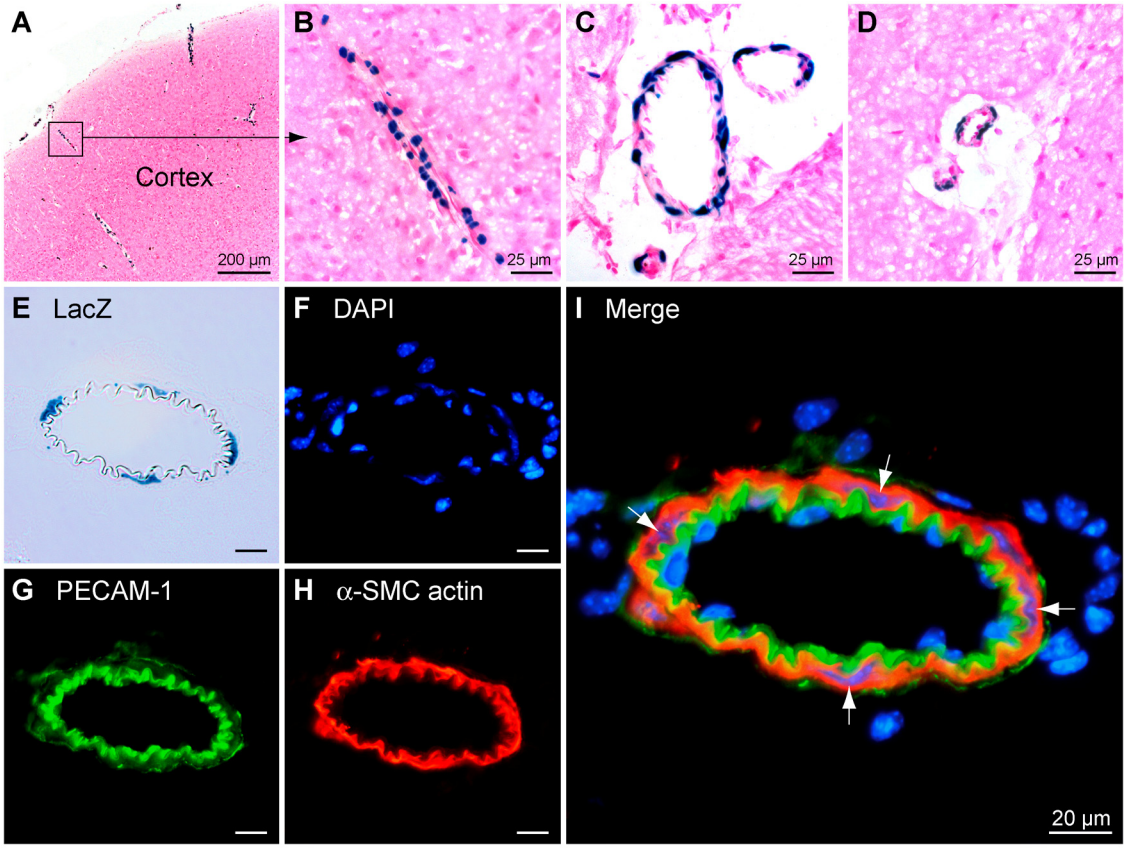


**Fig. 4:** Colocalization of LacZ expression with cell type-specific markers in brain vessels. LacZ-positive cells were ubiquitously present and appeared to be attached either outside of or inserted into the basal lamina (A-D). For colocalization (E-I), frozen sections were assayed for LacZ activity followed by immunohistochemistry with antibodies detecting PECAM-1 (G, green signal) or α-SMC actin (H, red signal). Cell nuclei were visualized with DAPI (F, blue signal). LacZ-positive cells colocalized with α-SMC actin expression (arrows in I).

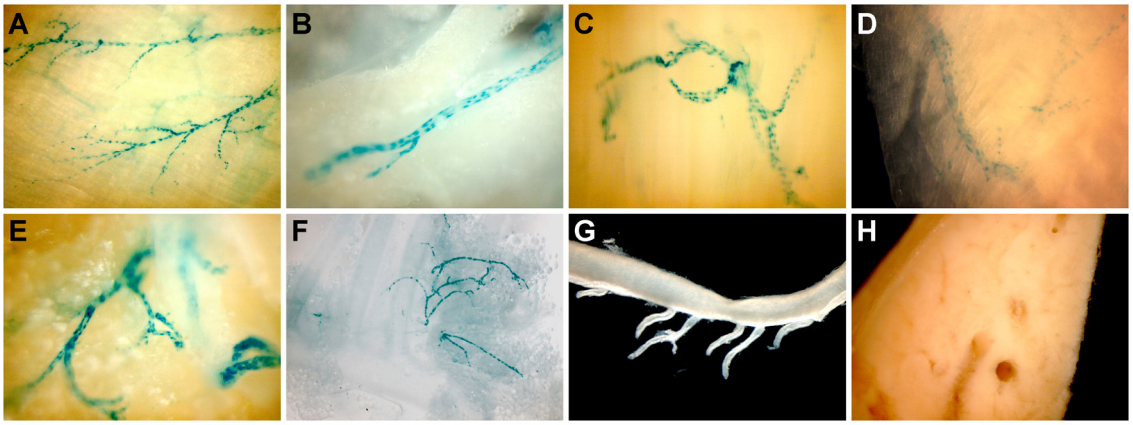


**Fig. 5:** Whole mount X-gal staining of various tissues. LacZ reporter gene expression was detected in smaller vessels of multiple tissues including the peritoneum (A), white fat (B), hamstring skeletal muscle (C), heart (D), adipose tissue (f), small arterioles of the *Vasa vasorum* in the outer layer of the aorta (E), and mesenteric arterioles (F). LacZ-positive cells were absent in the aorta (G) and liver (H).

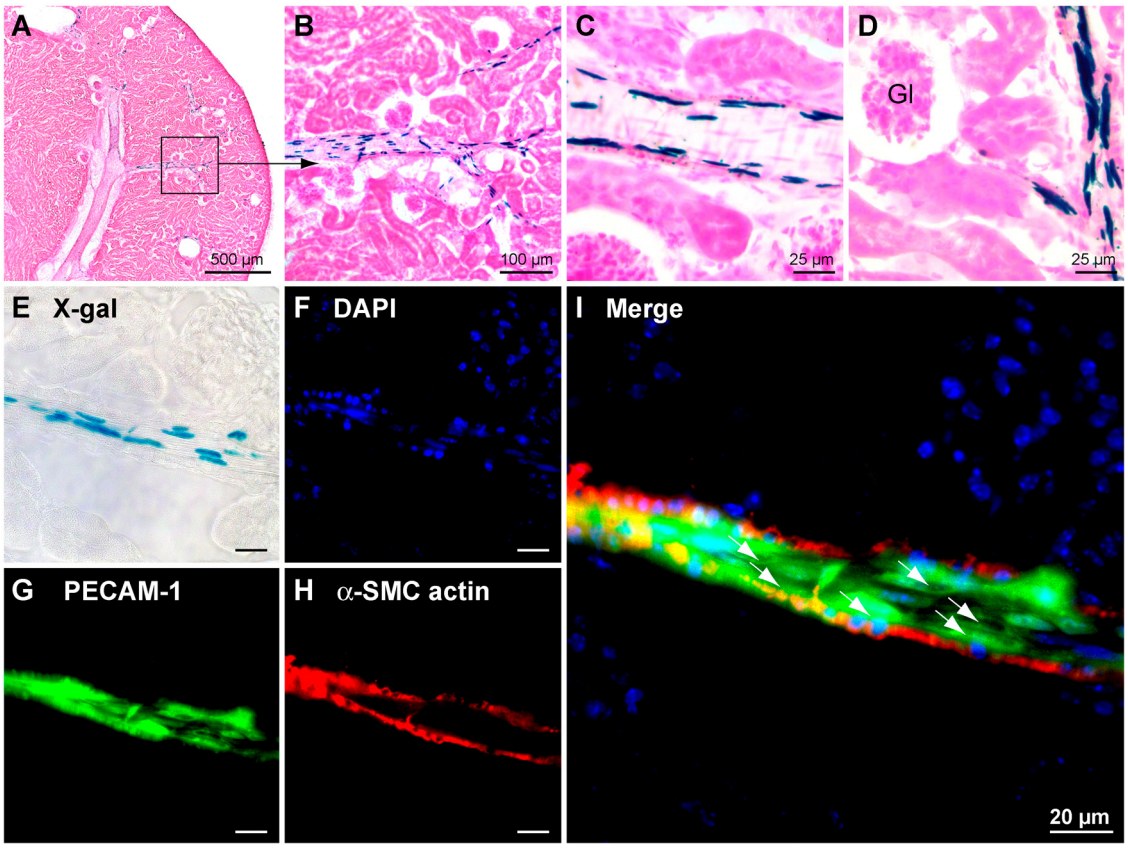


**Fig. 6:** Colocalization of LacZ expression with cell type-specific markers in the kidney. LacZ-positive cells were located at the luminal site of smaller arteries (i.e. arcuate and interlobular arteries) and in afferent arterioles supplying the glomeruli (A-D). For colocalization (E-I), frozen sections were assayed for LacZ activity followed by immunohistochemistry with antibodies detecting PECAM-1 (G, green signal) or α-SMC actin (H, red signal). Cell nuclei were visualized with DAPI (F, blue signal). LacZ-positive cells colocalized with PECAM-1 expression (arrows in I). Gl, glomerulus.

Previous RT-PCR results indicated prominent expression of Gpr30 in the stomach and pancreas of wildtype mice. Indeed, strong LacZ activity was detected in the gastric fundus of Gpr30-lacZ mice. LacZ-positive cells were exclusively located at the base of fundic glands (Fig. 7A-D). Within this area, gastric chief (zymogenic) cells and entero-endocrine cells are the most prominent cell populations. However, only chief cells are exclusively present in fundic glands and absent in cardiac or pyloric glands known to express enteroendocrine cells. Therefore, LacZ-positive cells at the base of fundic glands likely represent gastric chief cells. In the pancreas, LacZ activity was exclusively detected in the vessel system. However, the LacZ assay requires weak fixation, otherwise the enzyme becomes overfixed. This may lead to the rapid degradation of the LacZ enzyme due to active digestive enzymes in the pancreas.

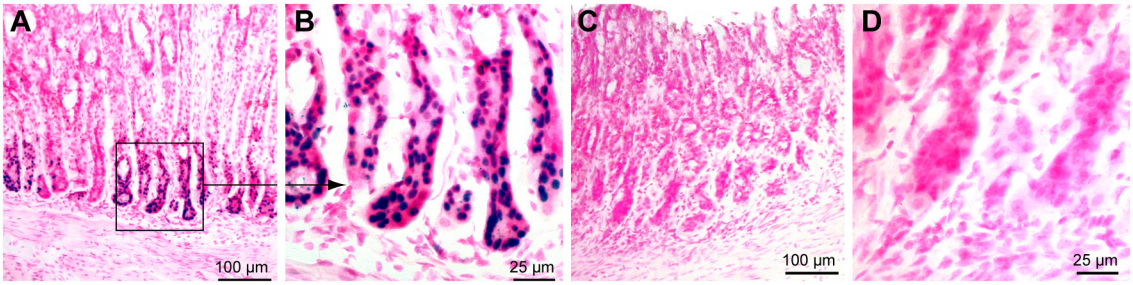


**Fig. 7:** X-gal staining of frozen sections from the stomach of heterozygous Gpr30-lacZ mice (A,B) and wildtype controls (C,D). LacZ-positive cells were found in the gastric fundus and likely represent gastric chief cells (blue nuclei in A, B).

To unravel expression of Gpr30 within the endocrine system, several glands and in the gonads were analyzed for LacZ-acitivity. LacZ expression was located in blood vessels in most of these tissues (i.e. thyroid gland, salivary gland, ovary, and testis). In addition, LacZ-positive cells were found in the medulla of the adrenal gland (Fig. 8A,B). The adrenal medulla contains chromaffin cells which secrete catecholamines such as epi-nephrine, norepinephrine, and dopamine into the blood. LacZ activity was also present in cells located in the intermediate and anterior lobe (adenohypophysis) of the pituitary gland (Fig. 8C,D). The LacZ staining was not nuclear, but scattered all over the cell body in the adrenal and pituitary gland indicating cell-type specific processing/transport of the β-galactosidase enzyme.

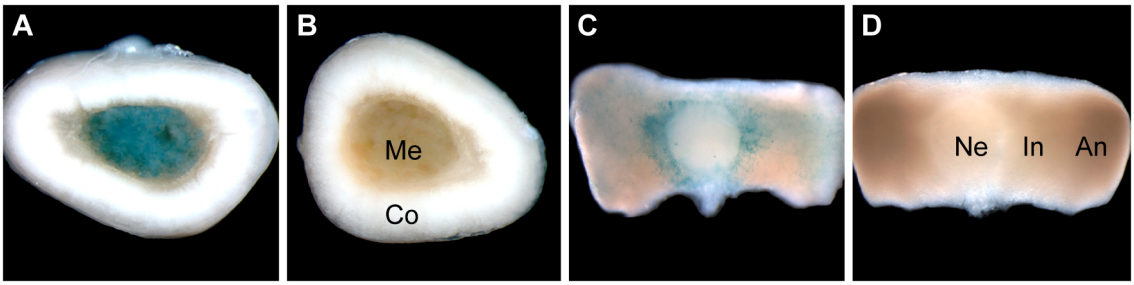


**Fig. 8:** Whole mount X-gal staining of the adrenal (A,B) and pituitary gland (C,D). LacZ-positive cells were located in the medulla of the adrenal gland (A) and in the intermediate and anterior lobe of the pituitary gland (C). The LacZ activity was absent in corresponding wildtype controls (B,D). Me, medulla; Co, cortex; Ne, neurohypophysis; In, intermediate lobe; An, anterior lobe.

Since non vessel-associated LacZ-positive cells were present in cortical areas of the brain, coronal sections of whole brains were analyzed in detail. Two distinct brain structures containing non vessel-associated LacZ-positive cells were found and classified according to the Allen Brain Reference Atlas (Lein et al. 2007). The first region containing these cells was located in the lateral part of the second layer of the cerebral cortex in the ectorhinal area (Fig. 9). The second structure that contained LacZ-positive cells was the polymorph layer of the dentate gyrus which is a part of the hippocampal formation.

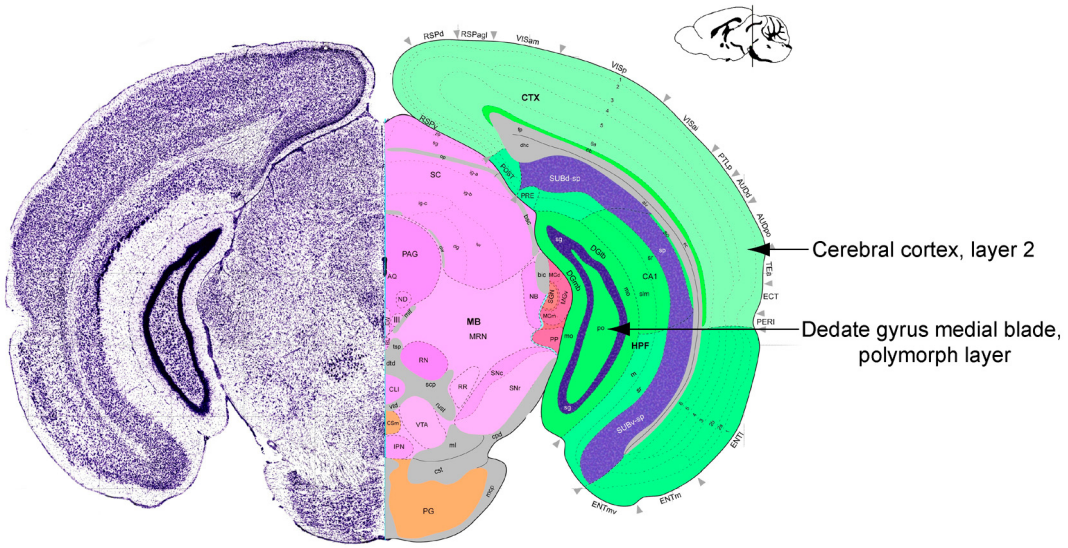


**Fig. 9:** Localization of nonvessels-associated LacZ-positive cells in a coronal section of the mouse brain. The left part shows the Nissl staining; in the right part all brain structures are designated. The arrows indicate the areas containing LacZ-positive cells. The image was downloaded from the Allan Brain Atlas (http://www.brain-map.org, Coronal section 90).

The X-gal staining colocalized with fluorescent Nissl staining used as a general marker for neuronal cells and not with the astrocyte marker glial fibrillary acidic protein (GFAP), PECAM-1 or α-SMC actin (Fig 10E-N). Therefore, these LacZ-positive cells are in fact neuronal subpopulations.

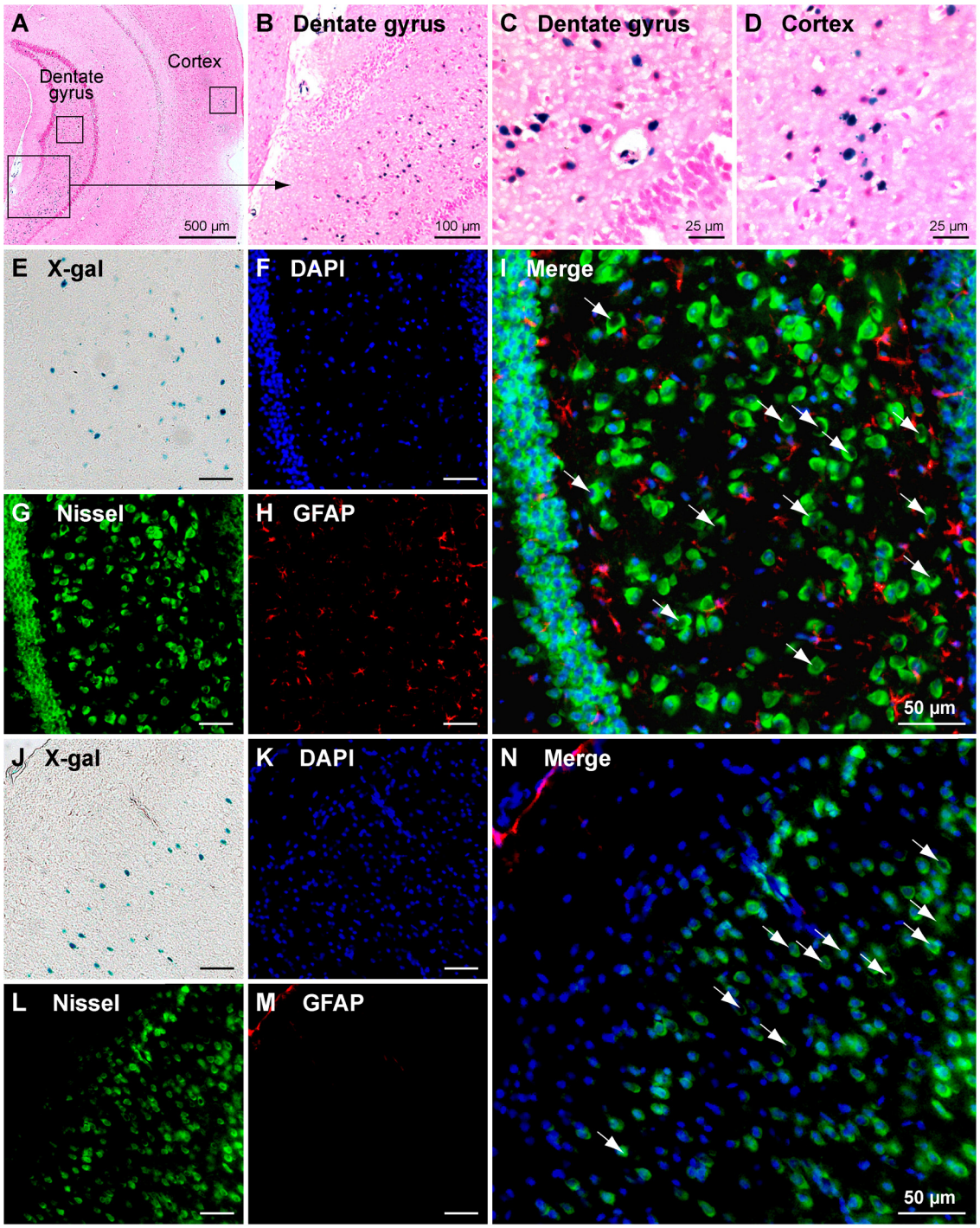


**Fig 10:** X-gal staining followed by immunohistochemistry and Nissl staining of frozen brain sections. LacZ-positive cells were present in the polymorphic layer of the dentate gyrus (A-C) and in the cortex (A,D). LacZ-positive cells colocalized with the fluorescent Nissel staining used as a marker for neuronal cells (green signal) and not with the astrocyte marker GFAP (red signal) in the dentate gyrus (E-I) and in the cortex (J-N). Cell nuclei were visualized with DAPI (F,K, blue signal). LacZ-positive nuclei are indicated by arrows in the merged images (I,N).

## 3.3 Detection of GPR30 Protein with Antibodies

Considerable efforts were undertaken to detect the GPR30 protein with western blotting, immunocyto- or immunohistochemistry. First of all different commercially available antibodies directed against the N-terminal, 1st extracellular, 3rd extracellular, and an antiserum detecting the C-terminal domain of human GPR30 (kindly provided by Prof. Eric Prossnitz, University of New Mexico, Albuquerque, USA) were tested on ectopically expressed human GPR30 with a C-terminal EGFP-tag in transfected HeLa cells. Two of these antibodies (3rd extracellular domain antibody, C-terminal domain antiserum) detected human GPR30 in transiently transfected HeLa cells (Fig. 11A). Tagged and untagged GPR30 seemed to be retained in the endoplasmatic reticulum and was not processed to the membrane in HeLa cells (Fig. 11A,B). The antibody directed against the 3rd extracellular domain also detected human GPR30 by western blotting in cell lysates from transfected HeLa cells (Fig. 11B).

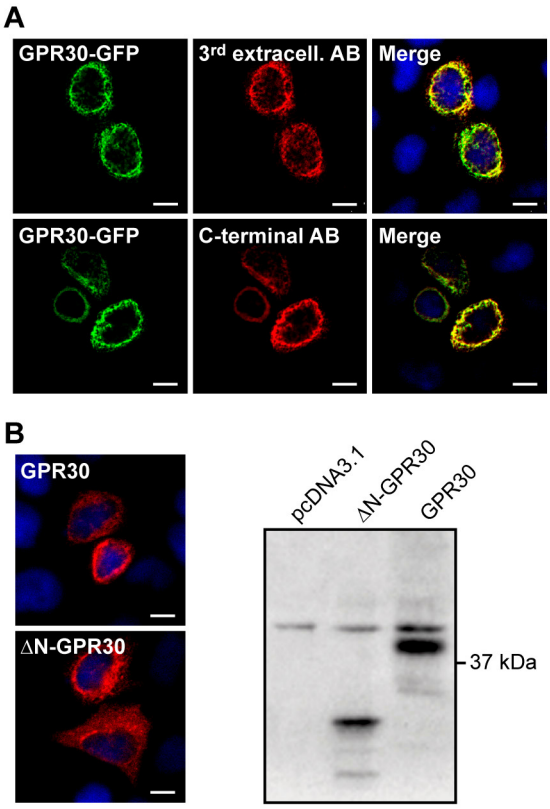


**Fig. 11:** HeLa cells were transiently transfected with EGFP-tagged human GPR30 and stained with antibodies detecting the 3rd extracellular domain (upper panel) or C-terminal domain (lower panel) of GPR30 (A). The EGFP signal (green) and the antibody signal (red) colocalized for both antibodies (yellow signal in the merged images, scale bar = 10 µm). HeLa cells were transiently transfected and cell lysates were immunoblotted with the 3rd extracellular domain antibody (B). The antibody specifically detected full-length GPR30 and N-terminally truncated GPR30 with the expected molecular weight.

In subsequent experiments, all antibodies were tested by immunohistochemistry on sections from different tissues of wildtype as well as Gpr30-lacZ mice. The antibodies were applied on frozen sections after methanol, ethanol, acetone and PFA-fixation as well as on PFA-fixed paraffin-embedded sections (see 2.5). At least brain and kidney sections were analyzed with each antibody. For these experiments cross-species reactivity was assumed, since all antibodies were generated against human peptides. However, the protein is highly conserved between human and mouse with 87% sequence identity, whereas most amino acid exchanges are within the N-terminal domain (56% sequence identity). The N-terminal domain antibody detected smooth muscle cells in paraffin-embedded sections of multiple tissues of murine and human origin, but the signal remained unchanged in Gpr30-lacZ mice and overlapped only partially with the LacZ expression. With the first extracellular domain antibody, no signals were obtained in frozen and paraffin-embedded sections. The C-terminal domain antiserum produced signals in different structures and cell types in frozen- and paraffin-embedded sections of Gpr30-lacZ and wildtype mice. The 3$^{rd}$ extracellular antibody nicely detected LacZ-positive cells in frozen sections of the brain, but the signal was unchanged in Gpr30-lacZ mice (Fig. 12). In subsequent experiments on kidney sections, this antibody failed to detect LacZ-positive cells.

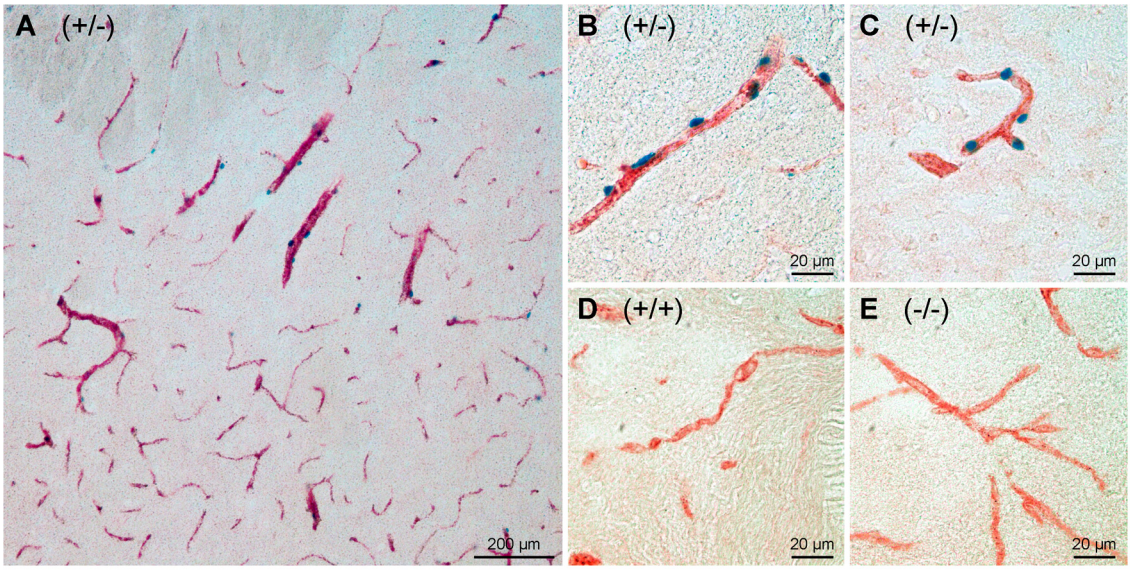


**Fig. 12:** X-gal staining followed by immunohistochemistry with an antibody directed against the 3rd extracellular domain of human GPR30 (A-C). LacZ-positive cells colocalized with the antibody signal. However, staining of frozen sections of wildtype (D) or homozygous Gpr30-lacZ mice (E) revealed that the signal was unchanged in Gpr30-lacZ mice. For immunohistochemistry, frozen brain sections (hypothalamus, 20 µm thick) were fixed with methanol and consecutively incubated with the primary antibody, a biotinylated secondary antibody, and a streptavidin-horseradish peroxidase complex (Strept ABComplex/HRP). Finally, the sections were stained with AEC solution (red dye).

Furthermore, several antibodies directed against different domains of human GPR30 (1st extracellular domain, 3rd extracellular domain, and C-terminal domain) were tested by western blotting on total cell lysates and membrane fractions of the hippocampus and stomach of Gpr30-lacZ and wildtype controls (see 2.4.3). However, specific bands that clearly represent Gpr30 were not detected so far (data not shown). Therefore, the LacZ expression profile and the absence of Gpr30 expression in Gpr30-lacZ mice could not be confirmed at the protein level.

## 3.4 Phenotypic Assessment of Gpr30-lacZ Mice

To gain insight into the function of Gpr30 *in vivo*, Gpr30-lacZ mice were extensively analyzed to identify alterations when compared with wildtype littermates. At the age of genotyping (4-6 weeks), Gpr30-LacZ mice were found at the expected Mendelian ratio on the C57BL/6J as well 129OlaHsd background. Significant differences concerning the survival rate upon aging were absent between Gpr30-LacZ mice and wildtype littermates up to 16 months of age. A general necropsy and histopathological examination of sectioned tissues did not reveal any abnormalities in Gpr30-lacZ mice (data not shown). The body weight as well as lean and fat mass determined by magnetic resonance imaging was not different in homozygous Gpr30-lacZ mice compared to wildtype littermates.

In parallel, a primary phenotype screen was performed at the German Mouse Clinic (GMC, http://www.mouseclinic.de; (Gailus-Durner 2005)), which included the following methods: behaviour (open field, acoustic startle, prepulse inhibition), cardiovascular (blood pressure, heart weight, echocardiography), clinical chemistry (simplified intraperitoneal glucose tolerance test, clinical chemical analysis, hematology), dysmorphology (Dual- Energy X-ray absorptiometry), energy metabolism (calorimetry), eye (eye size, ophthalmoscopy, slit lamp), immunology and allergy (FACS analysis of peripherial blood cells, immune globulin concentrations), lung function (plethysmography), neurology (mod. SHIRPA protocol, grip strength, rotarod), nociception (hot plate), pathology (macro & microscopic analysis), steroid metabolism (dehydroepiandrosterone, testosterone), and molecular phenotyping (cDNA microarrays). Major differences in Gpr30-lacZ mice when compared with wildtype siblings were found in the immunology screen. Under baseline conditions, the proportion of T cells in peripheral blood leukocytes (CD45+) was significantly decreased in Gpr30-lacZ mice. The fraction of CD4+ T cells was reduced by 24.8% in females and by 30.2% in males.

The number of CD8+ T cells was lowered by 20.6% in females and by 28.2% in males. Moreover, the proportion of cells expressing CD62L within the T cell compartment was significantly lower in Gpr30-lacZ mice (59.0% in females, 44.9% in males). These results have been confirmed with a second bleeding in an independent group. Full reports of the immunology screen with detailed information concerning the leukocyte subsets are shown in Tab. 5. In the hematology screen, white and red blood cell counts as well as platelet numbers were not significantly altered in Gpr30-lacZ mice. However, mutants displayed a slightly increased mean corpuscular volume of red blood cells, leading to an increased hematocrit (≈3%). This finding is of unclear relevance and strain-specific differences in the corpuscular volume are known.

Moreover, significant differences were found in the behavior screen. In the Open Field Test, Gpr30-lacZ mice moved less during the first, initial 5 min interval in this novel environment ($p < 0.05$), entered the exposed area, i.e. the centre of the Open Field, later than controls ($p < 0.05$) and moved with slower velocity in the centre ($p < 0.05$). This behavioral pattern indicates a subtle increase in anxiety-related behavior, in the absence of general changes in locomotor or exploratory activity.

Parts of the primary phenotype assessment at the GMC were performed following the EMPReSSslim protocols (Mallon *et al.* 2008). Therefore, the dataset will be available soon on the EuroPhenome webpage (http://www.europhenome.org/) which is an integrated resource that provides access to data and procedures for mouse phenotyping.

**Tab. 5:** Frequencies of main leukocyte subsets in blood of male and female Gpr30-lacZ mice and wildtype littermates analyzed by flow cytometry. The results of two independent bleedings are shown as percentage of all CD45+ viable leukocytes (n=10 per group). The experiments were performed in collaboration with Dr. Thure Adler (German Mouse Clinic, Institute of Experimental Genetics, Helmholtz Zentrum München).

| Parameter | 1st bleeding Gpr30-lacZ | Wildtype | p - value | 2nd bleeding Gpr30-lacZ | Wildtype | p - value |
|---|---|---|---|---|---|---|
| **Females** | | | | | | |
| CD3+ | 21.5 ± 0.9 | 26.6 ± 1.6 | <0.05 | 18.7 ± 0.9 | 24.0 ± 1.7 | <0.05 |
| CD3e+/CD4+ | 9.7 ± 0.5 | 12.9 ± 1.1 | <0.05 | 8.5 ± 0.4 | 11.6 ± 1.0 | <0.05 |
| CD3e+/CD8a+ | 8.5 ± 0.4 | 10.7 ± 0.6 | <0.05 | 7.4 ± 0.4 | 9.9 ± 0.7 | <0.01 |
| CD3e+/CD4+/CD25+ | 6.4 ± 0.5 | 4.9 ± 0.4 | <0.05 | 7.5 ± 0.6 | 5.6 ± 0.5 | <0.05 |
| CD3e+/gd+ | 0.38 ± 0.02 | 0.46 ± 0.03 | n.s. | 0.35 ± 0.02 | 0.4 ± 0.02 | n.s. |
| CD4+/CD62L+ | 16.8 ± 4.8 | 40.1 ± 6.4 | <0.01 | 25.6 ± 5.2 | 58.9 ± 6.0 | <0.001 |
| CD4+/CD44+ | 70.4 ± 0.8 | 73.1 ± 1.5 | n.s. | 72.9 ± 0.8 | 75.4 ± 0.9 | n.s. |
| CD8a+/CD62L+ | 19.0 ± 5.6 | 47.4 ± 7.2 | <0.01 | 29.8 ± 5.6 | 66.3 ± 6.8 | <0.001 |
| CD8a+/CD44+ | 58.1 ± 0.9 | 58.8 ± 1.2 | n.s. | 64.1 ± 0.8 | 62.4 ± 0.9 | n.s. |
| CD11b+/Gr1+ | 7.6 ± 0.9 | 6.3 ± 0.4 | n.s. | 16.4 ± 2.1 | 12.6 ± 0.6 | n.s. |
| CD11b+/nonGra/nonNK | 6.2 ± 1.0 | 5.9 ± 0.4 | n.s. | 4.3 ± 0.6 | 3.9 ± 0.5 | n.s. |
| NK+/CD5+ | 0.3 ± 0.01 | 0.3 ± 0.02 | n.s. | 0.3 ± 0.02 | 0.4 ± 0.02 | n.s. |
| NK+/CD5- | 3.6 ± 0.3 | 3.8 ± 0.2 | n.s. | 3.4 ± 0.7 | 3.7 ± 0.3 | n.s. |
| CD19+ | 58.9 ± 1.7 | 54.3 ± 2.1 | n.s. | 53.7 ± 2.2 | 50.3 ± 1.9 | n.s. |
| CD19+/IgD+ | 92.8 ± 0.3 | 92.6 ± 0.4 | n.s. | 92.8 ± 0.8 | 90.7 ± 0.9 | n.s. |
| CD19+/CD5+ | 2.5 ± 0.1 | 2.6 ± 0.2 | n.s. | 1.9 ± 0.1 | 2.5 ± 0.2 | <0.01 |
| CD19+/MHC II+/B220+ | 81.8 ± 1.2 | 85.2 ± 0.9 | <0.05 | 84.1 ± 1.0 | 82.8 ± 1.0 | n.s. |
| CD11b+/NK+ | 45.4 ± 1.8 | 51.8 ± 2.4 | <0.05 | 39.6 ± 1.9 | 44.4 ± 2.4 | n.s. |
| **Males** | | | | | | |
| CD3+ | 13.6 ± 1.3 | 18.7 ± 1.0 | <0.01 | 12.3 ± 1.0 | 17.2 ± 1.0 | <0.01 |
| CD3e+/CD4+ | 6.0 ± 0.6 | 8.6 ± 0.6 | <0.01 | 5.1 ± 0.5 | 7.4 ± 0.6 | <0.01 |
| CD3e+/CD8a+ | 5.6 ± 0.5 | 7.8 ± 0.5 | <0.01 | 5.9 ± 0.5 | 8.1 ± 0.4 | <0.01 |
| CD3e+/CD4+/CD25+ | 7.1 ± 0.5 | 5.9 ± 0.5 | n.s. | 8.3 ± 0.5 | 6.2 ± 0.6 | <0.05 |
| CD3e+/gd+ | 0.27 ± 0.03 | 0.3 ± 0.02 | n.s. | 0.25 ± 0.03 | 0.3 ± 0.02 | n.s. |
| CD4+/CD62L+ | 22.6 ± 7.1 | 43.4 ± 7.1 | n.s. | 16.8 ± 2.8 | 42.6 ± 7.9 | <0.01 |
| CD4+/CD44+ | 70.5± 1.0 | 72.0 ± 0.9 | n.s. | 69.3 ± 1.2 | 70.5 ± 0.9 | n.s. |
| CD8a+/CD62L+ | 28.2 ± 7.1 | 48.6 ± 7.2 | n.s. | 24.2 ± 3.4 | 50.1 ± 8.1 | <0.05 |
| CD8a+/CD44+ | 65.4 ± 1.8 | 63.8 ± 1.9 | n.s. | 66.2 ± 0.8 | 64.3 ± 1.3 | n.s. |
| CD11b+/Gr1+ | 9.6 ± 1.8 | 8.0 ± 0.9 | n.s. | 16.4 ± 1.1 | 14.7 ± 1.0 | n.s. |
| CD11b+/nonGra/nonNK | 6.3 ± 0.7 | 6.0 ± 0.6 | n.s. | 3.3 ± 0.1 | 3.4 ± 0.2 | n.s. |
| NK+/CD5+ | 0.3 ± 0.03 | 0.3 ± 0.01 | n.s. | 0.3 ± 0.02 | 0.3 ± 0.03 | n.s. |
| NK+/CD5- | 3.3 ± 0.2 | 3.2 ± 0.2 | n.s. | 4.2 ± 0.3 | 3.7 ± 0.3 | n.s. |
| CD19+ | 66.8 ± 2.4 | 63.6 ± 1.9 | n.s. | 60.3 ± 1.9 | 57.4 ± 1.5 | n.s. |
| CD19+/IgD+ | 92.7 ± 0.3 | 93.5 ± 0.2 | <0.05 | 92.1 ± 0.5 | 92.2 ± 0.4 | n.s. |
| CD19+/CD5+ | 1.9 ± 0.1 | 2.4 ± 0.1 | <0.05 | 1.4 ± 0.1 | 1.9 ± 0.1 | <0.05 |
| CD19+/MHC II+/B220+ | 85.1 ± 0.7 | 85.7 ± 0.8 | n.s. | 81.4 ± 1.2 | 81.2 ± 1.2 | n.s. |
| CD11b+/NK+ | 29.7 ± 3.1 | 32.8 ± 2.4 | n.s. | 48.0 ± 3.5 | 45.4 ± 2.6 | n.s. |

Main lineages: T cells (CD3+), CD4+ T cells, CD8+ T cells, γδT cells, T reg cells (CD4+CD25+), B cells (CD19+, resp. B220+), B1 B cells (/CD5+), mature B cells (/IgD+), granulocytes (CD11b+Gr1++), NK cells (DX5+CD3-), NK T cells (DX5+ CD3+)
Subpopulations: Further subpopulations are identified by bi-variate gating with the following markers:
T cells/ non Tcells: CD25, CD62L, Ly-6C, CD44, CD45RB, CD103.
CD19+ cells: IgD, B220, CD11b, CD5, Gr1; CD19- cells: Gr1, B220, CD5, CD11b.

## 3.5 Yeast Two-Hybrid Screening

To identify interacting proteins, yeast two-hybrid screenings were performed with the N- and C-terminal domains of GPR30 (Fig. 13A, see also 2.2). The N- and C-terminal domains of GPR30 were selected, since they most likely adapt the native conformation when isolated from the receptor. To generate the yeast baits, sequences encoding the N-terminal amino acids 1-54 or the C-terminal amino acids 330-375 of the human GPR30 were subcloned downstream of LexA into the EcoRI/BamHI site of the bait vector pBTM116 (Fig. 13B). The bait vector generates a fusion protein of the subcloned sequence N-terminally tagged with LexA when transformed into yeast (Fig. 13C). A human heart cDNA library subcloned in the XhoI restriction site of the pACT2 prey vector was co-transformed to screen for interacting proteins (Fig. 13B). The vector has a polylinker downstream of the GAL4 activation domain (amino acids 768–881) fused to an HA epitope tag. In yeast, pACT2 generates a fusion protein of the GAL4 domain, an HA epitope tag, and a protein encoded in the library if subcloned into the polylinker in the correct orientation and reading frame (Fig. 13C). Interaction of bait and prey proteins leads to the formation of an active transcription factor complex that induces the expression of the two reporter genes HIS3 and lacZ in LV40 yeasts (Fig. 13D).

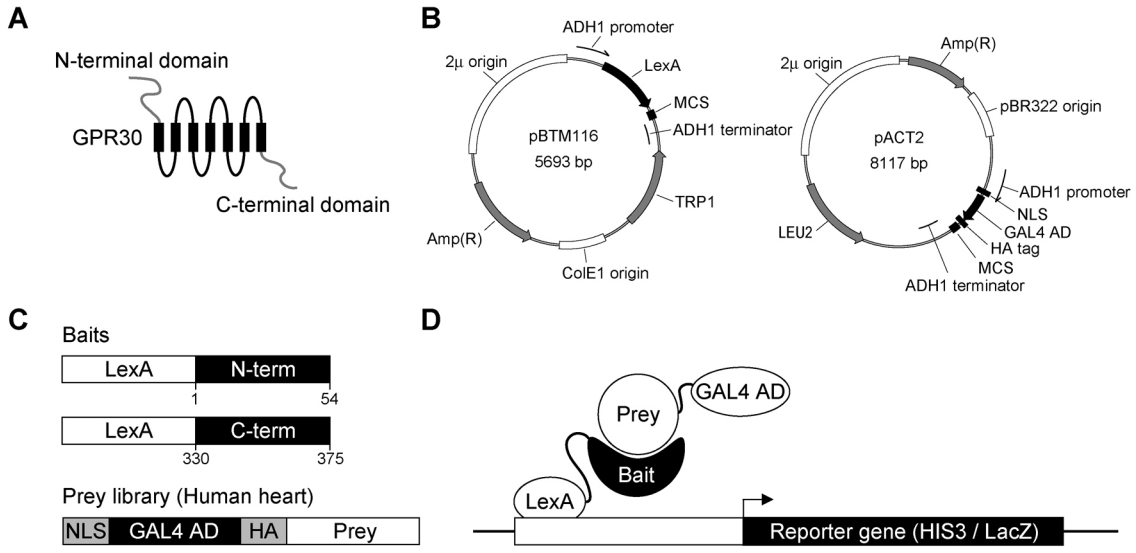


**Fig. 13:** Screening for interacting proteins using the yeast two-hybrid system. The N- and C-terminal domains of GPR30 (A) were subcloned into the bait vector pBTM116 (B) and expressed as fusion proteins with the LexA DNA-binding domain (C) in LV40 yeast. A human heart cDNA library subcloned into the prey vector pACT2 (B) was co-transformed to screen for interacting proteins. Interaction of bait and prey proteins leads to the formation of an active transcription factor complex that induces the expression of the reporter gene HIS3 and LacZ (D). MCS, multiple cloning site; NLS, nuclear localization signal; HA, hemagglutinin epitope tag; TRP1, N-(5'-phosphoribosyl)anthranilate isomerase; LEU2, 3-isopropylmalate dehydrogenase; GAL4 AD, GAL4 activation domain; ADH1, alcohol dehydrogenase 1.

For both baits (i.e. the N- and C-terminal domain baits) > 200 colonies were obtained in two independent screens. Prey plasmids were isolated from 20 (N-terminal bait) and 30 (C-terminal bait) randomly selected clones and sequenced. Informative sequencing results were obtained for 19 clones from the N-terminal screen and 22 clones from the C-terminal screen, respectively. Blast analysis against the human genome revealed that most sequences mapped to PDZ domain-containing 2 (PDZD2) for the N-terminal screen, as well as Pals1-associated tight junction protein (PATJ) and FUN14 domain-containing 2 (FUNDC2) for the C-terminal screen (Tab. 6). Clones encoding genomic sequences without homology to known genes were found in the N-terminal (N13) and C-terminal screen (C22).

**Tab. 6:** Interaction partners of the N- and C-terminal domains of GPR30 identified by yeast two-hybrid screening.

| Gene Symbol or clone ID | Description | No of clones | E value |
|---|---|---|---|
| **N-terminal domain** | | | |
| PDZD2 | PDZ domain containing 2 | 16 | 0.0 |
| ZBTB16 (PLZF) | Zinc finger and BTB domain containing 16 | 1 | 0.0 |
| N13 | Intergenic region | 1 | 0.0 |
| **C-terminal domain** | | | |
| PATJ (INADL) | Pals1-associated tight junction protein | 11 | 0.0 |
| FUNDC2 | FUN14 domain containing 2 | 10 | 0.0 |
| ZBTB16 (PLZF) | Zinc finger and BTB domain containing 16 | 2 | 0.0 |
| MORC2 | MORC family CW-type zinc finger 2 | 1 | 0.0 |
| C22 | Intergenic region | 1 | 0.0 |

Interaction between bait and preys was confirmed by re-transformation of bait and prey plasmids back into yeast. True positive interacting clones grew again on selective agar plates and were positive in LacZ activity filter assays (Fig. 14). Two controls were always included: (i) Clones co-transformed with the bait vector pBTM116-Nterm or pBTM116-Cterm as well as the empty prey vector pACT2 and (ii) clones co-transformed with the empty bait vector pBTM116 as well as the prey vector encoding the candidate sequence.

For all clones of the N-terminal screen either LacZ activity was detected in the controls (PDZD2, ZBTB16) or the clones did not grew again after retransformation (N13) (Fig. 14A). Using the C-terminal domain of Gpr30 as bait, clones encoding sequences

of PATJ, FUNDC2, the MORC family CW-type zinc finger 2 (MORC2), and C22 were positive in LacZ activity filter assays without signals in the negative controls. However, several of the candidates were considered as false positives and excluded from further analysis. C22 maps to intergenic regions on the mitochondrial genome as well as chromosome 3, 5, and 11. Translation of the sequence revealed a stop codon after eight amino acids and the resulting peptide was not related to a known protein. Zinc finger and BTB domain-containing protein 16 (ZBTB16) was found in the N- as well as C-terminal screen. Weak activation of the LacZ reporter occurred in the absence of the bait proteins which indicates auto-activating properties of ZBTB16 (Fig. 14A,B).

In conclusion, the efforts to identify proteins which interact with the N- or C-terminal domain of GPR30 using the yeast two-hybrid system ended up with three candidates (MORC2, PATJ, FUNDC2) for the C-terminal domain screen. To further narrow down the interaction sites of the candidates with the C-terminal domain of GPR30, the prey sequences were translated and aligned with the corresponding full-length proteins (Fig. 15). The potential interaction site of PATJ was within three C-terminal PDZ domains (amino acids 1381-1801). FUNDC2 bound GPR30 with its FUN14 domain (amino acids 47-189). MORC2 interacted with GPR30 within the C-terminal amino acids 814-970. Since MORC2 contains a CW-type zinc finger domain known to be involved in DNA binding, it was assumed that MORC2 likely represents a nuclear protein indicating an artificial nature of the interaction. Due to this fact, the interaction was not further analyzed here. PATJ is a multiple PDZ domain containing protein which associates with tight junction complexes. The interaction of PATJ with GPR30 was verified by co-immunoprecipitation by the PhD student Valeria Zazzu and will be further analyzed by her. Within the scope of this thesis, the potential interaction of FUNDC2 with the C-terminal domain of GPR30 was investigated by co-immuno-precipitation and colocalization in transfected cell lines in more detail.

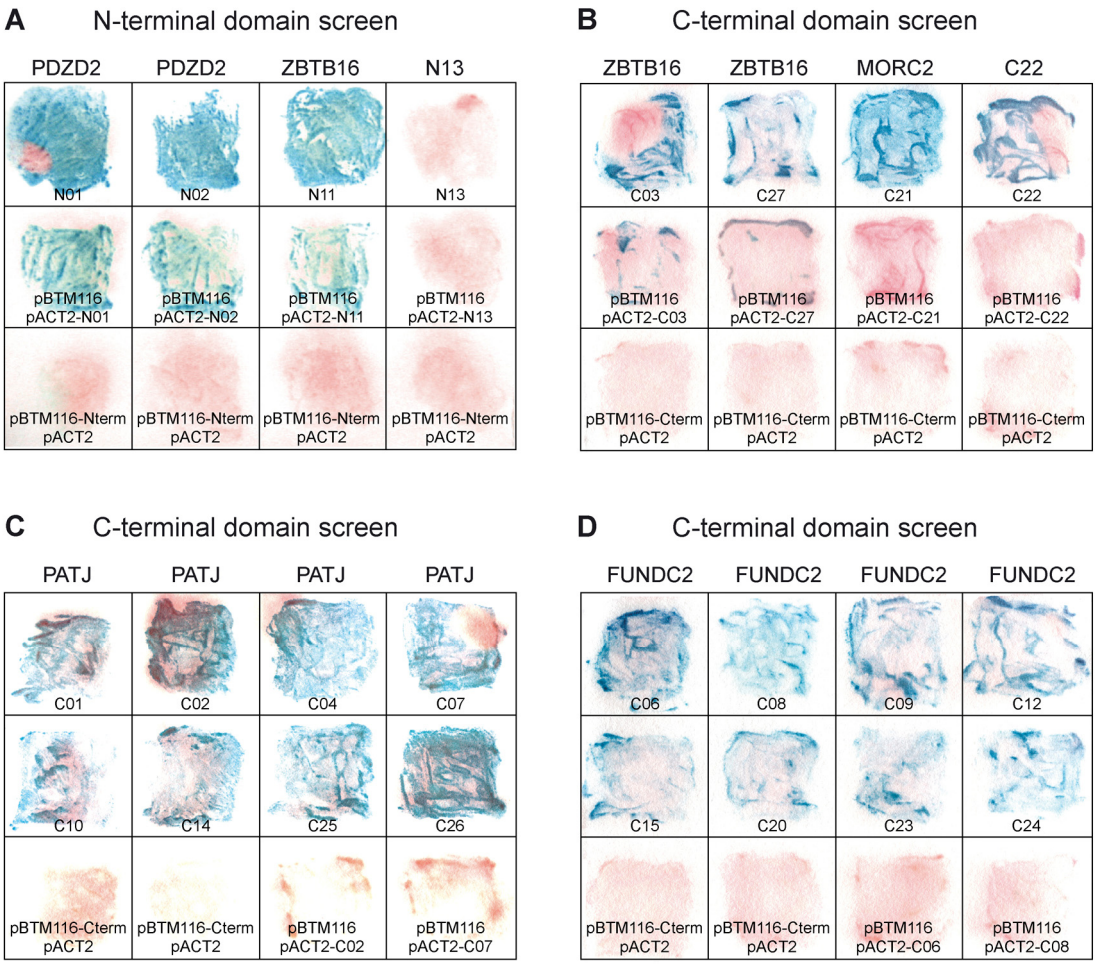


**Fig. 14:** LacZ activity filter assays performed after retransformation of bait and prey plasmids back into yeast. Results of the N-terminal (A) and C-terminal screen (B-C) are shown. Controls without either bait or prey proteins are included for each candidate. Several independent clones are shown for PDZD2, ZBTB16, PATJ, and FUNDC2.

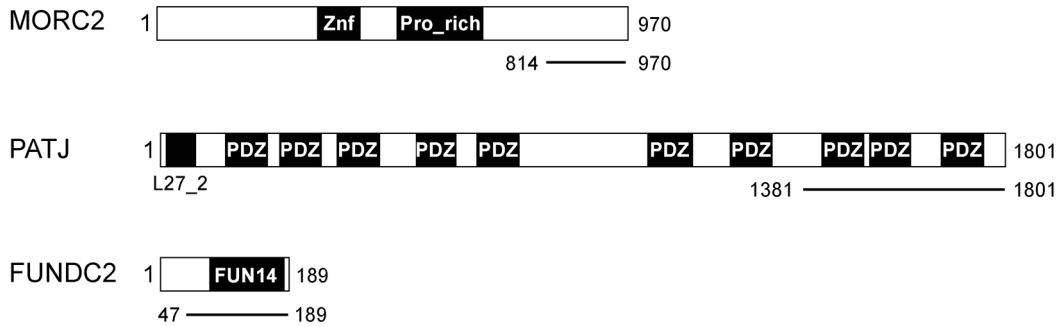


**Fig. 15:** Interaction sites within the proteins identified by yeast two-hybrid screening. The overall structure of the interacting proteins is shown, relevant domains are highlighted. The amino acid stretch encoded in the isolated prey clones (overlap of all sequenced clones) is indicated by the bars below the protein structures. Znf, Zinc finger (CW-type); Pro_rich, Proline-rich region; PDZ, PDZ domain; L27_2, L27_2 domain; FUN14, FUND14 domain.

## 3.6 Co-immunoprecipitation of GPR30 and FUNDC2

Interactions identified by yeast two-hybrid screening have to be verified by an independent approach. Therefore, co-immunoprecipitations were performed with HEK293 cells transiently co-expressing N-terminally HA-tagged GPR30 (HA-GPR30) and N-terminally Myc-tagged FUNDC2 (Myc-FUNDC2). N-terminally tagged constructs were selected, since the interaction was found to engage the C-terminus of GPR30 and the C-terminal FUN14 domain of FUNDC2 by yeast two-hybrid screening. The used RIPA-buffer based protocol (see 2.4.4) was already successfully applied to co-immunoprecipitate 7TMRs with interacting proteins (Rondou *et al.* 2008). As shown in Fig. 16, HA-GPR30 (lanes 2 and 4) and Myc-FUNDC2 (lanes 3 and 4) were properly expressed in total cell lysate of transfected HEK293 cells. The two bands of similar molecular weight found in lysates of HA-GPR30 transfected cells probably indicate posttranslational modifications of GPR30. Myc-FUNDC2 was successfully bound to the protein G sepharose beads by the anti-Myc antibody. However, HA-GPR30 was absent in the immunoprecipitate (no band using the anti-HA antibody in lane 4 after immunoprecipitation). Therefore, the interaction of GPR30 with FUNDC2 could not be verified using this approach.

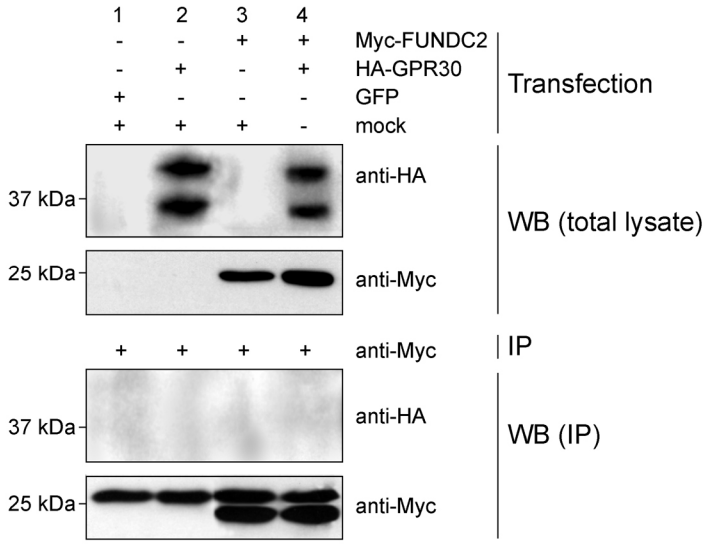


**Fig. 16:** Co-immunoprecipitation of GPR30 and FUNDC2. HEK293 cells were transiently transfected with N-terminally HA-tagged GPR30 and/or N-terminally Myc-tagged FUNDC2. Immunoprecipitation and Western blotting were performed using a mouse monoclonal anti-Myc and anti-HA antibodies. The potential interaction of both proteins could not be verified using this approach.

## 3.7 FUNDC2 Proteins Interact in Transfected HeLa Cells

Initially, the subcellular localization of FUNDC2 tagged N-terminally with YFP (YFP-FUNDC2) was investigated in transfected HeLa cells for colocalization studies with GPR30. However, YFP-FUNDC2 clearly localized to an unknown compartment or formed protein aggregates within the cell (Fig 17D) and did not colocalize with GPR30 (data not shown). To rule out an influence of the tag on the intracellular localization of FUNDC2, different FUNDC2 constructs with various N- or C-terminal terminal tags were constructed using a Gateway based cloning strategy (see 2.1.11). A strong impact of the N-terminal tag on the intracellular localization of FUNDC2 was observed by confocal immunoflourescence. The intracellular distribution was scattered over the whole cytoplasm in case of Myc- or FLAG-tag and was clearly different from HA- or YFP-FUNDC2 (Fig 17A-D). To verify the correct in frame expression of FUNDC2 with the respective N-terminal tag, western blotting with a commercial FUNDC2-specific antibody was performed (Fig 17E). The antibody detected all FUNDC2 constructs with the expected size in cell lysates from transfected HeLa cells. Moreover, endogenous expression of FUNDC2 was absent in HeLa cells. Therefore, the detection of untagged FUNDC2 was required to clarify the real intracellular localization in transfected cell lines and in cell lines endogenously expressing the protein. However, the antibody did not work in immunocyto- or immunohistochemistry (frozen brain sections) so far, which may indicate that the antibody recognizes only the denatured protein.

Cotransfection of Myc-, FLAG, or HA-FUNDC2 along with YFP-FUNDC2 revealed that all three N-terminally tagged FUNDC2 variants colocalized always with YFP-FUNDC2 in double transfected cells (Fig 18). This observation led to the hypothesis that FUNDC2 proteins form dimers or even multimers within the cell. In subsequent co-immunoprecipitations, the interaction of YFP-FUNDC2 and Myc-FUNDC2 was analyzed in detail (Fig. 19). As shown in lanes 7-9, both constructs were expressed in transfected Hela cells. YFP-FUNDC2 and Myc-FUNDC2 were enriched on the beads after immunoprecipitating with anti-YFP (lane 5) or anti-Myc (lane 4) antibodies, respectively. Immunoprecipitation with an anti-Myc antibody verified the interaction, since the GFP band appeared in lane 4. However, the interaction could not be verified vice versa, since unspecific bands overlapped with the expected Myc-signal at 25 kDa (lane 1 and 5).

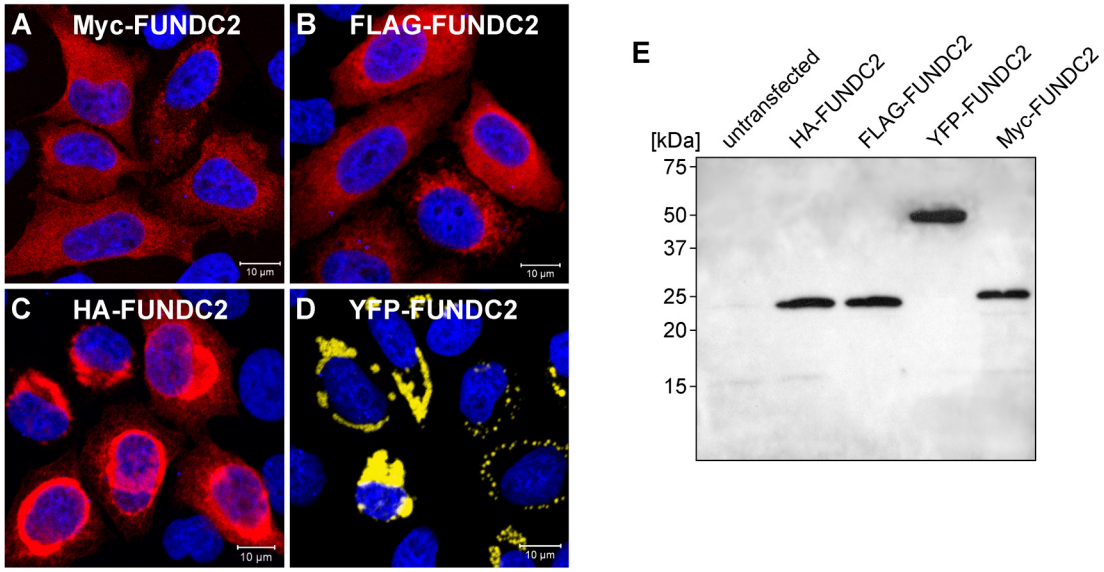


**Fig 17:** Expression of human FUNDC2 with N-terminal Myc-, FLAG-, HA-, or YFP-tags in transiently transfected HeLa cells. The intracellular distribution of FUNDC2 was analysed by confocal microscopy with monoclonal antibodies directed against Myc (A), FLAG (B), and HA (C) or the fluorescence signal of YFP (D). The intracellular localization of FUNDC2 differed depending on the N-terminal tag. All constructs were detected at the expected size of 23.7 kDa (HA-FUNDC2), 23.1 kDa (FLAG-FUNDC2), 49.1 kDa (YFP-FUNDC2), or 23.2 kDa (Myc-FUNDC2) by immunoblotting with a FUNDC2-specific monoclonal antibody (E). Scale bar = 10 µm.

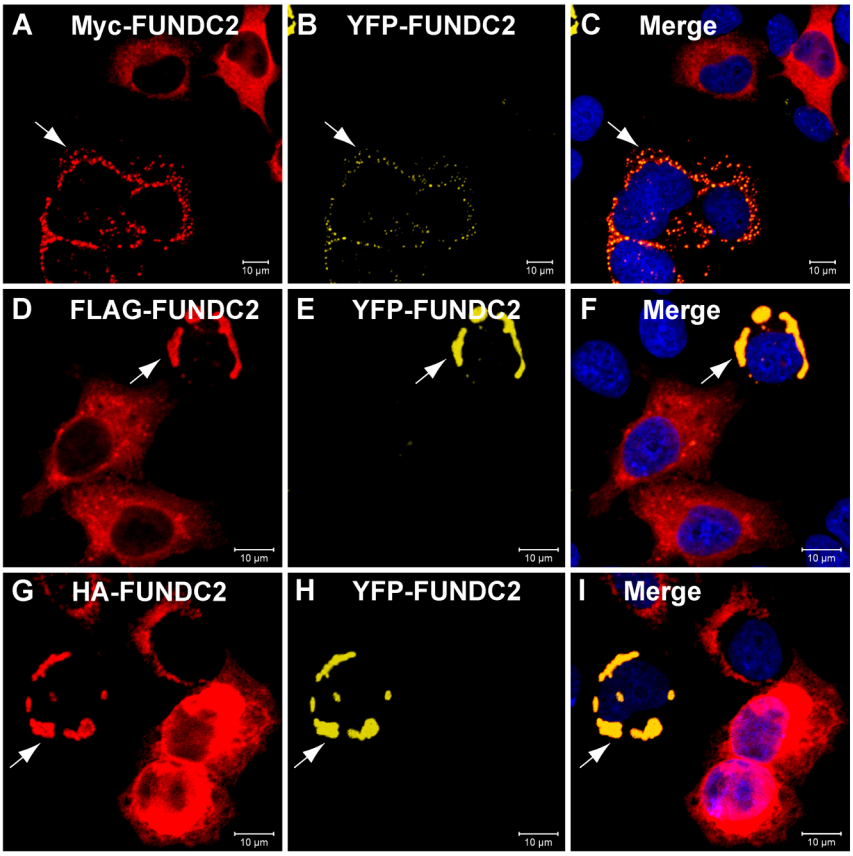


**Fig 18:** Cotransfection of N-terminally Myc- (A-C), FLAG- (D-F), or HA-tagged FUNCD2 (G-I) and YFP-FUNDC2. Of note, YFP-FUNDC2 always colocalized with Myc- FLAG, or HA-FUNDC2 in cotransfected cells (white arrows). Scale bar = 10 µm.

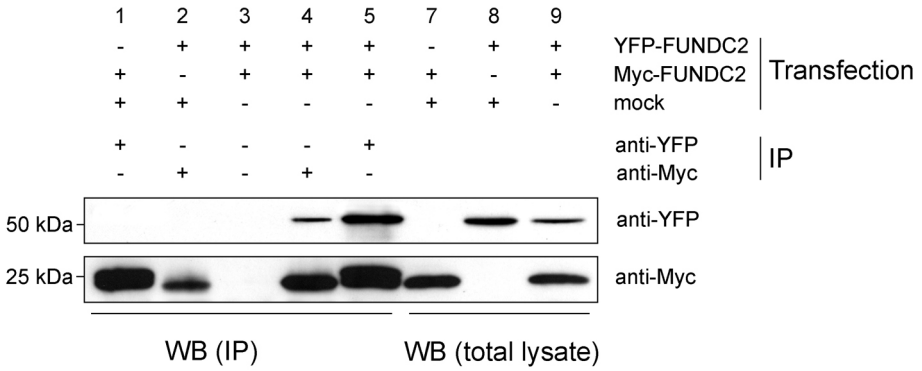


**Fig. 19:** Dimerization of FUNDC2. HeLA cells were transiently transfected with YFP-FUNDC2, Myc-FUNDC2 or both constructs. Immunoprecipitation and Western blotting were performed using a mouse monoclonal anti-YFP antibody and a rabbit polyclonal anti-Myc antibody.

# 4 DISCUSSION

This thesis aimed to contribute to the functional analysis of the seven-transmembrane receptor GPR30. Previous results suggested that GPR30 might be an estrogen receptor of novel type that binds estrogens at the plasma or endoplasmic reticulum membrane and mediates the rapid activation of signaling pathways in the absence of classical nuclear ERs (Filardo *et al.* 2007; Prossnitz *et al.* 2008). However, other groups could not reproduce these findings in independent experiments and still consider GPR30 as an orphan receptor with unknown function (Pedram *et al.* 2006; Otto *et al.* 2008b). Therefore, definitive proof for GPR30 being an estrogen receptor awaits binding studies with pure detergent-solubilized receptor and better studies of the downstream signaling pathways. Moreover, the physiological role of GPR30 *in vivo* remained unknown due to the lack of knowledge concerning the expression of GPR30 at the cell type level and the comprehensive analysis of Gpr30-deficient and transgenic mouse models.

To tackle these questions, the expression profile of a LacZ reporter and the phenotype caused by Gpr30-deficiency was analyzed in a mutant mouse model that harbors a LacZ reporter (Gpr30-lacZ) in the Gpr30 locus leading to a partial deletion of the coding sequence. Using this model, a cellular basis for the function of Gpr30 *in vivo* was established. To further gain information about the signaling complex of human GPR30 at the molecular level, yeast two-hybrid screens were performed with the N- and C-terminal domains as bait.

## 4.1 Endogenous Expression Pattern of GPR30

A prerequisite for the analysis of the physiological role of Gpr30 is a detailed knowledge about the tissue distribution at the cell type level. Several studies investigated the expression of Gpr30 by real-time PCR (Martensson *et al.* 2008), RNase protection assays (Otto *et al.* 2008a), northern blotting (Owman *et al.* 1996; Carmeci *et al.* 1997; Feng and Gregor 1997), or western blotting (Pedram *et al.* 2006; Wang *et al.* 2007) in various tissues of rodent and human origin, suggesting expression of the receptor at low levels in multiple tissues. However, due to a lack of specific methods that enable the detection of Gpr30 protein within tissues, the cellular basis of the expression profile remained unknown. Therefore, LacZ reporter mice were used here allowing the identification of Gpr30-positive cells within tissues. Since the LacZ assay facilitates remarkable signal amplification, this approach is especially useful if low expression levels are assumed. To validate that the expression of the targeted LacZ transcript

resembles the expression of the endogenous wildtype Gpr30 transcript, both alleles were quantified by real-time PCR in various tissues of heterozygous Gpr30-lacZ mice. The results revealed that the expression of the wildtype and the targeted allele correlated significantly, showing that the integration of the cassette did not affect the Gpr30 promoter activity. In agreement with prominent LacZ activity in SMCs and pericytes of the brain, highest expression of Gpr30 mRNA was detected in isolated brain vessels. A ubiquitous expression of Gpr30 mRNA at low levels might correspond to LacZ-positive vessel-associated cells found in multiple tissues of Gpr30-lacZ mice. Published data obtained by RNase protection assays revealed prominent expression of Gpr30 mRNA in the stomach, followed by the adrenal gland (Otto *et al.* 2008a). These findings are consistent with LacZ-positive gastric chief cells and chromaffin cells in the medulla of the adrenal glands. In line with published findings (Martensson *et al.* 2008; Otto *et al.* 2008a), Gpr30 mRNA as well as LacZ reporter activity were absent in the liver and thymus. In summary, Gpr30-lacZ mice likely represent a valid Gpr30 reporter model.

The identified LacZ-positive cells were characterized by colocalization of LacZ along with cell type specific markers. Using this strategy, the following cell populations were identified: (i) an endothelial cell subpopulation in small arterial vessels of multiple tissues (e.g. kidney, heart, peritoneum, genital tract), (ii) smooth muscle cells and pericytes in the brain, (iii) gastric chief cells in the stomach, (iv) neuronal subpopulations in layer II of the cortex as well as in the polymorph layer of the dentate gyrus, and (v) cell populations in the intermediate and anterior lobe of the pituitary gland as well as (vi) chromaffin cells in the medulla of adrenal glands.

In previous reports, the cell type-specific expression of Gpr30 was predominantly investigated in the rat brain (Brailoiu *et al.* 2007; Sakamoto *et al.* 2007; Matsuda *et al.* 2008). The expression of Gpr30 was determined by immunohistochemistry using a polyclonal antiserum directed against the C-terminal domain of the human GPR30 (Brailoiu *et al.* 2007; Sakamoto *et al.* 2007) and *in situ* hybridization (Sakamoto *et al.* 2007), whereas the signal obtained by both methods overlapped partially. Matsuda *et al.* reported the expression of rat GPR30 in pyramidal cells of the hippocampal regions CA1-3 and granule cells of the dentate gyrus (Matsuda *et al.* 2008). LacZ-positive neurons were found in the dentate gyrus of Gpr30-lacZ mice as well, but the expression was restricted to interneurons in the polymorphic layer.

Two other studies found that Gpr30 is expressed by magnocellular oxytocin-positive neurons in the paraventricular and supraoptic nuclei of the rat hypothalamus (Brailoiu *et al.* 2007; Sakamoto *et al.* 2007). Since oxytocin is known to regulate reproductive functions including parturition, milk ejection, and sexual as well as maternal behavior (Russell and Leng 1998), the authors speculate that estrogen influences oxytocin-positive neurons by activating Gpr30. In contrast to these reports, no LacZ-positive neurons were observed in the paraventricular and supraoptic nuclei of Gpr30-lacZ mice. In the hypothalamus, all identified LacZ-positive cells were associated to vessels and colocalized with α-SMC actin.

A heterogeneous and sexually dimorphic distribution pattern of Gpr30 mRNA has been reported for hypothalamic, amygdalar, and cerebellar areas of the hamster brain (Canonaco *et al.* 2008). Although the LacZ reporter assay is not quantitative, LacZ activity was found in the vasculature without differences between sexes at the cell type level. The heterogeneous expression profile observed by Canonaco *et al.* might also be caused by sex-specific differences in vessel size and abundance.

In addition to oxytocin-positive neurons (Sakamoto *et al.* 2007), granulosa cells of preantral follicles as well as mammary and uterine epithelial cells were found to express Gpr30 in an estrous-cycle-dependent manner (Wang *et al.* 2007; Prossnitz *et al.* 2008), supporting the hypothesis that Gpr30 mediates estrogen responses in reproductive organs. Conversely, granulosa cells, mammary and uterine epithelial cells were negative for LacZ expression in Gpr30-lacZ mice. However, LacZ-positive cells were located in blood vessels of Gpr30-lacZ mice, which may explain the expression of Gpr30 mRNA in these tissues.

Several reasons need to be considered to explain the inconsistency between the LacZ expression pattern and previous reports employing *in situ* hybridization or immunohistochemistry. The major drawback of these studies is the lack of critical experiments clearly confirming the specificity of used antibodies and probes. So far, no study reported the absence of a signal obtained by immunohistochemistry or western blotting in a Gpr30-deficient mouse model (Martensson *et al.* 2008; Otto *et al.* 2008a; Wang *et al.* 2008a). Within the scope of this thesis, several commercial antibodies and the mentioned antiserum directed against the C-terminal domain of human GPR30 were tested without success on sections of wildtype and homozygous Gp30-lacZ mice assuming cross-reactivity of the applied antibodies. These findings underline the difficulty to detect murine Gpr30 protein in tissues, probably due to low expression levels, the

lipophilic properties, and the lack of antibodies specifically recognizing the murine receptor with high affinity. Nevertheless, cell type-specific differences in the activity of the IRES element allowing nonclassical cap-independent translation of LacZ may also influence the results masking low expression of Gpr30. It is well known that endogenous mammalian IRES elements such as the FGF-2 or c-*myc* IRES are regulated during development or in a cell type-specific manner (Creancier *et al.* 2000; Creancier *et al.* 2001), but the used viral *Encephalomyocarditis* virus (EMCV) IRES has been shown to be ubiquitously active in various tissues (Creancier *et al.* 2001) and was frequently employed to express LacZ in reporter models. However, using IRES-lacZ cassettes introduced into the Lmo2 gene, which is ubiquitously expressed in embryonic endothelial cells, Chung *et al.* compared the activity of the EMCV IRES and the hepatitis C virus (HCV) IRES by LacZ assays in embryonic tissues (Chung *et al.* 2003). They found that the HCV IRES, but not the EMCV IRES, is used efficiently for protein synthesis in embryonic endothelial cells. Indeed, LacZ activity was absent in embryonic endothelial cells of Gpr30-lacZ mice at different stages of embryonic development (data not shown). Therefore, the observation that LacZ activity was restricted to special vascular beds in adult mice might also be caused by cell type-specific differences in the activity of the EMCV IRES. Cell type-specific IRES activity could not be excluded in Gpr30-lacZ mice, but the presented LacZ data are in good accordance with RT-PCR, real-time PCR and RNase Protection assays. The LacZ data presented here may not comprise all Gpr30-expressing cell types, but provides clear evidence that various cell types not identified by the C-terminal antiserum or *in situ* hybridization in previous reports express the receptor.

Concerning the expression of GPR30 in humans, three early reports investigated GPR30 mRNA expression by Northern blotting in multiple human tissues, but the findings were contradictory for several tissues (e.g. lung, liver, placenta) (Owman *et al.* 1996; Carmeci *et al.* 1997; Feng and Gregor 1997). Later studies applied the C-terminal antiserum to detect GPR30 in human paraffin embedded sections and found immunoreactivity in breast and endometrial carcinomas (Filardo *et al.* 2006; Smith *et al.* 2007) as well as in bone (Heino *et al.* 2008). In line with our findings in Gpr30-lacZ mice, expression of GPR30 mRNA was recently reported for human internal mammary arteries and saphenous veins (Haas *et al.* 2007), but more studies are needed to translate the findings observed in rodent models to humans.

## 4.2 Phenotype Assessment of Gpr30-lacZ Mice

To ensure the successful disruption of the Gpr30 coding sequence, the integration of the cassette into the mouse genome was analyzed by Southern blotting with three probes that hybridized 5' and 3' of the homology arms as well as in the cassette. The results confirmed the accurate integration of the cassette into the Gpr30 locus leading to the deletion of the sequence encoding the first two transmembrane domains and loops. Since the targeting construct did not include a polyadenylation site terminating transcription 3' of the neomycin resistance, a fusion transcript composed of the neomycin resistance and the truncated exon 3 of Gpr30 was expressed in Gpr30-lacZ mice. Nevertheless, expression of a truncated protein with persistent functionality is unlikely, since (i) several stop codons terminate the neomycin resistance, (ii) the neomycin resistance is not in frame with Gpr30, (iii) no translational start sites are known within the truncated Gpr30 transcript, and (iv) the mutation probably disrupts the functionality of Gpr30.

Three other Gpr30 knockout mouse models (Gpr30KO) were published during the preparation of this thesis (Martensson *et al.* 2008; Otto *et al.* 2008a; Wang *et al.* 2008a). At the age of weaning, Gpr30-LacZ mice and other Gpr30KOs (Otto *et al.* 2008a; Wang *et al.* 2008a) were found with the expected Mendelian ratio and survival rates were not compromised during adulthood up to an age of at least 16 months.

Gpr30-lacZ mice were fertile without any reproductive abnormalities. Otto *et al.* (2008) recently analyzed the function of Gpr30 in the reproductive system in detail using a Gpr30-deficient model ($Gpr30KO^{O}$) generated with the Cre/LoxP system (Otto *et al.* 2008a). Although Gpr30 mRNA was expressed in all reproductive organs of wildtype females, histopathological analysis of $Gpr30KO^{O}$ mice did not reveal any abnormalities. Moreover, estrogenic responses in the uterus and the mammary gland were unchanged in different assays such as morphological measures, cellular proliferation and target gene expression. In conclusion, these findings demonstrate that Gpr30 is dispensable for the mediation of estrogen effects in reproductive organs *in vivo*.

In a study by Martensson *et al.* (2008), the metabolic consequences of Gpr30 gene deletion were investigated in a knockout mouse model ($Gpr30KO^{M}$) (Martensson *et al.* 2008). They found that female, but not male $Gpr30KO^{M}$ mice had hyperglycemia and impaired glucose tolerance, reduced body weight, increased blood pressure, and reduced serum insulin-like growth factor-I levels. Female $Gpr30KO^{M}$ mice exhibited an age-dependent reduction of the body weight (-9.6% at 5 months of age) which correlated with a proportional decrease in skeletal growth of the axial and the appendicular

skeleton. The organ weight to body weight ratio for several major organs and the fat mass was unaffected indicating a proportional growth disturbance in female Gpr30KO$^{M}$ mice. In contradiction to these results, no significant differences concerning the body weight and fat mass were detected in male and female Gpr30-lacZ mice. However, the results in Gpr30-lacZ mice are in line with another Gpr30-deficient model (Gpr30KO$^{O}$) on a pure C57BL/6 background which did not exhibit body weight phenotype as well (Otto *et al.* 2008a). Since Gpr30KO$^{M}$ mice were on a mixed background (backcrossed for 6 generations) and it remained unclear if the control groups were littermates or C57BL/6 mice, strain specific differences may have influenced the results. Moreover, the applied Southern blot strategy used to evaluate the successful deletion of Gpr30 in Gpr30KO$^{M}$ mice was not appropriate to ensure proper integration of the 5'-arm and the single integration of the targeting vector into the genome. Therefore, multiple integrations into the Gpr30 locus or random integration into other loci may have caused a phenotype unrelated to Gpr30-deficiency. Furthermore, Martensson *et al.* observed significant difference in the glucose homeostasis while glucose tolerance testing indicated by a more rapid early increase and a sustained elevation of the plasma glucose levels (Martensson *et al.* 2008). In contrast, glucose tolerance testing of Gpr30-lacZ mice performed by us or at the German Mouse Clinic did not reveal significant differences in the glucose homeostasis. In further experiments, Martensson *et al.* showed that Gpr30 deletion abolished the E2-stimulated release of insulin *in vivo* in ovariectomized females and *in vitro* in isolated islets. However, the baseline insulin release upon glucose stimulation was already reduced by 50% in Gpr30KO$^{M}$ mice compared to wildtype controls, which may indicate that a more general disturbance of insulin release caused the observed phenotype.

In line with the finding that LacZ expression is prominent in small arterial vessels of multiple tissues, a slightly elevated blood pressure and an increased media:lumen ratio of 2$^{nd}$ order mesenteric arteries was observed in female 9 months old Gpr30KO$^{M}$ mice (Martensson *et al.* 2008). Our own attempts to detect blood pressure changes in Gpr30-lacZ mice failed so far, probably because the mice were of younger age.

To gain insight into the function of Gpr30, an extensive primary phenotype screen was performed at the German Mouse Clinic. Major alterations were observed only in the Immunology screen. Flow cytometric analysis of peripheral blood revealed statistically lower frequencies of CD4+ and CD8+ single positive T cells in Gpr30-lacZ mice compared to wildtype littermates. This went together with a lower proportion of CD62L

(L-selectin) expressing cells within the T cell cluster. Since CD62L+ T cells represent the naive T cell compartment newly produced in the thymus (Blais *et al.* 2008), the phenotype of Gpr30-lacZ mice might be explained by a lower rate of T cells produced in the thymus.

A T-cell phenotype has been already reported in a Gpr30-deficient mouse model ($Gpr30KO^{W}$) by Wang *et al.*, whereas the authors suggested a function of Gpr30 for thymocyte apoptosis during estrogen induced thymic atrophy (Wang *et al.* 2008a). In agreement with our findings, the apoptosis rate of TCR $\beta^{-/low}$ double positive (CD4+, CD8+) thymocytes (DP thymocytes) was doubled in $Gpr30KO^{W}$ mice when compared with wildtype controls already after vehicle treatment. Therefore, the lower frequency of CD4+ and CD8+ T cells in the peripheral blood found in Gpr30-lacZ mice can be explained by increased apoptosis of these cells within the thymus. These findings indicate an anti-apoptotic function of Gpr30 in thymocytes that is not sexually dimorphic in Gpr30-lacZ mice and therefore unlikely induced by the action of endogenous estrogens. In contrast, Wang *et al.* claimed a pro-apoptotic function of Gpr30 for DP thymocytes, since the induction of apoptosis by E2 was prevented in $Gpr30KO^{W}$ mice. However, it is also possible that the doubled apoptosis rate of these cells in $Gpr30KO^{W}$ mice under baseline conditions masks the effect of E2. If the apoptosis rate is already near the maximum under baseline conditions, an induction by E2 is not feasible anymore.

Since the reduction of thymic mass after E2 treatment is not completely prevented in ERα-deficient mice, Wang *et al.* speculate that apart from ERα another receptor (e.g. Gpr30) may be involved. However, this observation was made with the first hypomorphic ERα knockout strain (ERKO) from Ken Korach known to express functional splicing variants (Pendaries *et al.* 2002). In their own experiments, Wang *et al.* demonstrate a strong upregulation of ERα splicing variants in the thymus of ERKO mice. They argue that these splicing variants are inactive, whereas it has been demonstrated that they are active, e.g. in the cardiovascular system (Pendaries *et al.* 2002). Most likely, these splicing variants are also active in the thymus and explain the partial phenotype in ERKO mice. In contrast to the findings of Wang *et al.* suggesting that E2 induces a developmental blockage of DN thymocytes and increased apoptosis of DP thymocytes, another group reported that pregnancy or estrogen-induced thymic atrophy is not accompanied by a significant increase in thymocyte apoptosis, but mainly caused by a loss of early thymocyte precursors and the inhibition of thymocyte proliferation (Zoller and Kersh 2006; Zoller *et al.* 2007). Moreover, the experimental animals used

by Wang *et al.* were offspring of homozygous matings and not littermates. This leads to a genetic shift and to epigenetic modifications that can cause phenotypes that are not related to the mutation. The T cell phenotype identified in Gpr30-lacZ and Gpr30KO$^{W}$ mice might also be caused by a linkage of the mutation to genes from the 129 strain or the presence of the neomycin cassette. For both models, ES cells of the 129Sv background have been used and neomycin cassettes have not been removed from the Gpr30 locus. Indeed, the gene upstream of Gpr30 named Gpr146 is known to be regulated during positive and negative thymic selection (Kasler and Verdin 2007). Neomycin resistance cassettes were already found to silence genes hundreds of kb away from the targeted gene and thus may produce phenotypes independent of the targeted gene (Pham *et al.* 1996). In contradiction to a direct function of Gpr30 in the thymus, Gpr30 mRNA expression as well as LacZ-positive cells were absent in the thymus. However, mature peripheral blood leukocytes were not analyzed for Gpr30 expression so far.

The increased anxiety-related behavior of GPR30-lacZ mice found in the Open Field Test is most likely related to the expression of GPR30 in the dentate gyrus, cerebral cortex, anterior pituitary gland, and medulla of the adrenal gland. The dentate gyrus is located within the hippocampus, which is a part of the neuronal circuitry known to mediate anxiety (Millan 2003). The anterior pituitary secretes several peptide hormones involved in the regulation of various physiological processes including the stress response. In particular, the release of adrenocorticotropic hormone (ACTH) from the anterior pituitary induces the production of corticosteroids such as cortisol in the cortex of the adrenal glands. LacZ activity was found the adrenal glands, but was located in the medulla. The medulla contains chromaffin cells, which are specialized ganglia of the sympathetic nervous system that release epinephrine (adrenaline) and norepinephrine (noradrenaline) as well as endorphins into the blood stream. As such, chromaffin cells play an important role for mediating the increased activity of the sympathetic nervous system during the flight-or-fight-response. This stress reaction acutely results in an increased heart rate and contractility, bronchial dilatation, and decreased blood supply to the splanchnic bed, the skin and the kidneys. The findings in Gpr30-lacZ mice therefore indicate a potential role of Gpr30 in the hypothalamic-pituitary-adrenal axis and sympathetic nervous system during stress responses.

In conclusion, more studies are awaited to delineate the function of Gpr30 *in vivo*. These studies, however, should be performed with mouse models on a pure genetic background that are devoid of resistance and reporter cassettes. Furthermore, the analy-

sis of conditional knockout mice may be necessary to dissect the functions of Gpr30 in different cell types. Since Gpr30-deficiency results in only subtle phenotypes under normal conditions, certain challenges are probably necessary to observe the phenotype. The absence of a clear phenotype in Gpr30-lacZ under basal conditions was not unexpected, since multiple GPCR knockout models do not show apparent alterations under baseline conditions. For instance the blood pressure is controlled by altering the heart rate, vascular resistance, and fluid/electrolyte balance in the kidney, each of which is regulated to a large degree by GPCRs (e.g. adrenergic, muscarinic, angiotensin II, bradykinin, and endothelin receptors). These systems are able to compensate blood pressure changes under normal conditions as evidenced by the absence of strong blood pressure phenotypes in several knockout models deficient for one of these receptors. According to the LacZ expression profile and the T cell phenotype especially cardio-vascular, metabolic, behavioral, or immunological challenges may be required.

## 4.3 Proteins Interacting with the C-terminus of Human GPR30

7TMRs are elements of signaling units composed of multiple proteins that interact with each other in a complex fashion as shown for the G protein heterotrimer or β-arrestin. Information about the nature of proteins associated with a 7TMR provides insight into its function and subcellular localization. To identify proteins interacting with human GPR30, yeast two-hybrid screens were performed with the N- and C-terminal domains as bait. These domains were selected, since they most likely adopt the native conformation when isolated from the receptor. C-terminal domains have been frequently used as baits in yeast two-hybrid screenings enabling the identification of numerous interaction partners (Bockaert *et al.* 2004). In contrast, intracellular loops like the I3 loop (third intracellular loop) that mainly contacts the G protein are unlikely to adopt the native conformation. Novel technologies such as the ubiquitin-split-system (Iyer *et al.* 2005; Dirnberger *et al.* 2008) facilitating the use of full-length receptors inserted into the yeast membrane may overcome this limitation in future studies. In line with the observation that the N-terminal domain of GPR30 is not well conserved between species and might therefore lack any functionality, no putative interaction partners were identified with the N-terminal domain. Using the C-terminal domain as bait, the two candidates PALS1-associated tight junction protein (PATJ), and FUN14 domain-containing 2 (FUNDC2) were found.

PATJ, also known as inactivation no afterpotential D-like (INADL), has partial homology to the *Drosophila* InaD protein. InaD is essential for the regulation of the electrical response to light in photoreceptor cells by scaffolding the rhodopsin signaling complex through PDZ-mediated interactions with phospholipase C-β, eye-specific protein kinase C, and transient receptor potential channels (Huber *et al.* 1996; Shieh and Zhu 1996; Chevesich *et al.* 1997; Tsunoda *et al.* 1997). Like InaD, PATJ contains multiple PDZ domains and was found to be essential for tight junction formation and cell polarity shown by knockdown of PATJ in canine epithelial cells (Shin *et al.* 2005). Moreover, PATJ is required for directional migration in wound-induced migration assays (Shin *et al.* 2007). Several splicing variants have been reported that encode up to 10 PDZ domains and an N-terminal L27 domain (Philipp and Flockerzi 1997; Lemmers *et al.* 2002; Roh *et al.* 2002). Through its PDZ domains, PATJ interacts with tight junction proteins such as claudins and zonula occludens 3 (ZO-3) (Lemmers *et al.* 2002; Margolis and Borg 2005). The L27 domain of PATJ binds a complex containing the protein associated with Lin seven 1 (PALS1), human lin-7 homologue (LIN-7) and crumbs protein homolog 3 (CRB3) (Lemmers *et al.* 2002; Roh *et al.* 2002). The CRB3-PALS1-PATJ complex is a key component required for cell polarization and localizes to tight junctions at the apical site of the cell (Straight *et al.* 2004).

The potential interaction site of PATJ with the C-terminal domain of GPR30 found by yeast two-hybrid screening was within the three C-terminal PDZ domains (amino acids 1381-1801). PDZ domains are recognized as scaffolding sites for the assembly of 7TMR signaling units and bind PDZ ligands expressed at the C-terminus of GPCRs (Bockaert *et al.* 2004). The PDZ ligands are usually composed of three or four amino acids at the extreme C-terminus, although residues upstream may influence the specificity (Sheng and Sala 2001). Three different groups of PDZ ligands are known: class I (-E-S/T-x-V/I), class II (-ϕ-x-ϕ), and class III (-ψ-x-ϕ), whereas ψ and ϕ are acidic and hydrophobic residues, respectively (Sheng and Sala 2001). The C-terminal sequence of GPR30 (S-S-A-V) is highly conserved and similar to class I PDZ ligands. Vaccaro *et al.* determined the consensus ligand for 7 isolated PDZ domains of human PATJ by screening a random peptide library displayed on the phage lambda and found that each PDZ domain had a unique peptide binding preference (Vaccaro *et al.* 2001). Remarkably, the consensus ligand of the eighth PDZ domain was -S-x-V indicating that the C-terminus of GPR30 likely interacts with this domain. The interaction has been verified by co-immunoprecipitation in transfected 293 cells (in collaboration with Valeria Zazzu),

but experiments with cells endogenously expressing GPR30 and PATJ are lacking. The function of PATJ was predominantly investigated in epithelial cell types so far. If GPR30-positive cell types (e.g. endothelial) also express PATJ, has not been investigated so far. Moreover, the C-terminal domain of GPR30 might interact with the closely related multiple PDZ domain protein (MPDZ, also known as MUPP1), which is highly related to PATJ and expressed in various tissues (Ullmer *et al.* 1998). MPDZ was already shown to scaffold 7TMR signaling complexes and binds C-terminal domains of several 7TMRs including the serotonin 5-hydroxytryptamine (5-HT) receptors (Ullmer *et al.* 1998), γ-aminobutyric acid type B receptors (Balasubramanian *et al.* 2007), and $Mt_1$ melantonin receptors (Guillaume *et al.* 2008). The serotonin 5-HT2A and 5-HT2C receptors express a PDZ ligand very similar to that of GPR30 (-S-C-V and -S-S-V, respectively). A stretch of up to four serine residues within the PDZ ligand is characteristic for many 7TMRs. The serine residues may be phosphorylated upon activation of the 7TMR by GRKs and second-messenger regulated kinases to disrupt the interaction with the PDZ domain containing protein (Cao *et al.* 1999; Gage *et al.* 2005). Class I PDZ ligands were found to be necessary and sufficient for efficient recycling of 7TMRs indicating that PDZ-mediated interactions may have a more general function in regulating GPCR trafficking (Gage *et al.* 2005).

In conclusion, the C-terminal tail of GPR30 likely represents a PDZ ligand that specifically binds a PDZ domain of PATJ or MPDZ. The interaction may tether GPR30 to a signaling complex and has likely implications for the internalization and trafficking of the receptor. However, functional assays providing experimental evidence for this concept have not been developed so far. Since PATJ was found to be essential for tight junction formation, a potential function of GPR30 might the regulation of tight junction integrity in endothelial cells (e.g. during leukocyte transmigration).

The second candidate FUNDC2 belongs to the family of FUN14 domain containing proteins. The FUN14 domain is evolutionary conserved and spans about 100 C-terminal amino acids. In humans and mice, the two highly related members FUNDC1 (155 amino acids) and FUNDC2 (189 amino acids) are known, which are both encoded on the X chromosome (Harsha *et al.* 2005). Human FUNDC2 also has a pseudogene located on chromosome 2p11.2. The function of FUNDC2 is unknown so far, although the gene is located in the gene dense region Xq28 which has been in the focus of genome research for the last 20 years. More than 40 diseases have been mapped to Xq28, which spans 7.75 Mb of genomic DNA and harbors 105 protein-coding genes

(Poustka *et al.* 1991; Kolb-Kokocinski *et al.* 2006). The causative genes have been already identified for 26 of these diseases, but low patient numbers and variable phenotypes limit the fine mapping for the remaining 17 diseases (Kolb-Kokocinski *et al.* 2006). Therefore, a systematic study analyzed the tissues distribution and subcellular localization of all genes located within Xq28 and compared the expression patterns with disease phenotypes (Kolb-Kokocinski *et al.* 2006). FUNDC2 was recognized as a candidate gene for early-onset parkinsonism and X-linked mental retardation, but other candidates appear more promising (Kolb-Kokocinski *et al.* 2006). The expression pattern of FUNDC2 determined by *in situ* hybridization and Northern blotting suggests predominant expression in the cardiovascular, musculoskeletal, endocrine, and nervous system (http://www.inet.dkfz-heidelberg.de/LIFEdb). In line with data presented here, transient expression of FUNDC2 tagged with CFP or YFP at the N- or C-terminus resulted in a scattered localization surrounding the nucleus, which may point towards mitochondrial expression (Simpson *et al.* 2000) (Pictures are posted at http://gfp-cdna.embl.de/loc-html/Q9BWH2.html). In contrast, N-terminal tagging of FUNDC2 with small peptides such as Myc, HA, or FLAG performed here revealed a different intracellular distribution. These findings suggest that large tags like fluorescent proteins affect the intracellular localization of FUNDC2. To overcome this limitation, the detection of untagged FUNDC2 in transfected cell lines and in cell lines endogenously expressing the protein was required. However, tests with a monoclonal antibody directed against FUNDC2 facilitated only the detection of the denatured protein by western blotting, but not the detection of the native protein by immunocytochemistry. Therefore, appropriate methods to detect the native protein need to be established in future studies. As shown by co-immunoprecipitation, FUNDC2 proteins form homodimers or even multimers within the cell. FUNDC2 proteins contain therefore at least a dimerization domain. However, the interaction of FUNDC2 with the C-terminus of GPR30 could not be verified by co-immunoprecipitation here. This might be caused by technical limitations, but may also indicate a false positive interaction in the yeast two-hybrid screening.

Concerning the *in vivo* function of FUNDC2 in humans, Sheen *et al.* reported a complex genomic rearrangement within Xq28 leading to the deletion of the Factor VIII (F8, causing hemophilia A) and the FUNDC2 gene as well as the duplication of the genes TMEM185A, HSFX1, MAGEA9, and MAGEA11 (Sheen *et al.* 2007). Since no clinically detectable phenotypes other than hemophilia A were detected in the male

patient, the FUNDC2 deletion seems to have no biological effects *in vivo*. However, this observation may also indicate that the highly related protein FUNDC1 is able to substitute the function of FUNDC2. This complicates the analysis of the gene function in mice, since double knockouts will be necessary to observe a phenotype.

## 4.4 Concluding Remarks and Outlook

Within the scope of this thesis, the expression profile of a LacZ reporter and the phenotype induced by Gpr30-deficiency was analyzed in a novel mouse model designated as Gpr30-lacZ mouse. Since the detection of the mouse Gpr30 protein within tissues using antibodies was not possible so far (Martensson *et al.* 2008; Otto *et al.* 2008a; Wang *et al.* 2008a), the generation and analysis of LacZ reporter mice was an important step to provide a cellular basis for the functions of Gpr30 *in vivo*. The LacZ expression profile presented here provides clear evidence that various cell types not identified by the C-terminal antiserum or *in situ* hybridizations in previous reports express the receptor. However, the validation of the LacZ expression pattern at the endogenous Gpr30 protein level should be addressed again in future studies with novel antibodies. Especially chicken IgY antibodies directed against the 3$^{rd}$ extracellular loop or C-terminal domain of murine Gpr30 should be generated, since these domains are not well conserved in the chicken.

The reduced numbers of naive T cells observed in Gpr30-lacZ mice indicate a potential role of Gpr30 for the immune system. Therefore, the host response to pathogen infections may be investigated in more detailed studies of Gpr30-deficient mouse models. Since prominent expression of Gpr30 was found in endothelial and smooth muscle cell subpopulations, the reaction of isolated blood vessels from Gpr30-deficient mice to vasoconstrictors and vasodilators need to be assessed. Gpr30-deficieny may alter the outcome in models of vascular stress such as hypertension (e.g. infusion of angiotensin or isoproterenol), arteriogenesis (e.g. vessel constrictions), or vascular injury. Furthermore, detailed behavioral and metabolic phenotyping may reveal novel functions of Gpr30 in the nervous and digestive system.

Although results of other Gpr30-deficient mouse models provide evidence that Gpr30 plays a role in estrogen-induced thymic atrophy (Wang *et al.* 2008a) and pancreatic insulin release (Martensson *et al.* 2008), more studies are awaited to proof that Gpr30 represents an estrogen receptor *in vivo*. The analysis of male and female Gpr30-lacZ mice did not reveal sexually dimorphic alterations of the body weight, which is consis-

tent with another Gpr30-deficient model (Otto *et al.* 2008a) and questions the function of Gpr30 during estrogen-induced pancreatic insulin release. These inconsistent findings suggest that the targeting strategy, strain or environmental factors (e.g. the diet, housing conditions, health state, and stress) may influence the phenotype. Therefore, novel studies should be performed with mouse models on a pure genetic background that are devoid of resistance and reporter cassettes. Moreover, conditional knockout models will be necessary to dissect the functions of Gpr30 in different cell types.

Concerning the GPR30 signaling complex, PATJ or the closely related MPDZ may represent scaffolding proteins that bind the C-terminus of GPR30 with a PDZ domain. Since the C-terminal amino acids of GPR30 (S-A-V) are highly similar to the consensus ligand of the eighth PATJ PDZ domain (S-x-V) (Vaccaro *et al.* 2001), further studies should focus on this PDZ domain to narrow down the interaction site. The interaction has to be verified in cell types endogenously expressing both proteins. Moreover, assays need to be developed to investigate the functional consequences of the interaction.

# 5 REFERENCES

Adams JS (2005). "Bound" to work: the free hormone hypothesis revisited. *Cell.* **122**(5): 647-9.

Aluvihare VR, Kallikourdis M and Betz AG (2004). Regulatory T cells mediate maternal tolerance to the fetus. *Nat Immunol.* **5**(3): 266-71. Epub 2004 Feb 1.

Ankrapp DP, Bennett JM and Haslam SZ (1998). Role of epidermal growth factor in the acquisition of ovarian steroid hormone responsiveness in the normal mouse mammary gland. *J Cell Physiol.* **174**(2): 251-60.

Antal MC, Krust A, Chambon P and Mark M (2008). Sterility and absence of histopathological defects in nonreproductive organs of a mouse ERbeta-null mutant. *Proc Natl Acad Sci U S A.* **105**(7): 2433-8. Epub 2008 Feb 11.

Balasubramanian S, Fam SR and Hall RA (2007). GABAB receptor association with the PDZ scaffold Mupp1 alters receptor stability and function. *J Biol Chem.* **282**(6): 4162-71. Epub 2006 Dec 4.

Bartel PL and Fields S (1995). Analyzing protein-protein interactions using two-hybrid system. *Methods Enzymol.* **254**: 241-63.

Blais ME, Brochu S, Giroux M, Belanger MP, Dulude G, Sekaly RP and Perreault C (2008). Why T cells of thymic versus extrathymic origin are functionally different. *J Immunol.* **180**(4): 2299-312.

Bockaert J, Fagni L, Dumuis A and Marin P (2004). GPCR interacting proteins (GIP). *Pharmacol Ther.* **103**(3): 203-21.

Bohn LM, Lefkowitz RJ, Gainetdinov RR, Peppel K, Caron MG and Lin FT (1999). Enhanced morphine analgesia in mice lacking beta-arrestin 2. *Science.* **286**(5449): 2495-8.

Bologa CG, Revankar CM, Young SM, Edwards BS, Arterburn JB, Kiselyov AS, Parker MA, Tkachenko SE, Savchuck NP, Sklar LA, Oprea TI and Prossnitz ER (2006). Virtual and biomolecular screening converge on a selective agonist for GPR30. *Nat Chem Biol.* **2**(4): 207-12. Epub 2006 Mar 5.

Brailoiu E, Dun SL, Brailoiu GC, Mizuo K, Sklar LA, Oprea TI, Prossnitz ER and Dun NJ (2007). Distribution and characterization of estrogen receptor G protein-coupled receptor 30 in the rat central nervous system. *J Endocrinol.* **193**(2): 311-21.

Brink CB, Harvey BH, Bodenstein J, Venter DP and Oliver DW (2004). Recent advances in drug action and therapeutics: relevance of novel concepts in G-protein-coupled receptor and signal transduction pharmacology. *Br J Clin Pharmacol.* **57**(4): 373-87.

Canonaco M, Giusi G, Madeo A, Facciolo RM, Lappano R, Canonaco A and Maggiolini M (2008). A sexually dimorphic distribution pattern of the novel estrogen receptor G-protein-coupled receptor 30 in some brain areas of the hamster. *J Endocrinol.* **196**(1): 131-8.

Cao TT, Deacon HW, Reczek D, Bretscher A and von Zastrow M (1999). A kinase-regulated PDZ-domain interaction controls endocytic sorting of the beta2-adrenergic receptor. *Nature.* **401**(6750): 286-90.

Carmeci C, Thompson DA, Ring HZ, Francke U and Weigel RJ (1997). Identification of a gene (GPR30) with homology to the G-protein-coupled receptor superfamily associated with estrogen receptor expression in breast cancer. *Genomics* **45**(3): 607-17.

Chambliss KL, Yuhanna IS, Mineo C, Liu P, German Z, Sherman TS, Mendelsohn ME, Anderson RG and Shaul PW (2000). Estrogen receptor alpha and endothelial nitric oxide synthase are organized into a functional signaling module in caveolae. *Circ Res.* **87**(11): E44-52.

Chevesich J, Kreuz AJ and Montell C (1997). Requirement for the PDZ domain protein, INAD, for localization of the TRP store-operated channel to a signaling complex. *Neuron.* **18**(1): 95-105.

Chung GT, Yamada Y, Pannell R, Forster A and Rabbitts TH (2003). The hepatitis C virus internal ribosome entry site facilitates efficient protein synthesis in blood vessel endothelium during tumour angiogenesis. *Nucleic Acids Res.* **31**(8): e46.

Conner DA, Mathier MA, Mortensen RM, Christe M, Vatner SF, Seidman CE and Seidman JG (1997). beta-Arrestin1 knockout mice appear normal but demonstrate altered cardiac responses to beta-adrenergic stimulation. *Circ Res.* **81**(6): 1021-6.

Creancier L, Mercier P, Prats AC and Morello D (2001). c-myc Internal ribosome entry site activity is developmentally controlled and subjected to a strong translational repression in adult transgenic mice. *Mol Cell Biol.* **21**(5): 1833-40.

Creancier L, Morello D, Mercier P and Prats AC (2000). Fibroblast growth factor 2 internal ribosome entry site (IRES) activity ex vivo and in transgenic mice reveals a stringent tissue-specific regulation. *J Cell Biol.* **150**(1): 275-81.

Davies MN, Secker A, Halling-Brown M, Moss DS, Freitas AA, Timmis J, Clark E and Flower DR (2008). GPCRTree: online hierarchical classification of GPCR function. *BMC Res Notes.* **1**: 67.

DeWire SM, Ahn S, Lefkowitz RJ and Shenoy SK (2007). Beta-arrestins and cell signaling. *Annu Rev Physiol.* **69**: 483-510.

Dirnberger D, Messerschmid M and Baumeister R (2008). An optimized split-ubiquitin cDNA-library screening system to identify novel interactors of the human Frizzled 1 receptor. *Nucleic Acids Res.* **36**(6): e37. Epub 2008 Mar 4.

Drews J (2000). Drug discovery: a historical perspective. *Science.* **287**(5460): 1960-4.

Edwards DP (2005). Regulation of signal transduction pathways by estrogen and progesterone. *Annu Rev Physiol* **67**: 335-76.

Erlandsson MC, Ohlsson C, Gustafsson JA and Carlsten H (2001). Role of oestrogen receptors alpha and beta in immune organ development and in oestrogen-mediated effects on thymus. *Immunology.* **103**(1): 17-25.

Feng Y and Gregor P (1997). Cloning of a novel member of the G protein-coupled receptor family related to peptide receptors. *Biochem Biophys Res Commun* **231**(3): 651-4.

Fields S and Song O (1989). A novel genetic system to detect protein-protein interactions. *Nature.* **340**(6230): 245-6.

Filardo E, Quinn J, Pang Y, Graeber C, Shaw S, Dong J and Thomas P (2007). Activation of the novel estrogen receptor, GPR30, at the plasma membrane. *Endocrinology* **22**: 22.

Filardo EJ, Graeber CT, Quinn JA, Resnick MB, Giri D, DeLellis RA, Steinhoff MM and Sabo E (2006). Distribution of GPR30, a seven membrane-spanning estrogen receptor, in primary breast cancer and its association with clinicopathologic determinants of tumor progression. *Clin Cancer Res.* **12**(21): 6359-66.

Filardo EJ, Quinn JA, Bland KI and Frackelton AR, Jr. (2000). Estrogen-induced activation of Erk-1 and Erk-2 requires the G protein-coupled receptor homolog, GPR30, and occurs via trans-activation of the epidermal growth factor receptor through release of HB-EGF. *Mol Endocrinol* **14**(10): 1649-60.

Filardo EJ, Quinn JA, Frackelton AR, Jr. and Bland KI (2002). Estrogen action via the G protein-coupled receptor, GPR30: stimulation of adenylyl cyclase and cAMP-mediated attenuation of the epidermal growth factor receptor-to-MAPK signaling axis. *Mol Endocrinol* **16**(1): 70-84.

Fredriksson R, Lagerstrom MC, Lundin LG and Schioth HB (2003). The G-protein-coupled receptors in the human genome form five main families. Phylogenetic analysis, paralogon groups, and fingerprints. *Mol Pharmacol.* **63**(6): 1256-72.

Gage RM, Matveeva EA, Whiteheart SW and von Zastrow M (2005). Type I PDZ ligands are sufficient to promote rapid recycling of G Protein-coupled receptors independent of binding to N-ethylmaleimide-sensitive factor. *J Biol Chem.* **280**(5): 3305-13. Epub 2004 Nov 17.

Gailus-Durner V, Fuchs H, Becker L, Bolle I, Brielmeier M, Calzada-Wack J, Elvert R, Ehrhardt N, Dalke C, Franz TJ, Grundner-Culemann E, Hammelbacher S, Hölter SM, Hölzlwimmer G, Horsch M, Javaheri A, Kalaydjiev S, Klempt M, Kling E, Kunder S, Lengger L, Lisse T, Mijalski T, Naton B, Pedersen V, Prehn C, Przemeck G, Rácz, Reinhard C, Reitmeir P, Schneider I, Schrewe A, Steinkamp R, Zybill C, Adamski J, Beckers J, Behrendt H, Favor J, Graw J, Heldmaier G, Höfler H, Ivandic B, Katus H, Kirchhof P, Klingenspor M, Klopstock T, Lengeling A, Müller W, Ohl F, Ollert M, Quintanilla-Martinez L, Schmidt J, Schulz H, Wolf E, Wurst W, Zimmer A, Busch DH, Hrabé de Angelis M (2005). Introducing the German Mouse Clinic: open access platform for standardized phenotyping. *Nat Methods*(2): 403-4.

Goodman OB, Jr., Krupnick JG, Santini F, Gurevich VV, Penn RB, Gagnon AW, Keen JH and Benovic JL (1996). Beta-arrestin acts as a clathrin adaptor in endocytosis of the beta2-adrenergic receptor. *Nature.* **383**(6599): 447-50.

Gottlicher M, Heck S and Herrlich P (1998). Transcriptional cross-talk, the second mode of steroid hormone receptor action. *J Mol Med* **76**(7): 480-9.

Greene GL, Gilna P, Waterfield M, Baker A, Hort Y and Shine J (1986). Sequence and expression of human estrogen receptor complementary DNA. *Science.* **231**(4742): 1150-4.

Guillaume JL, Daulat AM, Maurice P, Levoye A, Migaud M, Brydon L, Malpaux B, Borg-Capra C and Jockers R (2008). The PDZ protein mupp1 promotes Gi coupling and signaling of the Mt1 melatonin receptor. *J Biol Chem.* **283**(24): 16762-71. Epub 2008 Mar 31.

Haas E, Bhattacharya I, Brailoiu E, Damjanovic M, Brailoiu GC, Gao X, Mueller-Guerre L, Marjon NA, Gut A, Minotti R, Meyer MR, Amann K, Ammann E, Perez-Dominguez A, Genoni M, Clegg DJ, Dun NJ, Resta TC, Prossnitz ER and Barton M (2009). Regulatory Role of G Protein-Coupled Estrogen Receptor for Vascular Function and Obesity. *Circ Res* **29**: 29.

Haas E, Meyer MR, Schurr U, Bhattacharya I, Minotti R, Nguyen HH, Heigl A, Lachat M, Genoni M and Barton M (2007). Differential effects of 17beta-estradiol on function and expression of estrogen receptor alpha, estrogen receptor beta, and GPR30 in arteries and veins of patients with atherosclerosis. *Hypertension.* **49**(6): 1358-63. Epub 2007 Apr 23.

Hamm HE (1998). The many faces of G protein signaling. *J Biol Chem.* **273**(2): 669-72.

Hammes A, Andreassen TK, Spoelgen R, Raila J, Hubner N, Schulz H, Metzger J, Schweigert FJ, Luppa PB, Nykjaer A and Willnow TE (2005). Role of endocytosis in cellular uptake of sex steroids. *Cell.* **122**(5): 751-62.

Hammes SR and Levin ER (2007). Extranuclear steroid receptors: nature and actions. *Endocr Rev.* **28**(7): 726-41. Epub 2007 Oct 4.

Harsha HC, Suresh S, Amanchy R, Deshpande N, Shanker K, Yatish AJ, Muthusamy B, Vrushabendra BM, Rashmi BP, Chandrika KN, Padma N, Sharma S, Badano JL, Ramya MA, Shivashankar HN, Peri S, Choudhury DR, Kavitha MP, Saravana R, Niranjan V, Gandhi TK, Ghosh N, Chandran S, Menezes M, Joy M, Mohan SS, Katsanis N, Deshpande KS, Raghothama C, Prasad CK and Pandey A (2005). A manually curated functional annotation of the human X chromosome. *Nat Genet.* **37**(4): 331-2.

Heino TJ, Chagin AS and Savendahl L (2008). The novel estrogen receptor G-protein-coupled receptor 30 is expressed in human bone. *J Endocrinol.* **197**(2): R1-6.

Horn F, Bettler E, Oliveira L, Campagne F, Cohen FE and Vriend G (2003). GPCRDB information system for G protein-coupled receptors. *Nucleic Acids Res.* **31**(1): 294-7.

Huber A, Sander P, Gobert A, Bahner M, Hermann R and Paulsen R (1996). The transient receptor potential protein (Trp), a putative store-operated Ca2+ channel essential for phosphoinositide-mediated photoreception, forms a signaling complex with NorpA, InaC and InaD. *Embo J.* **15**(24): 7036-45.

Isensee J, Meoli L, Zazzu V, Nabzdyk C, Witt H, Soewarto D, Effertz K, Fuchs H, Gailus-Durner V, Busch D, Adler T, de Angelis MH, Irgang M, Otto C and Noppinger PR (2008). Expression Pattern of Gpr30 in LacZ Reporter Mice. *Endocrinology* **18**: 18.

Iyer K, Burkle L, Auerbach D, Thaminy S, Dinkel M, Engels K and Stagljar I (2005). Utilizing the split-ubiquitin membrane yeast two-hybrid system to identify protein-protein interactions of integral membrane proteins. *Sci STKE.* **2005**(275): pl3.

Jensen EV and DeSombre ER (1973). Estrogen-receptor interaction. *Science.* **182**(108): 126-34.

Johnson MS, Robertson DN, Holland PJ, Lutz EM and Mitchell R (2006). Role of the conserved NPxxY motif of the 5-HT2A receptor in determining selective interaction with isoforms of ADP-ribosylation factor (ARF). *Cell Signal.* **18**(10): 1793-800. Epub 2006 Mar 20.

Kasler HG and Verdin E (2007). Histone deacetylase 7 functions as a key regulator of genes involved in both positive and negative selection of thymocytes. *Mol Cell Biol.* **27**(14): 5184-200. Epub 2007 Apr 30.

Klein-Hitpass L, Schorpp M, Wagner U and Ryffel GU (1986). An estrogen-responsive element derived from the 5' flanking region of the Xenopus vitellogenin A2 gene functions in transfected human cells. *Cell* **46**(7): 1053-61.

Kohout TA, Lin FS, Perry SJ, Conner DA and Lefkowitz RJ (2001). beta-Arrestin 1 and 2 differentially regulate heptahelical receptor signaling and trafficking. *Proc Natl Acad Sci U S A.* **98**(4): 1601-6. Epub 2001 Feb 6.

Kolb-Kokocinski A, Mehrle A, Bechtel S, Simpson JC, Kioschis P, Wiemann S, Wellenreuther R and Poustka A (2006). The systematic functional characterisation of Xq28 genes prioritises candidate disease genes. *BMC Genomics.* **7**: 29.

Kuiper GG, Carlsson B, Grandien K, Enmark E, Haggblad J, Nilsson S and Gustafsson JA (1997). Comparison of the ligand binding specificity and transcript tissue distribution of estrogen receptors alpha and beta. *Endocrinology.* **138**(3): 863-70.

Kuiper GG, Enmark E, Pelto-Huikko M, Nilsson S and Gustafsson JA (1996). Cloning of a novel receptor expressed in rat prostate and ovary. *Proc Natl Acad Sci U S A.* **93**(12): 5925-30.

Kumar P, Wu Q, Chambliss KL, Yuhanna IS, Mumby SM, Mineo C, Tall GG and Shaul PW (2007). Direct Interactions with G alpha i and G betagamma mediate nongenomic signaling by estrogen receptor alpha. *Mol Endocrinol.* **21**(6): 1370-80. Epub 2007 Apr 3.

Kvingedal AM and Smeland EB (1997). A novel putative G-protein-coupled receptor expressed in lung, heart and lymphoid tissue. *FEBS Lett* **407**(1): 59-62.

Laporte SA, Miller WE, Kim KM and Caron MG (2002). beta-Arrestin/AP-2 interaction in G protein-coupled receptor internalization: identification of a beta-arrestin binging site in beta 2-adaptin. *J Biol Chem.* **277**(11): 9247-54. Epub 2002 Jan 2.

Lein ES, Hawrylycz MJ, Ao N, Ayres M, Bensinger A, Bernard A, Boe AF, Boguski MS, Brockway KS, Byrnes EJ, Chen L, Chen L, Chen TM, Chin MC, Chong J, Crook BE, Czaplinska A, Dang CN, Datta S, Dee NR, Desaki AL, Desta T, Diep E, Dolbeare TA, Donelan MJ, Dong HW, Dougherty JG, Duncan BJ, Ebbert AJ, Eichele G, Estin LK, Faber C, Facer BA, Fields R *et al.* (2007). Genome-wide atlas of gene expression in the adult mouse brain. *Nature.* **445**(7124): 168-76. Epub 2006 Dec 6.

Lemmers C, Medina E, Delgrossi MH, Michel D, Arsanto JP and Le Bivic A (2002). hINADl/PATJ, a homolog of discs lost, interacts with crumbs and localizes to tight junctions in human epithelial cells. *J Biol Chem.* **277**(28): 25408-15. Epub 2002 Apr 18.

Losel RM, Falkenstein E, Feuring M, Schultz A, Tillmann HC, Rossol-Haseroth K and Wehling M (2003). Nongenomic steroid action: controversies, questions, and answers. *Physiol Rev.* **83**(3): 965-1016.

Luttrell LM (2006). Transmembrane signaling by G protein-coupled receptors. *Methods Mol Biol.* **332**: 3-49.

Maggiolini M, Vivacqua A, Fasanella G, Recchia AG, Sisci D, Pezzi V, Montanaro D, Musti AM, Picard D and Ando S (2004). The G protein-coupled receptor GPR30 mediates c-fos up-regulation by 17beta-estradiol and phytoestrogens in breast cancer cells. *J Biol Chem* **279**(26): 27008-16. Epub 2004 Apr 16.

Mallon AM, Blake A and Hancock JM (2008). EuroPhenome and EMPReSS: online mouse phenotyping resource. *Nucleic Acids Res.* **36**(Database issue): D715-8. Epub 2007 Sep 28.

Margolis B and Borg JP (2005). Apicobasal polarity complexes. *J Cell Sci.* **118**(Pt 22): 5157-9.

Martensson UE, Salehi SA, Windahl S, Gomez MF, Sward K, Daszkiewicz-Nilsson J, Wendt A, Andersson N, Hellstrand P, Grande PO, Owman C, Rosen CJ, Adamo ML, Lundquist I, Rorsman P, Nilsson BO, Ohlsson C, Olde B and Leeb-Lundberg LM (2008). Deletion of the G protein-coupled Receptor GPR30 Impairs Glucose Tolerance, Reduces Bone Growth, Increases Blood Pressure, and Eliminates Estradiol-stimulated Insulin Release in Female Mice. *Endocrinology* **9**: 9.

Matsuda K, Sakamoto H, Mori H, Hosokawa K, Kawamura A, Itose M, Nishi M, Prossnitz ER and Kawata M (2008). Expression and intracellular distribution of the G protein-coupled receptor 30 in rat hippocampal formation. *Neurosci Lett.* **441**(1): 94-9. Epub 2008 Jun 5.

McKenna NJ and O'Malley BW (2002). Combinatorial control of gene expression by nuclear receptors and coregulators. *Cell* **108**(4): 465-74.

Mendelsohn ME and Karas RH (2005). Molecular and cellular basis of cardiovascular gender differences. *Science.* **308**(5728): 1583-7.

Millan MJ (2003). The neurobiology and control of anxious states. *Prog Neurobiol.* **70**(2): 83-244.

Moore CA, Milano SK and Benovic JL (2007). Regulation of receptor trafficking by GRKs and arrestins. *Annu Rev Physiol.* **69**: 451-82.

Mukku VR and Stancel GM (1985). Regulation of epidermal growth factor receptor by estrogen. *J Biol Chem.* **260**(17): 9820-4.

Nadal A, Rovira JM, Laribi O, Leon-quinto T, Andreu E, Ripoll C and Soria B (1998). Rapid insulinotropic effect of 17beta-estradiol via a plasma membrane receptor. *Faseb J.* **12**(13): 1341-8.

Nelson KG, Takahashi T, Bossert NL, Walmer DK and McLachlan JA (1991). Epidermal growth factor replaces estrogen in the stimulation of female genital-tract growth and differentiation. *Proc Natl Acad Sci U S A.* **88**(1): 21-5.

Otto C, Fuchs I, Kauselmann G, Kern H, Zevnik B, Andreasen P, Schwarz G, Altmann H, Klewer M, Schoor M, Vonk R and Fritzemeier KH (2008a). GPR30 Does Not Mediate Estrogenic Responses in Reproductive Organs in Mice. *Biol Reprod* **17**: 17.

Otto C, Rohde-Schulz B, Schwarz G, Fuchs I, Klewer M, Brittain D, Langer G, Bader B, Prelle K, Nubbemeyer R and Fritzemeier KH (2008b). GPR30 localizes to the endoplasmic reticulum and is not activated by estradiol. *Endocrinology* **19**: 19.

Owman C, Blay P, Nilsson C and Lolait SJ (1996). Cloning of human cDNA encoding a novel heptahelix receptor expressed in Burkitt's lymphoma and widely distrib-

uted in brain and peripheral tissues. *Biochem Biophys Res Commun* **228**(2): 285-92.

Pedram A, Razandi M and Levin ER (2006). Nature of functional estrogen receptors at the plasma membrane. *Mol Endocrinol.* **20**(9): 1996-2009. Epub 2006 Apr 27.

Pedram A, Razandi M, Sainson RC, Kim JK, Hughes CC and Levin ER (2007). A conserved mechanism for steroid receptor translocation to the plasma membrane. *J Biol Chem.* **282**(31): 22278-88. Epub 2007 May 29.

Peirson SN, Butler JN and Foster RG (2003). Experimental validation of novel and conventional approaches to quantitative real-time PCR data analysis. *Nucleic Acids Res.* **31**(14): e73.

Pendaries C, Darblade B, Rochaix P, Krust A, Chambon P, Korach KS, Bayard F and Arnal JF (2002). The AF-1 activation-function of ERalpha may be dispensable to mediate the effect of estradiol on endothelial NO production in mice. *Proc Natl Acad Sci U S A.* **99**(4): 2205-10.

Petrie HT, Hugo P, Scollay R and Shortman K (1990). Lineage relationships and developmental kinetics of immature thymocytes: CD3, CD4, and CD8 acquisition *in vivo* and *in vitro*. *J Exp Med.* **172**(6): 1583-8.

Pham CT, MacIvor DM, Hug BA, Heusel JW and Ley TJ (1996). Long-range disruption of gene expression by a selectable marker cassette. *Proc Natl Acad Sci U S A.* **93**(23): 13090-5.

Philipp S and Flockerzi V (1997). Molecular characterization of a novel human PDZ domain protein with homology to INAD from Drosophila melanogaster. *FEBS Lett.* **413**(2): 243-8.

Poustka A, Dietrich A, Langenstein G, Toniolo D, Warren ST and Lehrach H (1991). Physical map of human Xq27-qter: localizing the region of the fragile X mutation. *Proc Natl Acad Sci U S A.* **88**(19): 8302-6.

Premont RT and Gainetdinov RR (2007). Physiological roles of G protein-coupled receptor kinases and arrestins. *Annu Rev Physiol.* **69**: 511-34.

Prenzel N, Zwick E, Daub H, Leserer M, Abraham R, Wallasch C and Ullrich A (1999). EGF receptor transactivation by G-protein-coupled receptors requires metalloproteinase cleavage of proHB-EGF. *Nature.* **402**(6764): 884-8.

Prossnitz ER, Arterburn JB, Smith HO, Oprea TI, Sklar LA and Hathaway HJ (2008). Estrogen signaling through the transmembrane G protein-coupled receptor GPR30. *Annu Rev Physiol.* **70**: 165-90.

Razandi M, Alton G, Pedram A, Ghonshani S, Webb P and Levin ER (2003a). Identification of a structural determinant necessary for the localization and function of estrogen receptor alpha at the plasma membrane. *Mol Cell Biol.* **23**(5): 1633-46.

Razandi M, Oh P, Pedram A, Schnitzer J and Levin ER (2002). ERs associate with and regulate the production of caveolin: implications for signaling and cellular actions. *Mol Endocrinol.* **16**(1): 100-15.

Razandi M, Pedram A, Greene GL and Levin ER (1999). Cell membrane and nuclear estrogen receptors (ERs) originate from a single transcript: studies of ERalpha and ERbeta expressed in Chinese hamster ovary cells. *Mol Endocrinol.* **13**(2): 307-19.

Razandi M, Pedram A, Park ST and Levin ER (2003b). Proximal events in signaling by plasma membrane estrogen receptors. *J Biol Chem.* **278**(4): 2701-12. Epub 2002 Nov 5.

Revankar CM, Cimino DF, Sklar LA, Arterburn JB and Prossnitz ER (2005). A Transmembrane Intracellular Estrogen Receptor Mediates Rapid Cell Signaling. *Science* **10**: 10.

Revankar CM, Mitchell HD, Field AS, Burai R, Corona C, Ramesh C, Sklar LA, Arterburn JB and Prossnitz ER (2007). Synthetic estrogen derivatives demonstrate the functionality of intracellular GPR30. *ACS Chem Biol.* **2**(8): 536-44. Epub 2007 Jul 27.

Robertson DN, Johnson MS, Moggach LO, Holland PJ, Lutz EM and Mitchell R (2003). Selective interaction of ARF1 with the carboxy-terminal tail domain of the 5-HT2A receptor. *Mol Pharmacol.* **64**(5): 1239-50.

Roh MH, Makarova O, Liu CJ, Shin K, Lee S, Laurinec S, Goyal M, Wiggins R and Margolis B (2002). The Maguk protein, Pals1, functions as an adapter, linking mammalian homologues of Crumbs and Discs Lost. *J Cell Biol.* **157**(1): 161-72. Epub 2002 Apr 1.

Rondou P, Haegeman G, Vanhoenacker P and Van Craenenbroeck K (2008). BTB Protein KLHL12 targets the dopamine D4 receptor for ubiquitination by a Cul3-based E3 ligase. *J Biol Chem.* **283**(17): 11083-96. Epub 2008 Feb 26.

Ropero AB, Fuentes E, Rovira JM, Ripoll C, Soria B and Nadal A (1999). Non-genomic actions of 17beta-oestradiol in mouse pancreatic beta-cells are mediated by a cGMP-dependent protein kinase. *J Physiol.* **521**(Pt 2): 397-407.

Rovati GE, Capra V and Neubig RR (2007). The highly conserved DRY motif of class A G protein-coupled receptors: beyond the ground state. *Mol Pharmacol.* **71**(4): 959-64. Epub 2006 Dec 27.

Rozen S and Skaletsky H (2000). Primer3 on the WWW for general users and for biologist programmers. *Methods Mol Biol.* **132**: 365-86.

Russell JA and Leng G (1998). Sex, parturition and motherhood without oxytocin? *J Endocrinol.* **157**(3): 343-59.

Sakamoto H, Matsuda K, Hosokawa K, Nishi M, Morris JF, Prossnitz ER and Kawata M (2007). Expression of G protein-coupled receptor-30, a G protein-coupled membrane estrogen receptor, in oxytocin neurons of the rat paraventricular and supraoptic nuclei. *Endocrinology.* **148**(12): 5842-50. Epub 2007 Sep 13.

Schaefer M, Albrecht N, Hofmann T, Gudermann T and Schultz G (2001). Diffusion-limited translocation mechanism of protein kinase C isotypes. *Faseb J.* **15**(9): 1634-6.

Sheen CR, Jewell UR, Morris CM, Brennan SO, Ferec C, George PM, Smith MP and Chen JM (2007). Double complex mutations involving F8 and FUNDC2 caused by distinct break-induced replication. *Hum Mutat.* **28**(12): 1198-206.

Sheng M and Sala C (2001). PDZ domains and the organization of supramolecular complexes. *Annu Rev Neurosci.* **24**: 1-29.

Shieh BH and Zhu MY (1996). Regulation of the TRP Ca2+ channel by INAD in Drosophila photoreceptors. *Neuron.* **16**(5): 991-8.

Shin K, Straight S and Margolis B (2005). PATJ regulates tight junction formation and polarity in mammalian epithelial cells. *J Cell Biol.* **168**(5): 705-11.

Shin K, Wang Q and Margolis B (2007). PATJ regulates directional migration of mammalian epithelial cells. *EMBO Rep.* **8**(2): 158-64. Epub 2007 Jan 19.

Simoncini T, Hafezi-Moghadam A, Brazil DP, Ley K, Chin WW and Liao JK (2000). Interaction of oestrogen receptor with the regulatory subunit of phosphatidylinositol-3-OH kinase. *Nature.* **407**(6803): 538-41.

Simpson ER, Misso M, Hewitt KN, Hill RA, Boon WC, Jones ME, Kovacic A, Zhou J and Clyne CD (2005). Estrogen--the good, the bad, and the unexpected. *Endocr Rev.* **26**(3): 322-30. Epub 2005 Apr 7.

Simpson JC, Wellenreuther R, Poustka A, Pepperkok R and Wiemann S (2000). Systematic subcellular localization of novel proteins identified by large-scale cDNA sequencing. *EMBO Rep.* **1**(3): 287-92.

Smith HO, Leslie KK, Singh M, Qualls CR, Revankar CM, Joste NE and Prossnitz ER (2007). GPR30: a novel indicator of poor survival for endometrial carcinoma. *Am J Obstet Gynecol.* **196**(4): 386.e1-9; discussion 386.e9-11.

Snyder UK, Thompson JF and Landy A (1989). Phasing of protein-induced DNA bends in a recombination complex. *Nature.* **341**(6239): 255-7.

Staples JE, Gasiewicz TA, Fiore NC, Lubahn DB, Korach KS and Silverstone AE (1999). Estrogen receptor alpha is necessary in thymic development and estradiol-induced thymic alterations. *J Immunol.* **163**(8): 4168-74.

Straight SW, Shin K, Fogg VC, Fan S, Liu CJ, Roh M and Margolis B (2004). Loss of PALS1 expression leads to tight junction and polarity defects. *Mol Biol Cell.* **15**(4): 1981-90. Epub 2004 Jan 12.

Takada Y, Kato C, Kondo S, Korenaga R and Ando J (1997). Cloning of cDNAs encoding G protein-coupled receptor expressed in human endothelial cells exposed to fluid shear stress. *Biochem Biophys Res Commun* **240**(3): 737-41.

Thomas P, Pang Y, Filardo EJ and Dong J (2005). Identity of an estrogen membrane receptor coupled to a G protein in human breast cancer cells. *Endocrinology.* **146**(2): 624-32. Epub 2004 Nov 11.

Tsunoda S, Sierralta J, Sun Y, Bodner R, Suzuki E, Becker A, Socolich M and Zuker CS (1997). A multivalent PDZ-domain protein assembles signalling complexes in a G-protein-coupled cascade. *Nature.* **388**(6639): 243-9.

Ullmer C, Schmuck K, Figge A and Lubbert H (1998). Cloning and characterization of MUPP1, a novel PDZ domain protein. *FEBS Lett.* **424**(1-2): 63-8.

Vaccaro P, Brannetti B, Montecchi-Palazzi L, Philipp S, Helmer Citterich M, Cesareni G and Dente L (2001). Distinct binding specificity of the multiple PDZ domains of INADL, a human protein with homology to INAD from Drosophila melanogaster. *J Biol Chem.* **276**(45): 42122-30. Epub 2001 Aug 16.

Vandesompele J, De Preter K, Pattyn F, Poppe B, Van Roy N, De Paepe A and Speleman F (2002). Accurate normalization of real-time quantitative RT-PCR data by geometric averaging of multiple internal control genes. *Genome Biol.* **3**(7): RESEARCH0034.

Vivacqua A, Bonofiglio D, Recchia AG, Musti AM, Picard D, Ando S and Maggiolini M (2006). The G protein-coupled receptor GPR30 mediates the proliferative ef-

fects induced by 17beta-estradiol and hydroxytamoxifen in endometrial cancer cells. *Mol Endocrinol.* **20**(3): 631-46. Epub 2005 Oct 20.

Voigt P, Brock C, Nurnberg B and Schaefer M (2005). Assigning functional domains within the p101 regulatory subunit of phosphoinositide 3-kinase gamma. *J Biol Chem.* **280**(6): 5121-7. Epub 2004 Dec 20.

Wang C, Dehghani B, Magrisso IJ, Rick EA, Bonhomme E, Cody DB, Elenich LA, Subramanian S, Murphy SJ, Kelly MJ, Rosenbaum JS, Vandenbark AA and Offner H (2008a). GPR30 contributes to estrogen-induced thymic atrophy. *Mol Endocrinol.* **22**(3): 636-48. Epub 2007 Dec 6.

Wang C, Prossnitz ER and Roy SK (2007). Expression of G protein-coupled receptor 30 in the hamster ovary: differential regulation by gonadotropins and steroid hormones. *Endocrinology.* **148**(10): 4853-64. Epub 2007 Jul 19.

Wang C, Prossnitz ER and Roy SK (2008b). G protein-coupled receptor 30 expression is required for estrogen stimulation of primordial follicle formation in the hamster ovary. *Endocrinology.* **149**(9): 4452-61. Epub 2008 May 22.

Warner M and Gustafsson JA (2006). Nongenomic effects of estrogen: why all the uncertainty? *Steroids.* **71**(2): 91-5. Epub 2005 Oct 25.

Wyckoff MH, Chambliss KL, Mineo C, Yuhanna IS, Mendelsohn ME, Mumby SM and Shaul PW (2001). Plasma membrane estrogen receptors are coupled to endothelial nitric-oxide synthase through Galpha(i). *J Biol Chem.* **276**(29): 27071-6. Epub 2001 May 21.

Xue Y, Ren J, Gao X, Jin C, Wen L and Yao X (2008). GPS 2.0, a tool to predict kinase-specific phosphorylation sites in hierarchy. *Mol Cell Proteomics.* **7**(9): 1598-608. Epub 2008 May 6.

Zoller AL and Kersh GJ (2006). Estrogen induces thymic atrophy by eliminating early thymic progenitors and inhibiting proliferation of beta-selected thymocytes. *J Immunol.* **176**(12): 7371-8.

Zoller AL, Schnell FJ and Kersh GJ (2007). Murine pregnancy leads to reduced proliferation of maternal thymocytes and decreased thymic emigration. *Immunology.* **121**(2): 207-15. Epub 2007 Jan 23.

# ACKNOWLEDGEMENTS

First and foremost, I would like to say that I had a great time at the Center for Cardiovascular Research and would like to thank all of you who made this time so pleasant and scientifically fruitful.

In particular, I wish to express my deep gratitude to **Patricia Ruiz Noppinger**, my principle supervisor, who supported me and my work since 2004 with tremendous efforts. Without your encouragement and guidance, I could have never conducted this dissertation. You gave me the change to become a self-confident researcher and fully supported my work. Dear Patricia, thank you so much for these years.

Special thanks go to **Carola Geiler** for her excellent technical assistance and support. Dear Carola, I really enjoyed to work with you every day. Thank you for sharing all your expert knowledge with me.

I would like to express my sincere gratitude to all my colleagues in the AG Ruiz which all contributed to this work. Thanks go to **Jutta Bebla** for organizing everything, **Henning Witt and Markus Irgang** for your helpful comments and discussions, **Dian Soewarto** for teaching me basics of mouse breeding and handling, **Valeria Zazzu**, **Luca Meoli**, **Christoph Nabzdyk**, **Daniel Ciera**, **Aydah Sabah**, **Beata Thalke**, and **Carsta Werner** for being wonderful colleagues.

I thank **Dr. Christiane Otto**, Therapeutic Research Group Women's Healthcare, Bayer Schering Pharma AG, for critical discussions and fruitful collaboration.

I thank **Dr. Valérie Gailus-Durner, Dr. Thure Adler, Dr. Helmut Fuchs** and all members of the German Mouse Clinic, Helmholtz Zentrum München, Institute of Experimental Genetics, for collaboration concerning the phenotyping of Gpr30-lacZ mice.

My most heartfelt thanks go to my beloved **Sabina**. Liebe Sabina, ich danke Dir für Deine Liebe und die schöne Zeit mit Dir.

Deep gratitude goes to my parents **Merja** and **Jürgen Isensee**. Ich liebe Euch für all Eure Unterstützung auf diesem langen Weg.

The studies were supported by the Research and Training Group 754 "Sex- and Gender-specific Mechanisms in Myocardial Hypertrophy" (German Research Council, DFG).

# PUBLICATIONS

## Peer Reviewed Publications

Isensee, J., L. Meoli, V. Zazzu, C. Nabzdyk, H. Witt, D. Soewarto, K. Effertz, H. Fuchs, V. Gailus-Durner, D. Busch, T. Adler, M. H. de Angelis, M. Irgang, C. Otto and P. Ruiz Noppinger (2008). *Expression Pattern of Gpr30 in LacZ Reporter Mice.* **Endocrinology** 18: 18. Epub 2008 Dec 18 (doi:10.1210/en.2008-1488)

Isensee, J., H. Witt, R. Pregla, R. Hetzer, V. Regitz-Zagrosek and P. Ruiz Noppinger (2008). *Sexually dimorphic gene expression in the heart of mice and men.* **J Mol Med.** 86(1): 61-74. Epub 2007 Jul 24.

Isensee, J. and P. Ruiz Noppinger (2007). *Sexually dimorphic gene expression in mammalian somatic tissue.* **Gend Med.** 4(Suppl B): S75-95.

## Abstracts

ELSO/EMBO Meeting 2008
*Deciphering the function of the G-protein Coupled Receptor GPR30*
Isensee J, Meoli L, Zazzu V, Effertz K, Ruiz Noppinger P
30/09 – 02/10/2008, Nice, France

XX International Congress of Genetics
*Deciphering the function of the G-protein Coupled Receptor GPR30*
Isensee J, Meoli L, Zazzu V, Effertz K, Ruiz Noppinger P
12-17/08/2008, Berlin, Germany

11th Meeting of the European Council for Cardiovascular Research
*Towards Deciphering the Function of the G-Protein coupled receptor GPR30*
Isensee J, Zazzu V, Meoli L, Effertz K, Ruiz Noppinger P
29/09 – 01/10/2006, Nice, France

Keystone Symposia, Molecular Biology of the Vasculature
*Deciphering the Function of the potential Estrogen Receptor GPR30 in the Vasculature*
Isensee J, Ruiz Noppinger P, Effertz K
02-07/03/2006, Keystone USA

## Invited Guest Speaker

Frühjahrskongress der Apothekerkammer Schleswig-Holstein
*Molekularbiologische Grundlagen für Geschlechterunterschiede in der Medizin*
12/04/2008, Ostseebad Damp, Germany

2nd International Congress of Gender Medicine
*Elucidating the function of the G-protein coupled receptor GPR30*
02/06/2007, Vienna, Austria

Expert Meeting GenderBasic
*Sexually dimorphic gene expression in somatic tissues*
26/01/2007, Maastricht, Netherlands

## Scholarships & Awards

| | |
|---|---|
| 10/2004 – 09/2007 | Scholarship of the German Research Council, Research training group GK 754-II "Sex-specific mechanisms in myocardial hypertrophy" |
| 09/2006 | Price for best Poster Presentation, Annual Meeting of the European Council for Cardiovascular Research (ECCR), Nice, France |
| 04/2006 | Keystone Symposia Scholarship, Molecular Biology of the Vasculature, Keystone, USA |

# EIDESSTATTLICHE ERKLÄRUNG

Hiermit erkläre ich, dass ich die vorliegende Dissertation selbständig und nur unter Verwendung der angegebenen Hilfsmittel erarbeitet und verfasst habe. Diese Arbeit wurde keiner anderen Prüfungsbehörde vorgelegt.

Berlin, 18. August 2009.

(Jörg Isensee)